uOttawa

L'Université canadienne
Canada's university

FACULTÉ DES ÉTUDES SUPÉRIEURES ET POSTOCTORALES

uOttawa

L'Université canadienne
Canada's university

FACULTY OF GRADUATE AND POSDOCTORAL STUDIES

Kelly Patterson
AUTEUR DE LA THÈSE / AUTHOR OF THESIS

M.Sc. (Biochemistry)
GRADE / DEGREE

Faculty of Medicine
FACULTÉ, ÉCOLE, DÉPARTEMENT / FACULTY, SCHOOL, DEPARTMENT

Biochemical Characterization of Indian Hedgehog Mutations Associated with Brachydactyly Type A1 and Acrocapitofemoral Dysplasia

TITRE DE LA THÈSE / TITLE OF THESIS

Dennis Bulman
DIRECTEUR (DIRECTRICE) DE LA THÈSE / THESIS SUPERVISOR

CO-DIRECTEUR (CO-DIRECTRICE) DE LA THÈSE / THESIS CO-SUPERVISOR

EXAMINATEURS (EXAMINATRICES) DE LA THÈSE / THESIS EXAMINERS

Marie-Andrée Akimenko

Martin Holcik

Gary W. Slater
Le Doyen de la Faculté des études supérieures et postdoctorales / Dean of the Faculty of Graduate and Postdoctoral Studies

Biochemical characterization of Indian Hedgehog mutations associated with Brachydactyly type A1 and Acrocapitofemoral Dysplasia

Kelly Patterson

Thesis submitted to the
Faculty of Graduate and Postdoctoral Studies

In partial fulfillment of the requirements for the Master of Science degree in
Biochemistry with a Specialization in Human and Molecular Genetics

Department of Biochemistry, Microbiology, and Immunology
Faculty of Medicine
University of Ottawa

Your file Votre référence
ISBN: 978-0-494-61209-5
Our file Notre référence
ISBN: 978-0-494-61209-5

Abstract

Indian hedgehog (IHH) is involved in regulating bone development, playing a particularly important role in endochondral ossification. Mutations in the *IHH* gene have been implicated in two human genetic diseases, brachydactyly type A1 and acrocapitofemoral dysplasia. This project involves characterizing these mutations and elucidating the resulting defect in IHH function. Nine mutant IHH constructs were created using site-directed mutagenesis to induce point mutations into full-length *IHH* cDNA, and HEK293 cell lines stably expressing each of the mutant constructs were established. Attempts to characterize the mutant IHH constructs using *in vitro* models of chondrogenesis were unsuccessful due to a lack of long-term expression and low transfection efficiency. The HEK293[IHH] stable lines were co-cultured with SHH-Light II cells (a hedgehog-responsive cell line) to measure the activity of the mutant constructs and compare to IHH^{WT}. Secretion and processing of the mutant IHH constructs were assessed by ELISA and western blotting, respectively. Overall, the mutations result in decreased intracellular levels of the IHH, with additional defects in processing and signaling for several of the mutants.

Acknowledgements

I would first like to thank Dennis, my supervisor and mentor, for all of his guidance and encouragement over the past two years. I am very grateful for the many conversations and all of the advice about lab work, my career, and life in general! And thanks to all of the people in the Bulman lab, past and present: Graeme Cunningham, Stuart Douglas, Alexis Given, Nancy Laurin, Heather MacDonald, Lem Racacho, Tara Read, Amanda Smith, Fengxia Xiao, and Roubing Zou. I hope I'm lucky enough to work in a lab as friendly and fun as this one again!

Thanks also to the members of the Parks, Picketts, and Wallace labs for reagents, equipment, and help with troubleshooting (especially Dr. Robin Parks, Kathy Poulin, Mike Huh, Maureen Curtin, Dr. Valerie Wallace, Shawn Beug, and Sherry Thurig,).

I would also like to thank OGSST and the University of Ottawa for funding, as well as the department of BMI, the FGPS, and Dr. Dennis Bulman for the travel grants which allowed me to present at the BRS/BSMB conference.

I am very grateful to Dr. Benjamin Alman and Claire Hsu from the Hospital for Sick Children (Toronto, ON) for teaching me the primary chondrocyte culture techniques.

I would also like to express my appreciation to my thesis advisory committee members, Dr. Valerie Wallace and Dr. Maxwell Hincke for their guidance and helpful advice.

Finally, I would like to thank my family and friends for their support and encouragement, especially my parents, my sister Melissa, Christian, and Maureen. I would not be where (or who) I am today without you.

Table of Contents

List of Figures

List of Tables

List of Abbreviations

×	symbol for multiplication
×g	g-force
2D	two dimensional
3D	three dimensional
A	alanine (Ala)
ACFD	Acrocapitofemoral dysplasia
Ad5	adenovirus type 5
amp	ampicillin
BDA1	Brachydactyly type A1
BMP	bone morphogenetic protein
BOC	brother of CDO
bp	base pair
BrdU	bromodeoxyuridine
c.	indicates cDNA sequence
cDNA	complementary DNA
cm	centimetre
CM	conditioned media
CMV	cytomegalovirus
CSPG	chondroitin sulfate proteoglycan
C-terminal	carboxy-terminal
D	aspartic acid (Asp)
ddH_2O	double distilled water
DHH	Desert Hedgehog
Disp	Dispatched
DMEM	Dulbecco's Modified Eagle medium
DMSO	dimethyl sulfoxide
DNA	deoxyribonucleic acid
dNTP	deoxyribonucleotide triphosphate
E	glutamic acid (Glu)
E. coli	*Escherichia coli*
EBSS	Earle's Balanced Salt Solution
ECL	enzymatic chemiluminescence

ECM	extracellular matrix
EGFP	enhanced green fluorescent protein
ER	endoplasmic reticulum
FBS	fetal bovine serum
FGF	fibroblast growth factor
GAG	glycosaminoglycan
Gas1	growth-arrest-specific 1
GH	growth hormone
h	hour
HDAC4	histone deacetylase-4
HEK	Human embryonic kidney
Hh	*Drosophila* hedgehog or hedgehog proteins in general
Hhat	Hedgehog acyltransferase
Hip	Hedgehog interacting protein
HS	heparan sulfate
HSPG	heparan sulfate proteoglycan
I	isoleucine (Ile)
IFT	intraflagellar transport protein
IGF	insulin-like growth factor
IHH	Indian Hedgehog protein
IHH	Indian Hedgehog gene (italics)
IHH-N	amino-terminal fragment of IHH
K	lysine (Lys)
kDa	kiloDalton
L	leucine (Leu)
LB	Luria-Bertani
LBMC	limb bud mesenchymal cell
MEF2C	myocyte enhancer factor-2
MEM	Minimal Essential Medium
min	minute
mL	milliliters
mM	millimolar
mShh	mouse sonic hedgehog
MWCO	molecular weight cut-off

N	asparagine (Asn)
ng	nanogram
nm	nanometre
N-terminal	amino-terminal
OHRI	Ottawa Hospital Research Institute
P	proline (Pro)
p.	indicates protein sequence
PBS	phosphate-buffered saline
PCR	polymerase chain reaction
pen/strep	penicillin/streptomycin
PFA	paraformaldehyde
Ptc	Patched
PTHrP	parathyroid hormone-related peptide
PTM	post-translational modification
PVDF	polyvinylidene difluoride
Q	glutamine (Gln)
R	arginine (Arg)
rpm	revolutions per minute
RT	room temperature
s	second
sddH_2O	sterile double distilled water
SDM	site-directed mutagenesis
SDS	sodium dodecyl sulfate
SHH	Sonic Hedgehog
Smo	Smoothened
T	threonine (Thr)
T3	triiodothyronine thyroid hormone
TBE	Tris-Borate-EDTA
TBS	Tris-Borate saline
TBS-T	Tris-Borate saline Tween-20
U	unit
UPR	unfolded protein response
UV	ultraviolet

V	volt
V	valine (Val)
WT	wild type
X	symbol for times (concentration)
Δ	delta symbol for change (deletion)
μg	microgram
μL	microlitre
μM	micromolar
μm	micrometre

Chapter 1: Introduction

Bone growth is a highly orchestrated process, involving many different players with interactions between multiple signaling pathways. Dysregulation of a single pathway can disrupt the balance of proliferation and differentiation of cells within the growth plate, leading to skeletal abnormalities. Indian hedgehog, (IHH) is one of the major players in the process of endochondral ossification and this research project attempts to decipher the resulting defect in bone development caused by mutations in *IHH*.

1.1. Hereditary disorders of bone development

1.1.1. Brachydactyly type A1

Brachydactyly was first described by William Farabee in his Ph.D. dissertation in 1903, making it the first human condition to be characterized by Mendelian autosomal dominant inheritance (Farabee, 1903). The families he described from Pennsylvania presented with short, broad hands and short stature. In England a few years later, Drinkwater described three families with the same condition (Drinkwater, 1908; Drinkwater, 1912; Drinkwater, 1915; Girirajan, and Elsea, 2005). Four decades later, Julia Bell created a classification system for brachydactyly, breaking it into five types (types A, B, C, D, and E) based on common phenotypes (Bell, 1951; Fitch, 1979). Brachydactyly type A was divided into three subtypes A1, A2, and A3.

Brachydactyly type A1 (BDA1) is a rare form of brachydactyly characterized by shortened middle phalanges of all digits of the hands and feet (Figure 1.1). In severe cases,

Figure 1.1. Morphological characteristics of hands of BDA1 patients. The various bones and digits of the hand are labelled in panel A, both an unaffected hand and a BDA1 hand are presented (modified from Girirajan and Elsea, 2005). Panel B illustrates the characteristics of a digit of an unaffected individual, as well as a BDA1 digit and a severe BDA1 digit (modified from Drinkwater, 1915). The severely affected digit has the middle phalanx fused to the distal, creating the characteristic pawn-shaped bone. An X-ray of a patient with shortened middle phalanges is shown in panel C (McCready, 2005; used with permission).

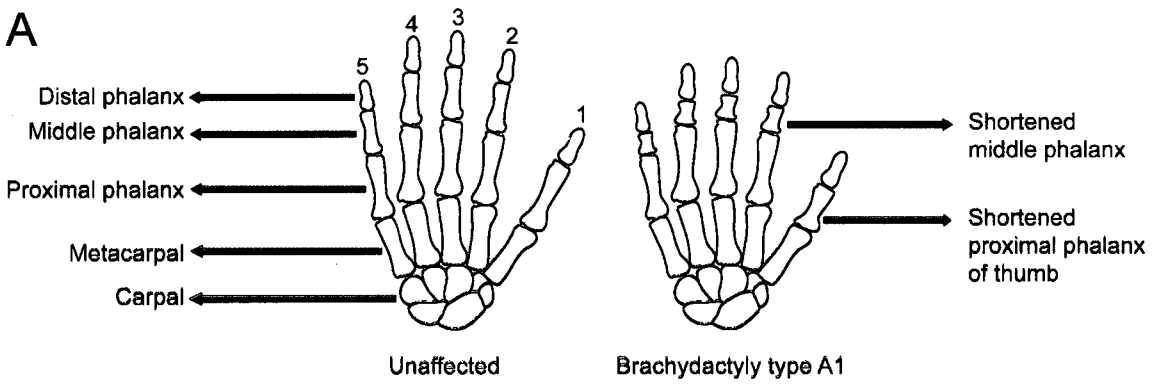
A
Distal phalanx
Middle phalanx
Proximal phalanx
Metacarpal
Carpal
5
4
3
2
1
Unaffected
Shortened middle phalanx
Shortened proximal phalanx of thumb
Brachydactyly type A1

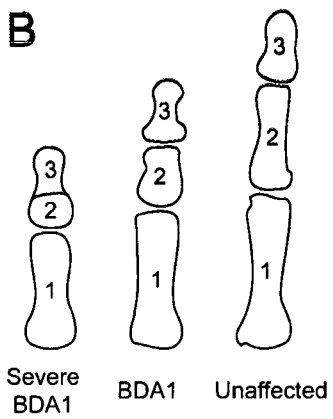
B
3
2
1
Severe BDA1
BDA1
Unaffected


C

the middle phalanges can also be fused to the proximal phalanges. There is also a shortening of the proximal phalanx in the thumb and big toe, and affected individuals are usually of short stature. Overall, the BDA1 phenotype is highly heterogeneous, and the severity of affected individuals varies even within the same family (Byrnes, Racacho, et al, 2009).

The locus for BDA1 was mapped to 2q35-q36 in two large unrelated Chinese families (Yang, She, et al, 2000). The following year, the same group identified three heterozygous missense mutations in the *IHH* gene in all affected members of three unrelated Chinese families (Gao, Guo, et al, 2001). To date, there have been six additional missense mutations and one deletion mutation identified in families of various ethnicity (Byrnes, Racacho, et al, 2009; Giordano, Gennari, et al, 2003; Kirkpatrick, Au, et al, 2003; Liu, Wang, et al, 2006; Lodder, Hoogeboom, et al, 2008; McCready, Sweeney, et al, 2002; McCready, Grimsey, et al, 2005; Stattin, Lindén, et al, 2009; Zhu, Ke, et al, 2007). This brings the total number of BDA1 mutations to ten, involving seven conserved residues in the amino terminal portion of IHH (Figure 1.2 and Table 1.1).

1.1.2. Acrocapitofemoral dysplasia

Acrocapitofemoral Dysplasia (ACFD) is another rare skeletal dysplasia that is caused by mutations in *IHH*. It is an autosomal recessive condition that has only been diagnosed in five individuals in two families of Belgian and Dutch origin (Hellemans, Coucke, et al, 2003; Mortier, Kramer, et al, 2003). The phenotype of patients with ACFD includes short stature and brachydactyly (Figure 1.3). Patients also had a narrow thorax, and a relatively large head. Premature epiphyseal closure was present in the phalanges and the proximal femur.

Figure 1.2. Localization of mutations within the amino-terminal fragment of *IHH*. The sequence alignment in panel A shows the location of all of the BDA1 (red) and ACFD (blue) mutations characterized in this study (modified from Byrnes *et al*, 2009). A 3D representation of IHH-N (modeled after Shh-N) is shown in panel B with the mutated residues highlighted. Residues 46 and 190 are mutated in ACFD (indicated in blue) and lie near the N- and C-termini. All other mutations are from BDA1 patients and cluster in the centre of the protein (modified from Byrnes *et al*, 2009).

A

P46L

```
Homo_sapiens_IHH        CGPGR-VVGSRRRPPRKLVPLAYKQFSPNVPEKTLGASGRYEGKIARSSERFKELTPNYN
Mus_musculus_IHH        CGPGR-VVGSRRRPPRKLVPLAYKQFSPNVPEKTLGASGRYEGKIARSSERFKELTPNYN
Gallus_gallus_IHH       CGPGR-VVGSRRRPPRKLIPLAYKQFSPNVPEKTLGASGRYEGKIARNSERFKELTPNYN
Danio_rerio_IHHa        CGPGR-GHG-KRRPPKKLTPLNYKQFSPNVAEKTLGASGRIEGKITRNSERFKELTPNYN
Danio_rerio_IHHb        CGPGR-GYG-KRRTPRKLTPLAYKQFSPNVAEKTLGASGRYEGKVTPSSERFKELTPNYN
Xenopus_laevis_IHH      CGPGR-VVGRRRRP-TKLSPLSYKQFSPNVPEKTLGASGRYEGKISRNSERFKELTPNYN
Homo_sapiens_SHH        CGPGR-GFG-KRRHPKKLTPLAYKQFIPNVAEKTLGASGRYEGKISRNSERFKELTPNYN
Homo_sapiens_DHH        CGPGRGPVGRRRYARKQLVPLLYKQFVPGVPERTLGASGPAEGRVARGSERFRDLVPNYN
```

D100N
E95K
T130N
R128Q
E131K

```
Homo_sapiens_IHH        PDIIFKDEENTGADRLMTQRCKDRLNSLAISVMNQWPGVKLRVTEGWDEDGHHSEESLHY
Mus_musculus_IHH        PDIIFKDEENTGADRLMTQRCKDRLNSLAISVMNQWPGVKLRVTEGWDEDGHHSEESLHY
Gallus_gallus_IHH       PDIIFKDEENTGADRLMTQRCKDRLNSLAISVMNQWPGVKLRVTEGWDEDGHHSEESLHY
Danio_rerio_IHHa        PDIIFKDEENTGADRLMTQRCKDKLNSLAISVMNMWPGVKLRVTEGWDEDGNHFEDSLHY
Danio_rerio_IHHb        PDIIFKDEENTGADRMMTQRCKDKLNSLAISVMNLWPGVRLRVTEGWDEDGLHSEESLHY
Xenopus_laevis_IHH      PDIIFKDEEITGADRLMTQRCKDRLNSLAISVMNQWPGVKLRVTEGWDEDGHHFEESLHY
Homo_sapiens_SHH        PDIIFKDEENTGADRLMTQRCKDKLNALAISVMNQWPGVKLRVTEGWDEDGHHSEESLHY
Homo_sapiens_DHH        PDIIFKDEENSGADRLMTERCKERVNALAIAVMNMWPGVRLRVTEGWDEDGHHAQDSLHY
```

T154I
V190A

```
Homo_sapiens_IHH        EGRAVDITTSDRDRNKYGLLARLAVEAGFDWVYYESKAHVHCSVKSEHSAAAKTGGCFPA
Mus_musculus_IHH        EGRAVDITTSDRDRNKYGLLARLAVEAGFDWVYYESKAHVHCSVKSEHSAAAKTGGCFPA
Gallus_gallus_IHH       EGRAVDITTSDRDRNKYGMLARLAVEAGFDWVYYESKAHIHCSVKSEHSAAAKTGGCFPG
Danio_rerio_IHHa        EGRAVDITTSDRDRNKYGMLARLAVEAGFDWVYYESKAHIHCSVKSEHSVAAKTGGCFPA
Danio_rerio_IHHb        EGRAVDITTSDRDRNKYRMLARLAVEAGFDWVYYESKGHVHCSVKSEHSVAAKTGGCFPG
Xenopus_laevis_IHH      EGRAVDITTSDRDRNKYGMLARLAVEAGFDWVYYESKAHIHCSVKSEHSAAAKTGGCFPG
Homo_sapiens_SHH        EGRAVDITTSDRDRSKYGMLARLAVEAGFDWVYYESKAHIHCSVKAENSVAAKSGGCFPG
Homo_sapiens_DHH        EGRALDITTSDRDRNKYGLLARLAVEAGFDWVYYESRNHVHVSVKADNSLAVRAGGCFPG
```

B

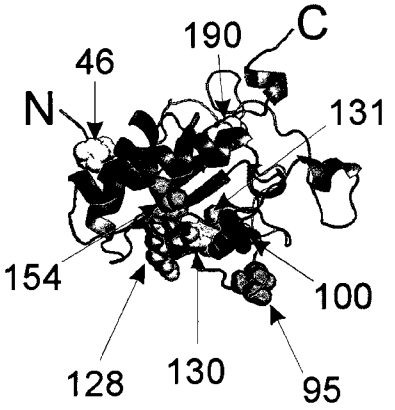

Table 1.1. Summary of mutations in *IHH* causing BDA1 and ACFD. The DNA mutations and resulting amino acid substitutions are listed for both BDA1 and ACFD. The ethnicity of the patients and the reference for the study in which the mutations were identified are also indicated (modified from Byrnes *et al*, 2009). Mutations marked with an asterisk were not investigated in this study.

DNA mutation	Amino Acid	Condition	Ethnicity	Reference
c.283G>A	p.E95K	BDA1	Chinese	Yang *et al*, 2000; Gao *et al*, 2001
c.284A>G	p.E95G*	BDA1	Mexican	Kirkpatrick *et al*, 2003
c.283_285 delGAG	p.ΔE95	BDA1	Dutch	Lodder *et al*, 2008
c.298G>A	p.D100N	BDA1	British	McCready *et al*, 2002; McCready *et al*, 2005
c.298G>A	p.D100N	BDA1	Italian	Giordano *et al*, 2003
c.298G>A	p.D100N	BDA1	Chinese	Zhu *et al*, 2007
c.298G>A	p.D100N	BDA1	New Zealand (British ancestors)	Byrnes *et al*, 2009
c.300C>A	p.D100E*	BDA1	Chinese	Gao *et al*, 2001
c.383G>A	p.R128Q	BDA1	American (Scottish, Irish, and German ancestors)	Byrnes *et al*, 2009
c.389C>A	p.T130N	BDA1	Indian	Byrnes *et al*, 2009
c.391G>A	p.E131K	BDA1	Chinese	Gao *et al*, 2001
c.391G>A	p.E131K	BDA1	Ashkenazi Jewish	Byrnes *et al*, 2009
c.461C>T	p.T154I	BDA1	Chinese	Liu *et al*, 2006
c.472C>T	p.R158C*	BDA1	Swedish	Stattin *et al*, 2009
c.137C>T	p.P46L	ACFD	Belgian	Hellemans *et al*, 2003
c.569T>C	p.V190A	ACFD	Dutch	Hellemans *et al*, 2003

Figure 1.3. Phenotypes of patients with ACFD. Panel A shows a 10.5 year-old Belgian girl with a P46L mutation who has brachydactyly and mild short stature. The boy in panel B is from the Dutch family with the V190A mutation. He is shown at nine years of age with short-limb dwarfism and a narrow thorax. In panel C is a radiograph of the left hand of the girl in panel A at 9.5 years of age. The radiograph in panel D is of the left hand of the boy in panel B at 11 years of age (Hellemans, 2003; used with permission).

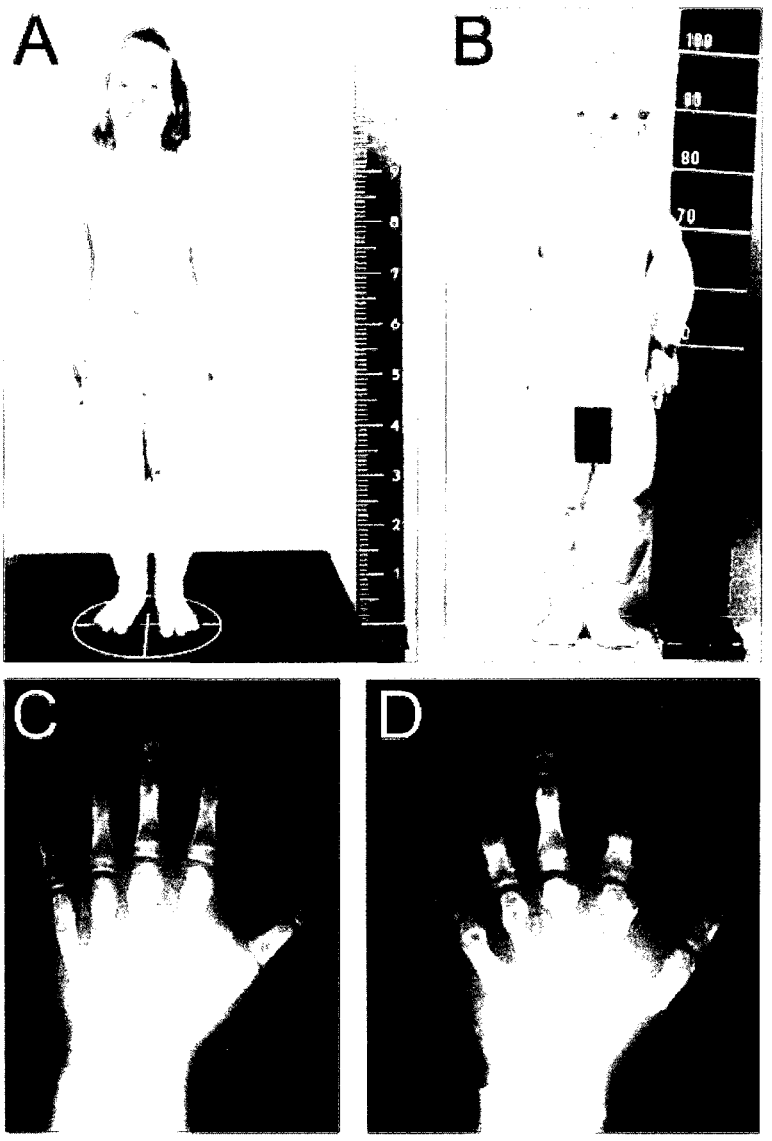
A
B
C
D

Prior to premature closure of the epiphysis, cone-shaped epiphysis were present in the shoulders, knees, ankles, proximal femur, and the middle and distal phalanges of the hands. The vertebrae of affected individuals were also ovoid in appearance, and the femur had a shortened neck with a small bony outgrowth. The affected individuals in the Dutch family had severely shortened tubular bones of the upper and lower limbs, however both affected individuals in the Belgian family had only a mild shortening.

Mutations in *IHH* were found in all affected individuals of both families in the same year that the condition was first identified (Hellemans, Coucke, et al, 2003). Both affected individuals in the Belgian family have a homozygous c.137C>T transition resulting in a p.P46L missense mutation. The parents of the affected children in the Belgian family were heterozygous for the p.P46L and had mild shortening of the middle phalanges, with severe shortening of the middle phalanx of digit V (the little finger). All three individuals in the Dutch family have a c.569T>C transition resulting in a p.V190A missense mutation. Only one set of parents in the Dutch family showed mild shortening of the metacarpals and proximal phalanges. The differences between ACFD and BDA1 mutations may be a result of different types of mutations (loss-of-function or gain-of-function) in the recessive and dominant conditions, respectively.

1.2. Hedgehog family of proteins

1.2.1. Processing of hedgehog proteins

IHH is a member of the hedgehog family of proteins that act as morphogens which are important in developmental processes. The hedgehog proteins are named as such because

the *Drosophila* hedgehog gene (Hh) was discovered during a screen for mutations in segment polarity genes, and the fruit flies with mutations in Hh had disrupted denticle formation resulting in the entire embryo being covered in bristles, resembling a hedgehog (Nusslein-Volhard, and Wieschaus, 1980). The mammalian orthologs were later discovered and were also named following the same theme: Sonic hedgehog (SHH), Indian hedgehog (IHH), and Desert hedgehog (DHH) (Echelard, Epstein, et al, 1993; Krauss, Concordet, and Ingham, 1993). SHH plays many roles during early development including determining left-right asymmetry, development of the central nervous system, and the anterior-posterior axis of the limb (reviewed in Chiang, Litingtung, et al, 1996; McMahon, Ingham, and Tabin, 2003). DHH is involved in spermatogenesis as well as myelination of the peripheral nervous system (Bitgood, Shen, and McMahon, 1996; Mirsky, Parmantier, et al, 1999). IHH is involved in the development of parts of the gastrointestinal tract (Bitgood, and McMahon, 1995) and is essential for the coordination of chondrocyte proliferation and differentiation at the growth plate during endochondral ossification (Lanske, Karaplis, et al, 1996; St-Jacques, Hammerschmidt, and McMahon, 1999), which will be discussed in detail later on.

The following summary of the processing of hedgehog proteins and the hedgehog signaling pathway will use results from studies where much of the work done has been on *Drosophila* Hh or SHH. However, due to the high level of conservation of hedgehog proteins among vertebrates, we will assume that the basics of processing and signal transduction are conserved for IHH as well.

The *IHH* gene has three exons and is translated into a protein that is 411 amino acids in length which also contains an amino-terminal signal peptide. The IHH full-length precursor is a 45 kiloDalton (kDa) protein consisting of the active signaling amino-terminal domain and the catalytic carboxy-terminal domain (Figure 1.4). The signal peptide targets the

Figure 1.4. Synthesis of the Indian hedgehog protein. The full-length protein is translated and undergoes autocleavage and cholesterol addition catalyzed by the C-terminal domain. The amino-terminal fragment (IHH-N) is then palmitoylated at the N-terminus by the acyltransferase Hhat.

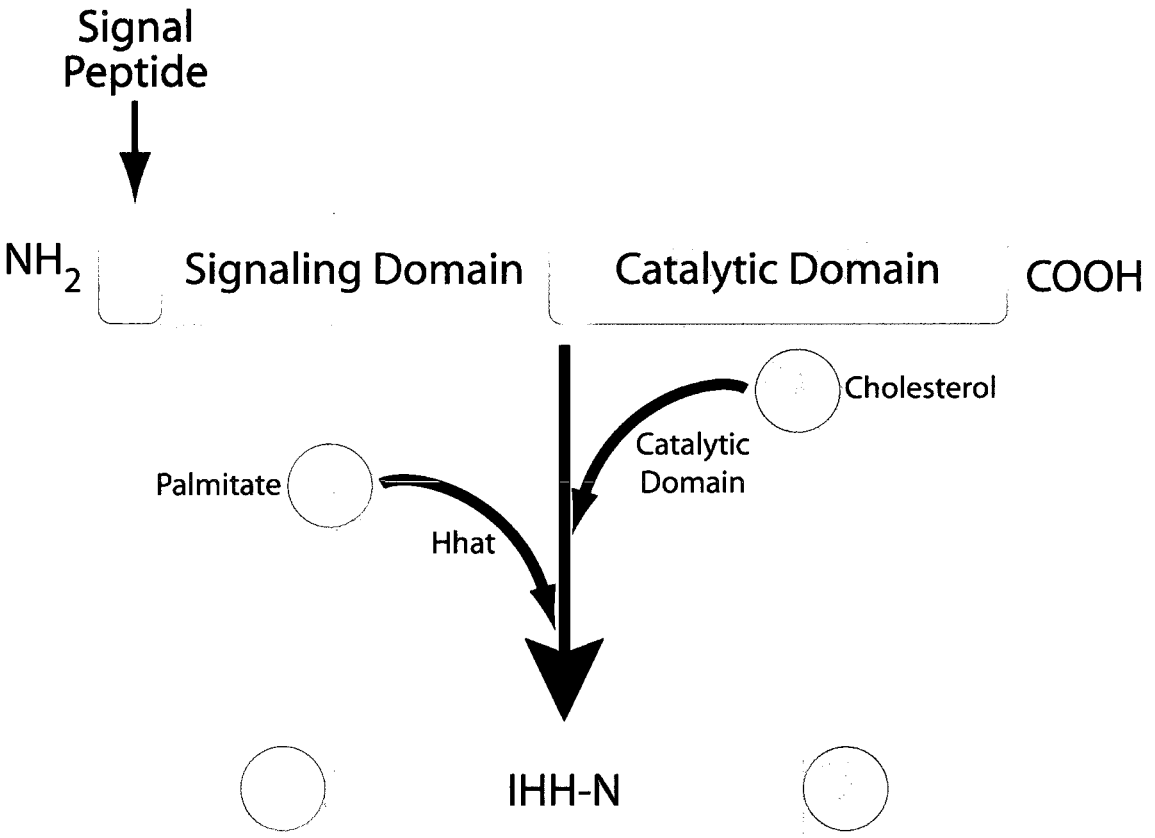
Signal
Peptide
NH2
Signaling Domain
Catalytic Domain
COOH
Cholesterol
Catalytic
Domain
Palmitate
Hhat
IHH-N

protein to the endoplasmic reticulum (ER) where it undergoes autocleavage catalyzed by the C-terminal domain to yield the 19 kDa N-terminal fragment, Hh-N (reviewed in Mann, and Beachy, 2004). The C-terminal domain also acts as a cholesterol transferase, and a cholesterol adduct is covalently attached to the new C-terminus of Hh-N during the autocleavage reaction (Porter, Young, and Beachy, 1996). The protein is palmitoylated at the amino-terminal cysteine (C24) of SHH-N (equivalent to residue C28 in IHH-N) which is exposed after signal peptide cleavage (Pepinsky, Zeng, et al, 1998). The palmitate is added via an amide linkage by the membrane-associated hedgehog acyltransferase (Hhat) (Buglino, and Resh, 2008) while passing through the secretory pathway. The active, dual lipid-modified Hh-N is then secreted from the cell by the membrane protein Dispatched (Disp), a 12-pass transmembrane protein which is related to the Hh receptor Patched (Ptc). Both Disp and Ptc are members of a group of proteins related to bacterial transmembrane transporters (Burke, Nellen, et al, 1999; Mann, and Beachy, 2004).

The dual lipid modifications are essential for proper Hh signaling and they serve as anchors to the cell membrane, allowing for proper gradient formation by preventing diffusion (Mann, and Beachy, 2004). Cholesterol targets the protein to lipid rafts in the cellular membrane (Chen, Li, et al, 2004) and is essential for multimerization (Zeng, Goetz, et al, 2001), while palmitoylation is important for potency (Pepinsky, Zeng, et al, 1998). Multimerization is essential for long-range signaling as it allows the hydrophobic hedgehog molecule to travel through the extracellular matrix (ECM) and it may occur via interactions with heparan sulfate proteoglycans (HSPGs) and lipoproteins (Chen, Li, et al, 2004; Eugster, Panáková, et al, 2007; Panáková, Sprong, et al, 2005; Zeng, Goetz, et al, 2001).

HSPGs consist of a core protein on which the heavily sulfated heparan sulfate (HS) glycosaminoglycan (GAG) chains are added. The core protein determines the localization

and function of the different HSPG family members such as glypicans (membrane), syndecans (transmembrane), and perlecans (ECM) (Ma, Xiao, and He, 2008). Chondroitin sulfate proteoglycans (CSPGs) are similar to HSPGs in that they consist of heavily sulfated chains attached to a core protein, however the composition of the chains are different (Cortes, Baria, and Schwartz, 2009). An example of a CSPG is aggrecan, which is located in the ECM at the growth plate (Cortes, Baria, and Schwartz, 2009). Hedgehog molecules bind to HSPGs and CSPGs via a conserved Cardin-Weintraub consensus sequence (XBBBXXBX) which is found at residue 36-43 in IHH (Cardin, and Weintraub, 1989; Cortes, Baria, and Schwartz, 2009; Rubin, Choi, and Segal, 2002). The positive charges of the conserved basic residues are essential for the Hh protein to bind to the negatively charged sulphated chains of the HSPGs and CSPGs (Cortes, Baria, and Schwartz, 2009; Rubin, Choi, and Segal, 2002). It has been recently shown that reduced HSPG and CSPG binding leads to a decreased range of IHH signaling at the growth plate (Cortes, Baria, and Schwartz, 2009).

1.2.2. The hedgehog signaling pathway

After secretion, multimerization, and trafficking through the ECM, IHH-N binds to its receptor Patched (Ptc) on hedgehog-responsive cells. In vertebrates, there are two Ptc isoforms, Ptc and Ptc2. However Ptc is thought to be the essential isoform because Ptc2 deficient mice are viable and have a mild phenotype compared to Ptc deficient mice (Goodrich, 1997). Ptc is a 12-pass transmembrane receptor which is functionally related to a family of bacterial transporters. Because of the transporter-like properties of Ptc, it has been suggested that Ptc represses Smo by pumping a small molecule inhibitor of Smo such

as vitamin D3 derivatives or oxysterols (Bijlsma, Spek, et al, 2006; Corcoran, and Scott, 2006). It has been suggested that one Ptc molecule can regulate approximately fifty Smo molecules (Taipale, Cooper, et al, 2002). When Smo is repressed, the Gli zinc-finger transcription factors are processed into their repressor forms, which then enter the nucleus and repress the transcription of target genes (Figure 1.5).

Mammals have three Gli transcription factors, Gli1, Gli2, and Gli3. Gli1 acts primarily as a transcriptional activator, Gli3 as a repressor, and Gli2 functions as both depending on its processing (reviewed in Ehlen, Buelens, and Vortkamp, 2006). When Hh binds to Ptc (which may exist as a trimer), the complex is internalized and degraded which lifts the repression of Smo to allow Smo to target to the membrane at the cilia (Lu, Liu, and Kornberg, 2006). Smo then inhibits the processing of the Gli2/3 into the repressor forms, and represses the sequestration of Gli2 and Gli1 in the cytoplasm to allow the activated forms of Gli to enter the nucleus and activate transcription of target genes which include Gli-1 and Ptc-1.

Recently there have been many studies implicating the primary cilium as having a role in vertebrate Hh signaling (reviewed in Simpson, Kerr, and Wicking, 2009; Singla, and Reiter, 2006). Primary cilia exist on most vertebrate cells and are solitary (one per cell) and non-motile (Huangfu, and Anderson, 2005). Intraflagellar transport proteins (IFTs) are involved in cilia growth and maintenance and are thus indirectly important for Hh signaling. IFTs also play a direct role in Hh signaling by modulating the localization of the Gli transcription factors at the cilia (Haycraft, Banizs, et al, 2005; Huangfu, and Anderson, 2005; Liu, Wang, and Niswander, 2005; May, Ashique, et al, 2005). It has been shown that Ptc localizes to the cilia and prevents Smo from accumulating there (Rohatgi, Milenkovic, and Scott, 2007). Smo can only localize to the cilia after Ptc is internalized following Hh binding (Lu, Liu, and Kornberg, 2006).

Figure 1.5. The hedgehog signaling pathway. Panel A represents a cell in the absence of IHH (arrows indicate induction, crossed lines indicate repression). Ptc is repressing Smo and the Gli transcription factors are processed into their repressor form (Gli2/3) and repress transcription of target genes. In panel B, IHH binds to Ptc and the complex is then internalized and degraded. This lifts the repression of Smo, allowing it to target to the membrane at the cilia and activate the signaling cascade. Smo represses the processing of Gli repressor forms, and also represses the sequestration of the Gli activator forms (Gli1/2) in the cilia. Through the action of various IFT proteins, the Gli activators enter the nucleus and activate transcription of target genes such as Ptc and Gli1.

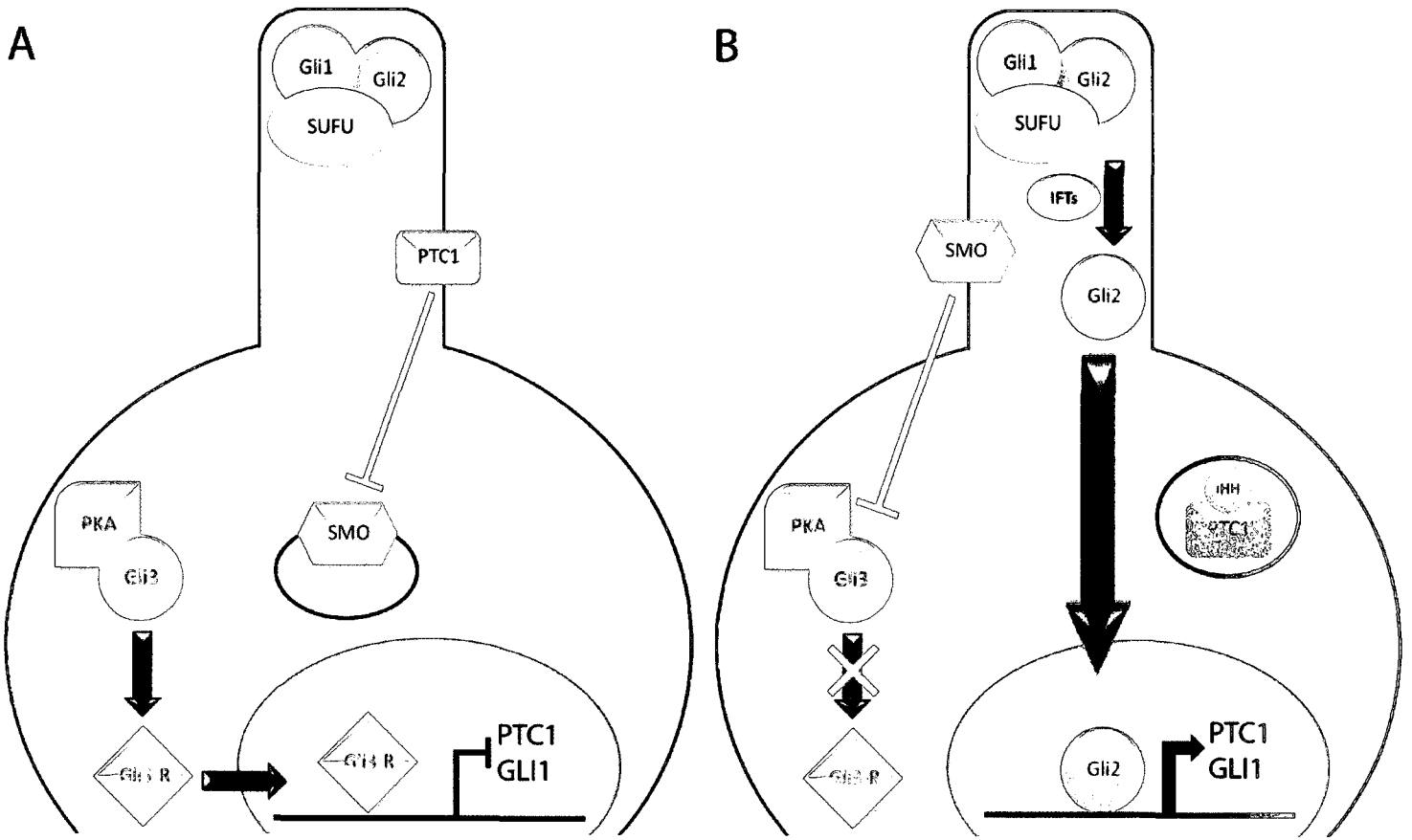
A
Gli1
Gli2
SUFU
PTC1
PKA
Gli3
SMO
PTC1
GLI1
B
Gli1
Gli2
SUFU
IFTs
SMO
Gli2
PKA
Gli3
IHH
PTC1
Gli2
PTC1
GLI1

There are a number of different receptors for Hh on target cells which help to precisely control the gradient of Hh through the developing tissue. These include receptors that either negatively or positively regulate Hh signaling. Hedgehog interacting protein (Hip) is a vertebrate hedgehog receptor that negatively regulates Hh signaling. Hip is a membrane-bound protein that competes with Ptc for Hh binding to restrict the movement of hedgehog molecules through the tissue (Chuang, and McMahon, 1999; Jeong, and McMahon, 2005).

CDO is a transmembrane protein that binds Hh in a calcium-dependent manner (McLellan, Zheng, et al, 2008). There are some conflicting reports as to whether CDO enhances Ptc binding Hh (Martinelli, and Fan, 2007) or competes with Ptc for Hh binding (McLellan, Zheng, et al, 2008). Brother of CDO (BOC) is another Hh receptor and is involved in regulating axon guidance by Shh (Okada, Charron, et al, 2006). Sequence similarity between BOC and CDO suggests that BOC may also bind Hh in a calcium-dependent manner (Tenzen, Allen, et al, 2006; Zhang, Kang, et al, 2006).

Growth-arrest-specific 1 (Gas1) is a receptor that acts as a positive regulator of the Hh pathway in vertebrates. Gas1 helps to increase the local concentration of Hh at the cell because of its high affinity for Hh (Allen, Tenzen, and McMahon, 2007; Lee, Buttitta, and Fan, 2001; Martinelli, and Fan, 2007). Calcium may also play a role in Hh binding to Gas1 (McLellan, Zheng, et al, 2008). Due to the importance of Hh signaling for development, multiple receptors have evolved to keep the Hh gradient tightly regulated.

1.3. Bone development

1.3.1. Endochondral ossification

Intramembranous ossification and endochondral ossification are two different processes by which the bones of the human skeleton are formed. Very few bones, such as the clavicle and the flat bones of the skull, undergo intramembranous ossification where mesenchymal cells differentiate directly into osteoblasts (reviewed in Zelzer, and Olsen, 2003). The long bones of the skeleton undergo endochondral ossification where mesenchymal cells first differentiate into chondroctyes to form the cartilage template before osteoblasts take over to start the ossification process to form bone (reviewed in Karsenty, 2003; Kronenberg, 2003; Mackie, Ahmed, et al, 2008).

Endochondral ossification begins when mesenchymal cells condense and differentiate into chondrocytes which then secrete cartilage ECM. This forms the cartilage model of the future bone. Chondrocytes at the centre of the condensation mature and undergo hypertrophy, leading to the development of the primary ossification centre.

A secondary ossification centre also forms at the epiphysis, which is the region at the end of the bone that forms the joint with adjacent bones. This leaves a region of cartilage sandwiched between the two ossification centres (called the growth plate or physis) which is responsible for the longitudinal growth of the bone.

Proliferation and differentiation of chondrocytes at the growth plate follows a well-defined pattern and the cells form distinct zones based on their level of maturation. In the resting zone, there is little to no proliferation of the chondrocytes and the cells are spaced far apart with ECM taking up most of the space (Ballock, and O'Keefe, 2003; Burdan, Szumiło, et al, 2009; Melrose, Smith, et al, 2008). These resting chondrocytes may act as

chondrocyte "stem-like" cells by producing daughter cells which then form the beginnings of new columns of proliferating chondrocytes (Abad, Meyers, et al, 2002).

In the proliferative zone, chondrocytes become flattened discs which divide longitudinally, forming columns of stacked cells. Cells then exit the proliferative zone, stop dividing and undergo differentiation into prehypertrophic chondrocytes, and later into hypertrophic chondrocytes. When the chondrocytes undergo hypertrophy, they grow ten times in size (Lefebvre, and Smits, 2005) contributing to the growth of the bone. Hypertrophic chondrocytes secrete type X collagen, orchestrate the mineralization of the surrounding ECM, and induce vascularization. Hypertrophic chondrocytes also induce the cells of the adjacent perichondrium (the outer layer of the cartilage model) to differentiate into osteoblasts which then form the bone collar. After all of this has been accomplished, the hypertrophic chondrocyte undergoes apoptosis and osteoblasts lay down bone matrix in its place. After adolescence, fusion of the growth plates occurs when the proliferative potential of the chondrocytes is exhausted (Weise, De-Levi, et al, 2001).

This process of differentiation is regulated by many different transcription factors, as well as systemic and locally secreted factors (Figure 1.6) (reviewed in Mackie, Ahmed, et al, 2008). Briefly, the systemic factors include growth hormone (GH), oestrogen, oxygen tension, and thyroid hormone (triiodothyronine, T3). GH induces proliferation of chondrocytes, oestrogen induces senescence, and T3 induces hypertrophy. Oxygen tension influences the expression of certain transcription factors which will be discussed later.

Insulin-like growth factor (IGF) and IHH are two locally secreted factors that induce proliferation of chondrocytes, while parathyroid hormone-related peptide (PTHrP) delays hypertrophy. Bone morphogenetic protein (BMP) induces proliferation and *IHH* expression, while fibroblast growth factors (FGFs) decrease proliferation and *IHH* expression, acting as a BMP antagonist.

Figure 1.6. Schematic representations of the signaling pathways involved in chondrocyte maturation. Panel A summarizes the various effects of transcription factors, systemic factors, and locally secreted factors (arrows indicate induction, crossed lines indicate repression; modified from Mackie *et al*, 2008). Panel B integrates the signaling pathways that regulate chondrocyte proliferation and hypertrophy (modified from Provot and Schipani, 2005).

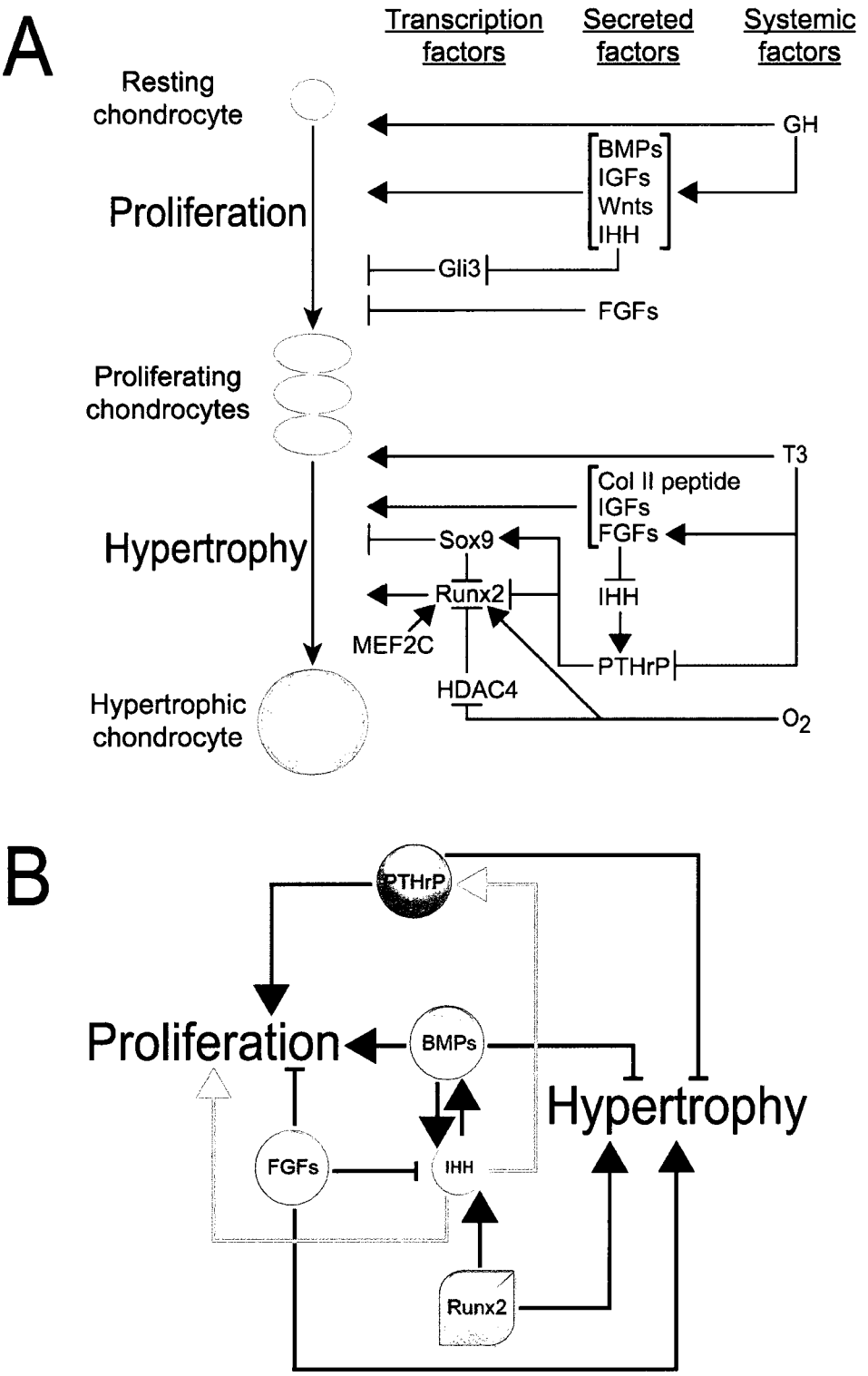
A
Transcription factors
Secreted factors
Systemic factors
Resting chondrocyte
Proliferation
Proliferating chondrocytes
Hypertrophy
Hypertrophic chondrocyte
GH
BMPs
IGFs
Wnts
IHH
Gli3
FGFs
T3
Col II peptide
IGFs
FGFs
Sox9
Runx2
MEF2C
HDAC4
IHH
PTHrP
O2
B
PTHrP
Proliferation
BMPs
Hypertrophy
FGFs
IHH
Runx2

Transcription factors that play a role in chondrocyte differentiation include SOX9, Runx2, Nkx3/Bapx1, myocyte enhancer factor-2 (MEF2C) and histone deacetylase-4 (HDAC4). SOX9 is expressed in the mesenchymal condensation stage to induce the cells to differentiate into chondrocytes (reviewed in Lefebvre, and Smits, 2005). SOX9 is also expressed in proliferating chondrocytes and induces the expression of collagen type II in those cells. Runx2 induces hypertrophy and *IHH* and *Col10a1* expression (Yoshida, Yamamoto, et al, 2004). PTHrP, SOX9, and HDAC4 all inhibit Runx2 (Guo, Chung, et al, 2006; Vega, Matsuda, et al, 2004; Zhou, Zheng, et al, 2006). Expression of Nkx3/Bapx1 is induced by PTHrP and it also inhibits Runx2 expression (Provot, Kempf, et al, 2006). MEF2C induces expression of *Col10a1* and there is a total lack of hypertrophy in Mef2c-null mice (Arnold, Kim, et al, 2007).

Oxygen tension also plays a role in chondrocyte hypertrophy by influencing Runx2 and HDAC4 expression. In hypoxic conditions, expression of HDAC4 is activated and Runx2 is repressed (Hirao, Tamai, et al, 2006). Most chondrocytes experience low oxygen tension compared to other tissues because cartilage is mostly avascular (Schipani, Ryan, et al, 2001). Blood vessels invade as the bone ossifies thus increasing the local oxygen concentration and influencing chondrocyte hypertrophy.

1.3.2. The IHH/PTHrP feedback loop

Two of the secreted factors mentioned briefly in the previous section, IHH and PTHrP, are involved in a negative feedback loop to regulate growth in the long bones (Karp, Schipani, et al, 2000; Kronenberg, 2003). It has been shown that *IHH* is expressed throughout the entire cartilage model early in mouse development, but at birth it is restricted

to the prehypertrophic chondrocytes (Bitgood, and McMahon, 1995; Lanske, Karaplis, et al, 1996; St-Jacques, Hammerschmidt, and McMahon, 1999; Vortkamp, Lee, et al, 1996).

The cells of the periarticular perichondrium secrete PTHrP, which indirectly represses the expression of *IHH* by inhibiting differentiation of the proliferating chondrocytes into prehypertrophic chondrocytes (Figure 1.7). Receptors for PTHrP are expressed in low levels in proliferating chondrocytes, and are highly expressed when the chondrocytes stop proliferating (Lee, Lanske, et al, 1996). As the bone lengthens, proliferating chondrocytes grow further away from the source of PTHrP. When proliferating chondrocytes no longer receive the repressive signal from PTHrP, they undergo differentiation into prehypertrophic chondrocytes. These cells then secrete IHH which induces proliferation of chondrocytes (Long, Zhang, et al, 2001) and also induces resting chondrocytes to become proliferative chondrocytes (Kobayashi, Soegiarto, et al, 2005). IHH also induces the expression of PTHrP in the periarticular perichondrium, which then inhibits hypertrophy; creating the negative feedback loop (Lanske, Karaplis, et al, 1996). This negative feedback loop between IHH and PTHrP regulates the rate at which chondrocytes exit the proliferative zone and ensures that the pool of proliferating chondrocytes is maintained (Karp, Schipani, et al, 2000; Kronenberg, 2003).

1.4. Thesis

1.4.1. Rationale

Many mutations in *IHH* had already been published at the beginning of this research project; however no studies had been published on the effect of these mutations on IHH function. Using a panel of eight BDA1 mutations and 2 ACFD mutations, this project aimed

Figure 1.7. IHH/PTHrP feedback loop in the developing long bone. Cells of the periarticular perichondrium secrete PTHrP which prevents the differentiation of the proliferating chondrocytes into prehypertrophic chondrocytes. PTHrP represses the expression of IHH indirectly by repressing the differentiation of proliferating chondrocytes into the IHH-producing prehypertrophic chondrocytes. As the proliferating chondrocytes grow further away from the source of PTHrP, they eventually escape the repression of PTHrP and undergo differentiation. IHH is secreted from the prehypertrophic chondrocytes and induces the proliferation. IHH also induces the expression of PTHrP, completing the feedback loop.

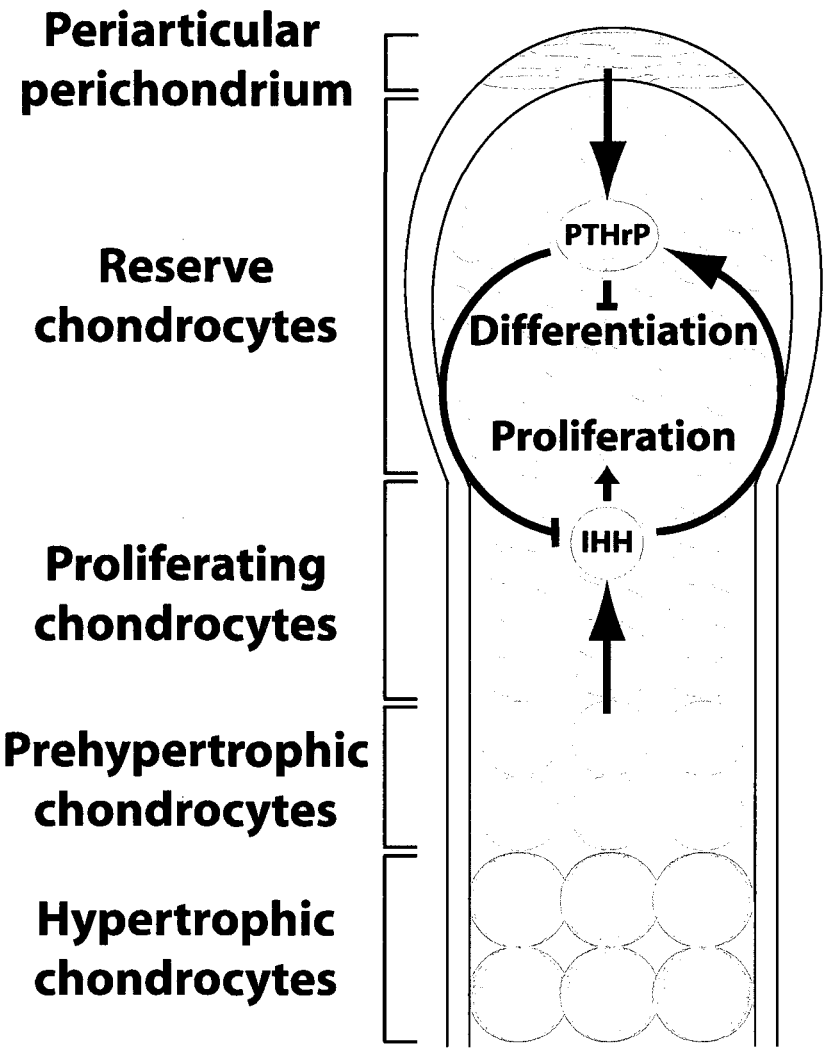
Periarticular perichondrium
Reserve chondrocytes
Proliferating chondrocytes
Prehypertrophic chondrocytes
Hypertrophic chondrocytes
PTHrP
Differentiation
Proliferation
IHH

at characterizing the resulting defect in IHH function at the protein level. Bacterial expression and purification of IHH proteins would have been a simple approach, however the resulting proteins would not be lipid-modified. Since the lipid modifications of hedgehog proteins are essential for proper function, a mammalian expression system was chosen to more accurately reproduce the physiological situation. Also, the constructs were cloned as full-length cDNA constructs to allow for cholesterol addition by the C-terminal domain. The resulting defect in the mutant IHH constructs could then be compared to the IHH^{WT} construct for different steps of IHH biogenesis including processing, secretion, and the ability to set off the signaling cascade.

1.4.2. Hypothesis

My hypothesis is that mutations in *IHH* cause BDA1 and ACFD by disrupting IHH signaling at the growth plate, leading to dysregulation of chondrocyte proliferation and differentiation. Since the mutations occur in different regions of the protein, they may interfere with IHH biogenesis in different ways, resulting in defective processing, secretion, and activity. The ACFD mutations may interfere with lipid modification due to their proximity to the amino- and carboxy-termini which would decrease the multimerization and activity of the mutant protein. The BDA1 mutations may interfere with Ptc binding and multimerization and decrease the activity of the mutant protein.

1.4.3. Objectives

- Create mutant vector constructs by site-directed mutagenesis (SDM) and create lipid mutant constructs as controls.
- Create ATDC5 clones stably expressing each of the mutant *IHH* constructs to look for differences in proliferation, differentiation, and apoptosis.
- Establish micromass cultures from primary mouse limb bud mesenchymal cells and transfect with mutant *IHH* constructs to repeat the above assays.
- Create HEK293 clones stably expressing each of the mutant *IHH* constructs to analyze defects in processing, secretion, and activity by comparing mutant to wild-type.

Chapter 2: Creation of the mutant IHH constructs

2.1. Introduction

The first goal of this research project was to create the mutant *IHH* constructs to be used in the *in vitro* assays. A previous graduate student, Graeme Cunningham, successfully cloned the full-length human *IHH* cDNA into the vector pBlueScript II KS+ and he created the mutant *IHH* constructs E95K, D100N, R128Q, E131K, and V190A (Cunningham, 2008). These were later subcloned into the mammalian expression vector pcDNA3.1+ to allow for high levels of expression of IHH under the cytomegalovirus (CMV) promoter. I also created four more mutant constructs (P46L, ΔE95, T130N, and T154I) and three constructs to act as controls for lipid modification. All constructs were subcloned into pcDNA3.1+ and verified by sequencing prior to use.

The controls for lipid-modification defects are IHH constructs that are unable to be modified by either cholesterol (IHH-N), palmitate (IHH^{C28S}) or both ($IHH\text{-}N^{C28S}$). Cloning only the N-terminal domain of *IHH* results in a protein that is not cholesterol-modified since the C-terminal domain, which is required for cholesterol addition, is missing (Figure 2.1). Palmitate is added to the N-terminal cysteine (C28) which is exposed after the signal peptide is cleaved (Pepinsky, Zeng, et al, 1998). Mutating this residue to a serine (C28S) results in a mutant IHH protein lacking palmitate because serine cannot act as an acceptor for palmitate (Buglino, and Resh, 2008).

Figure 2.1. Schematic of the IHH lipid mutant constructs. On the left, the cDNA of each construct is shown, the green bar represents the C28S mutation. On the right, the resulting IHH protein is shown, P represents palmitate and C represents cholesterol. Cholesterol addition only takes place when the C-terminal domain (IHH-C) is present, and palmitate cannot be added with the C28S mutation.

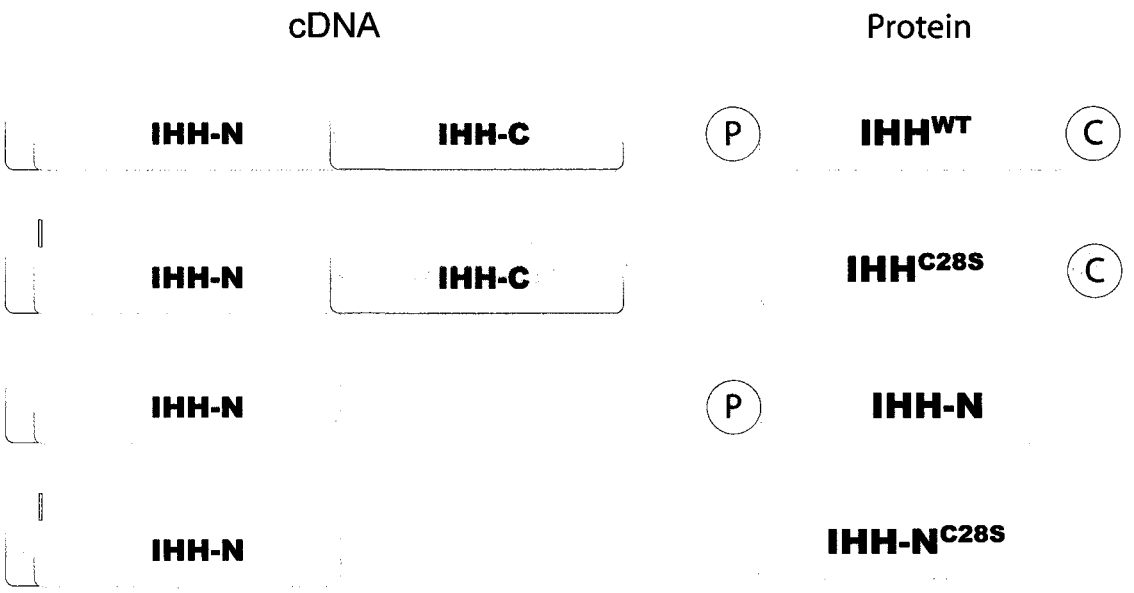
cDNA
Protein
IHH-N
IHH-C
P
IHH^WT
C
IHH-N
IHH-C
IHH^C28S
C
IHH-N
P
IHH-N
IHH-N
IHH-N^C28S

2.2. Materials and Methods

2.2.1. Primers

Primers for mutagenesis were designed by hand following the guidelines in the QuikChange site-directed mutagenesis kit manual (Stratagene, La Jolla, CA). Table 2.1 lists the sequences of all primers used in this research project. The primers contained the desired mutation flanked by ~15 bases of wild-type sequence on each side, and the forward and reverse primers were reverse complements of each other. Primers were synthesized by Sigma Genosys (Sigma-Aldrich, Oakville, ON) and resuspended in sddH_2O to make the 100 μM stock and the 10 μM working stock. Primer stocks were stored at -20°C.

2.2.2. Site-directed mutagenesis

The full-length *IHH* cDNA clone in the vector pBlueScript II KS+ (pBSII.IHH^{WT}) was used as the template to create the selected mutations. The protocol in the QuikChange site-directed mutagenesis kit (Stratagene, La Jolla, CA) was followed exactly. To summarize, the primers were used to introduce the mutation on both strands of the plasmid via polymerase chain reaction (PCR) amplification in an MBS Satellite 0.2G thermal cycler. Any leftover template (containing IHH^{WT} sequence) was removed by *Dpn*I digestion (the mutated plasmid amplified *in vitro* is not methylated, and thus not sensitive to *Dpn*I digestion). The plasmid was then transformed into XLI-Blue *Escherichia coli* competent cells which then repaired the nicks in the plasmid from the PCR amplification. The transformants were plated on Luria-Bertani/ampicillin (100 μg/mL) agar plates and single

Table 2.1. Primer sequences. The mutated bases (including the kozak sequence and stop codon) are indicated in italics and red, the restriction enzyme sites are indicated in blue and underlined. The red triangle in the E95del primers indicates a deletion of the second GAG codon. The P46L forward and reverse primers were made by a previous graduate student, Graeme Cunningham (Cunningham, 2008).

Primer Name	5′-3′ Sequence	Mutation, restriction sites, and other features
P46L-For	AAACTCGTGC *T* GCTCGCCTACAA	P46L
P46L-Rev	TTGTAGGCGAGC *A* GCACGAGTTT	P46L
E95del-For	GACATCATCTTCAAGGACGAG▲AACACAGGCGCCGACCGCCTCATG	ΔE95
E95del-Rev	CATGAGGCGGTCGGCGCCTGTGTT▲CTCGTCCTTGAAGATGATGTC	ΔE95
IHH.T130N.F	CGGTGTGAAGCTGCGGGTGA *A* CGAGGGCTGGGACGAGGAC	T130N
IHH.T130N.R	GTCCTCGTCCCAGCCCTCG *T* TCACCCGCAGCTTCACACCG	T130N
IHH.T154I.F	GGGCCGCGCGGTGGACATCA *T* CACATCAGACCGCGACCGC	T154I
IHH.T154I.R	GCGGTCGCGGTCTGATGTG *A* TGATGTCCACCGCGCGGCCC	T154I
IHH-N.F	CTAGTGGATCC*GCCGCC*ATGTCTCCCGCCCGGCTCCGG	*Bam*HI site and *kozak sequence*
IHH-N.R	CTAGGCGGCCGC*CTA*GCCGCCTGTCTTGGCTGCGG	*Not*I site and *stop codon*
IHH.3UTR.R	CTGGGTACCGGGCCCTCCCCAATG	*Apa*I site

colonies were isolated and grown in a 5 mL LB/amp broth culture for 16 h followed by plasmid purification using the QiaPrep spin mini prep kit (Qiagen, Mississauga, ON). Glycerol stocks of the cultures were prepared and kept at -80°C for long term storage.

2.2.3. Sequencing

Constructs were verified by sequencing using the T7 (5′-TAATACGACTCACTATAGGG-3′) and Sp6 (5′-ATTTAGGTGACACTATAG-3′) promoter primers. Reactions were prepared following the protocol for the BigDye™ Terminator v3.1 cycle sequencing kit (Applied Biosystems, Foster City, CA). The sequencing reaction buffer from the kit was used at 1X with 3.2 μM primer and 30 ng plasmid DNA as the template. The PCR program consisted of a one minute step at 96°C, followed by 25 cycles of 10 s at 96°C; 5 s at 50°C; and 4 min at 60°C. Amplified DNA was purified by ethanol precipitation and the purified DNA was subjected to capillary electrophoresis using the ABI 3130x1 Genetic Analyzer (Applied Biosystems, Foster City, CA). The sequences were then analyzed using the ABI Sequencing Analysis v5.2 software (Applied Biosystems, Foster City, CA) and DS Gene v1.5 (Accelrys, San Diego, CA).

2.2.4. Subcloning confirmed mutant constructs into pcDNA3.1+

2.2.4.1. Gel purification

After the sequences were verified, the *IHH* fragments were subcloned from pBlueScript II KS+ into the mammalian expression vector pcDNA3.1+. Both the pcDNA3.1+ vector and the respective pBSII.IHH vector were digested with *Bam*HI and *Apa*I. The digested DNA was loaded (in its entirety) on a 1% Tris-Borate-EDTA (TBE) agarose gel containing

0.5 μg/mL ethidium bromide and subjected to electrophoresis at 120 V for 1 h. The DNA was visualized under 302 nm UV light using the AlphaImager with the AlphaEase®FC v6.0.0 software (Alpha Innotech Corporation, San Leandro, CA). The DNA bands were excised and purified from the gel using the illustra GFX PCR DNA & Gel Band Purification kit (GE Healthcare, Buckinghamshire, UK) and eluted in sddH_2O. The concentration of the purified DNA was determined by loading 5-10 μL on a gel as described above, and the intensities of the bands were compared to the intensities of the known amounts of DNA in the bands of the HighRanger Plus 100 bp ladder (Norgen Biotech, Thorold, ON). The concentration was also confirmed by reading the absorbance at 260 nm using the NanoDrop ND-1000 spectrophotometer (NanoDrop Technologies, Wilmington, DE).

2.2.4.2. Ligation and transformation of Escherichia coli

Purified insert and vector DNA were ligated together with a 7:1 molar ratio of insert to vector in a 20 μL reaction volume. The ligation buffer was used at 1X with 1U of T4 DNA ligase (Invitrogen, Carlsbad, CA). The reaction was incubated at 14°C for 16 h in an MBS Satellite 0.2G thermal cycler (Thermo Electron Corporation, Milford, MA).

Subcloning efficiency DH5α *E. coli* competent cells were transformed with 2 μL of the ligation reaction (5-10 ng of DNA). The cells were mixed with the DNA and incubated on ice for 20 min followed by heat shock at 42°C for 45 s. The cells were incubated on ice for 2 min and then Luria-Bertani (LB) broth was added and the cells recovered at 37°C, shaking at 225 rpm for 1 h. The transformants were plated on LB/ampicillin (100 μg/mL) agar plates and colonies grew overnight at 37°C. Single colonies were picked to inoculate a 5 mL

LB/amp broth culture, which was grown at 37°C, shaking at 225 rpm for 16 h. Plasmid DNA was purified using the QiaPrep spin mini prep kit (Qiagen, Mississauga, ON).

2.2.5. Cloning IHH-N and creating lipid mutant controls

2.2.5.1. PCR amplification of IHH-N

The amino-terminal fragment of the *IHH* cDNA was amplified and a stop codon was introduced at the cleavage site to produce the IHH-N construct. The specifications for the Native *Pfu* Polymerase kit (Stratagene, La Jolla, CA) were followed, using 2.5U *Pfu* per reaction and the *Pfu* buffer at 1X. The template was 20 ng of pcDNA3.1.IHH^{WT} plasmid DNA, with 0.2 μM primers (IHH-N.F and IHH-N.R, see table 2.1) and 0.4 mM dNTPs. The PCR program consisted of one cycle at 95°C for 4 min, followed by 30 cycles of 30 s at 95°C; 1 min at 58°C; and 2 min at 72°C. The final 10 min elongation step was at 72°C.

2.2.5.2. Creation of IHH-N and IHH-N^{C28S} constructs

A flow chart in Figure 2.2 illustrates the experimental plan for creating the lipid mutant constructs. The PCR amplified IHH-N DNA was gel purified as described earlier. The purified IHH-N DNA and pcDNA3.1 plasmid DNA were digested with *Bam*HI and *Not*I followed by gel purification, ligation, and transformation into DH5α competent cells as described previously. Plasmid DNA was purified and verified by sequencing as described earlier. This process was repeated to create the IHH-N^{C28S} construct, except the template DNA for the PCR was the pcDNA3.1.IHH^{C28S} plasmid DNA to create a construct that contained both lipid mutations.

Figure 2.2. Flow chart of cloning the lipid mutant contructs. The plasmids used as templates for the PCR are listed in the coloured boxes, the details are listed in the white boxes (RE = restriction enzyme).

IHH-N:

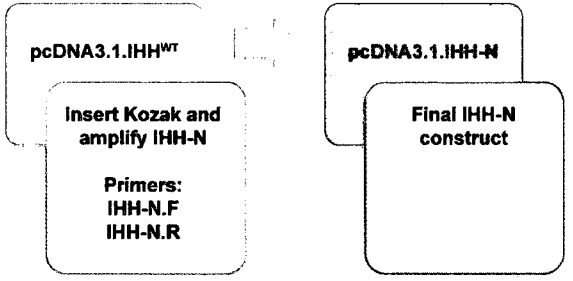

IHH^{C28S}:

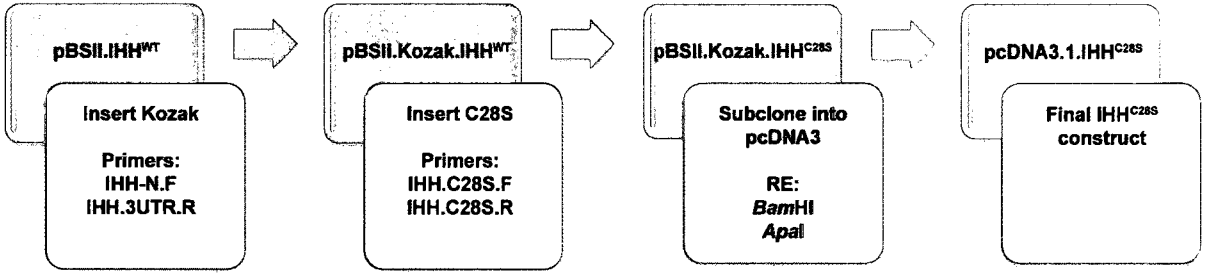

IHH-N^{C28S}:

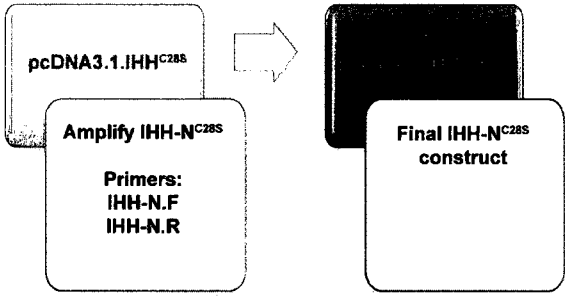

2.3. Results

The IHH^{P46L}, $IHH^{\Delta E95}$, IHH^{T130N}, and IHH^{T154I} mutations were successfully introduced into the full-length *IHH* cDNA and subcloned into pcDNA3.1 (Figure 2.3). Sequences were verified to ensure the correct mutation was introduced and no other mutations were caused by misincorporation during the PCR amplification. The lipid mutant constructs were successfully created and also confirmed by sequencing (Figure 2.4).

2.4. Discussion

We chose to use the full-length human cDNA of *IHH* for our mutant constructs so the final protein would have the proper lipid modifications. As discussed in the introduction, if only the *IHH-N* cDNA was used, the resulting protein would lack cholesterol. This produces a protein that is not tethered to the membrane as tightly and is easier to collect in the media of cells expressing the construct. However this does not accurately represent the natural state of IHH^{WT} so the dual lipid-modified constructs were made. We also chose a mammalian expression system for the same reasons, because although the constructs could be overexpressed and purified from *E. coli*, the resulting protein would lack both of the lipid modifications. The lipid-mutant constructs were created as controls and lack either one of the lipids or both (Figure 2.1).

The lipid mutant control constructs and $IHH^{\Delta E95}$ were created a year after the research project began. At this point it was noticed that the *IHH* mutant constructs did not contain a

Figure 2.3. Electropherograms of BDA1 and ACFD mutations in *IHH*. The top row of electropherograms show the induced mutation, while the bottom row shows the reference IHH^{WT} sequence. The dots indicate the mutated residues; the dot for the ΔE95 deletion is shown between residues, indicating the deletion of the second GAG codon.

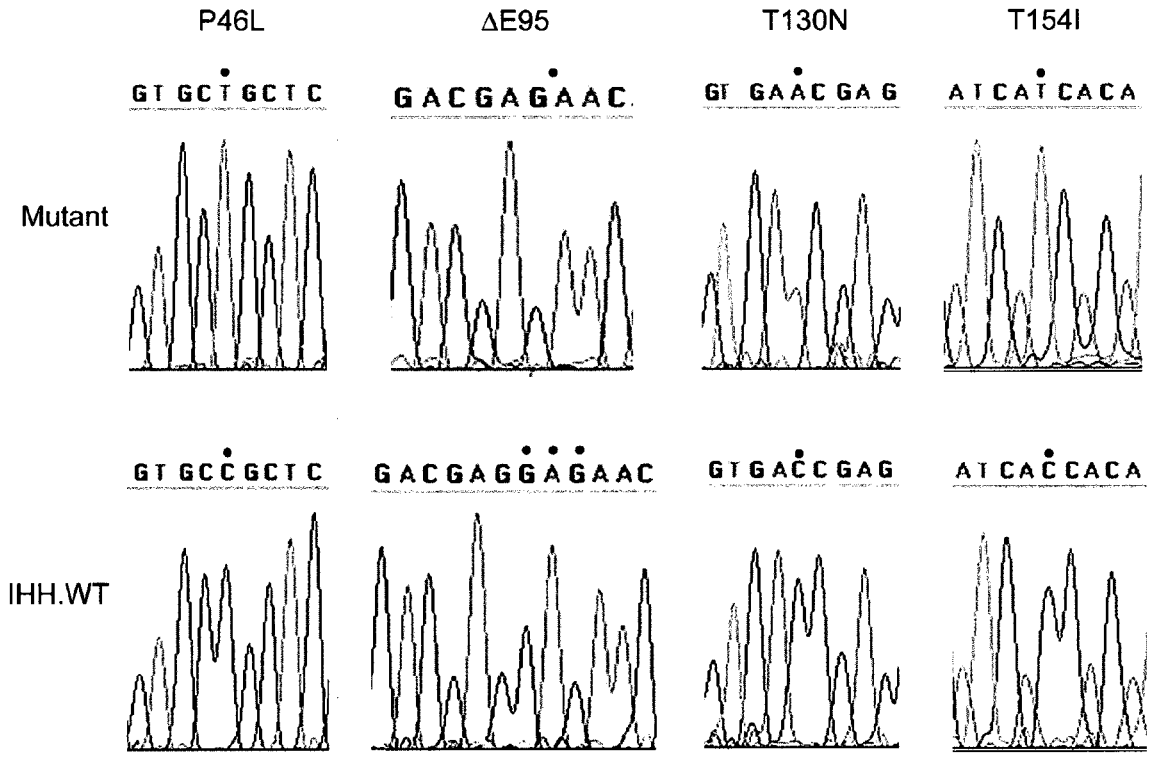
P46L
ΔE95
T130N
T154I
Mutant
IHH.WT

Figure 2.4. Electropherograms of the *IHH* lipid mutant constructs. In panel A, the top row of electropherograms show the induced mutation, while the bottom row shows the reference IHH^{WT} sequence. The dots indicate the mutated residues. The new stop codon (TAG) plus part of the *Not*I cloning site are shown for the IHH-N constructs. Both the p.C28S mutation (c.82T>A) and the IHH-N truncation are shown for the $IHH\text{-}N^{C28S}$ construct. Both the DNA and protein sequences are shown in panel B to illustrate the introduction of the premature stop codon to produce the IHH-N construct. The dot indicates the cleavage site in IHH^{WT}.

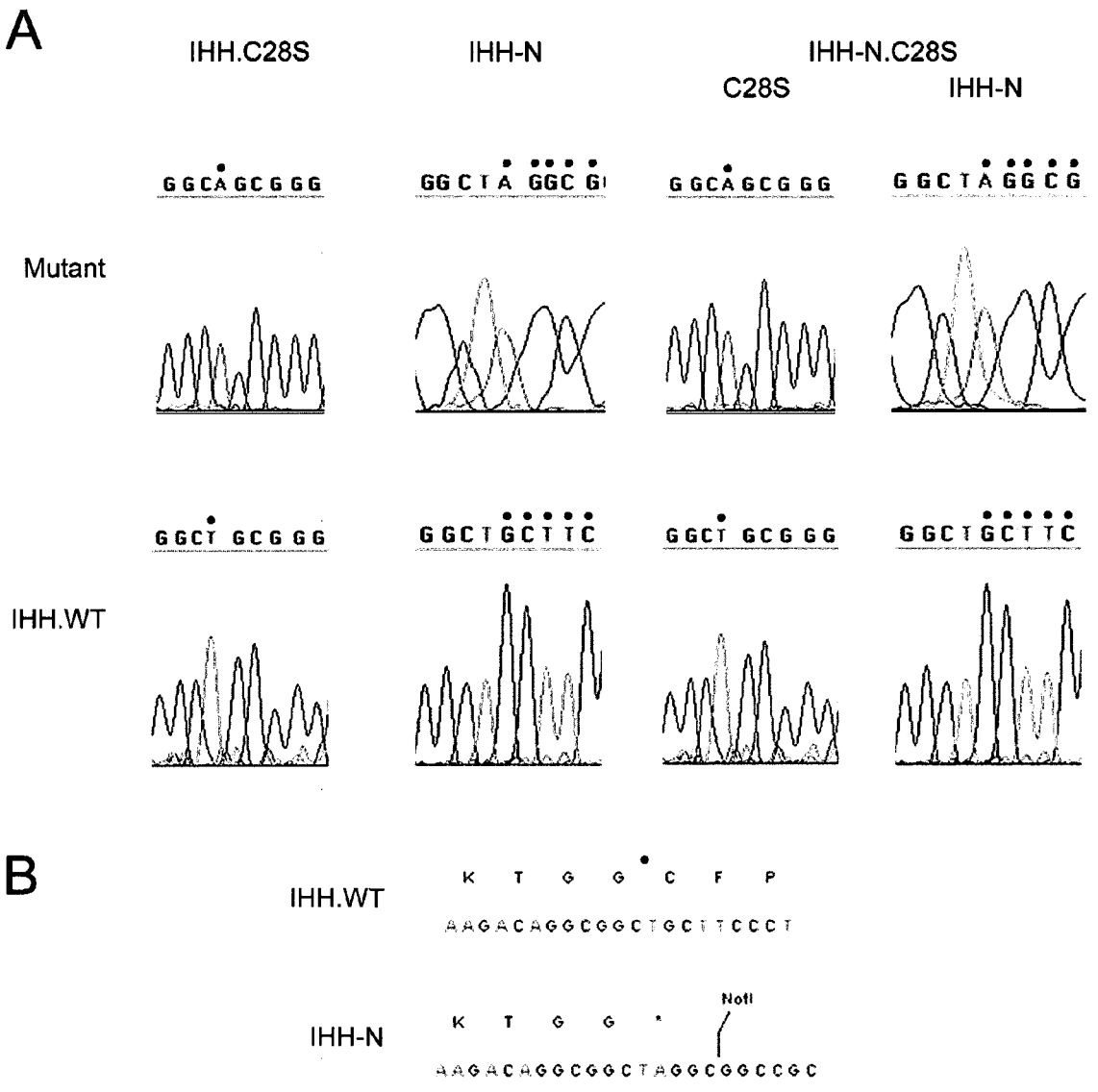
A
IHH.C28S
IHH-N
IHH-N.C28S
C28S
IHH-N
Mutant
IHH.WT
B
IHH.WT
K T G G C F P
AAGACAGGCGGCTGCTTCCCT
IHH-N
K T G G *
NotI
AAGACAGGCGGCTAGGCGGCCGC

Kozak sequence upstream of the start site. When the full-length human *IHH* cDNA was cloned by Graeme Cunningham, the *Bam*HI site was placed directly upstream of the start site, removing the endogenous Kozak sequence (5′-GCCGCC-3′) (Cunningham, 2008). At that point in the research project it was becoming apparent that expression of IHH protein in the HEK293 cell line tended to be low. In order to attempt to improve expression, this Kozak sequence was inserted into pBSII.IHH^{WT} for all future SDM constructs. For this reason, the IHH$^{\Delta E95}$ construct and the lipid mutant constructs all have a Kozak sequence, which could potentially improve expression of these constructs relative to the previous constructs that lack a Kozak sequence. However, this will not complicate the interpretation of the results because the assay data are always normalized to the stable expression level of IHH in each cell line, to account for differences in expression.

In summary, four new mutant constructs were successfully made to complete the panel of mutants to contain all known BDA1 and ACFD mutations at beginning of the research project. Three lipid mutant constructs were successfully created to act as controls. After the constructs were verified by sequencing they were ready to be transfected into various cell lines for the *in vitro* assays.

Chapter 3: *In vitro* models of chondrogenesis

3.1. Introduction

In vitro models of biological systems are useful tools for studying a particular protein or pathway of interest by decreasing the number of variables to consider as compared to *in vivo* models. However, there are always complications or limitations to *in vitro* models, and the challenge for culturing chondrocytes *in vitro* is the maintenance of the chondrocyte phenotype. After prolonged culture in monolayer, chondrocytes will undergo dedifferentiation into fibroblast-like cells (Stokes, Liu, et al, 2002).

In order to isolate a chondrogenic cell line, Atsumi *et al* first isolated a fibroblastic cell line (AT805) from mouse teratocarcinoma stem cells (Atsumi, Miwa, et al, 1990). They hoped to improve their chances of isolating a chondrogenic line by starting with a chondrogenic precursor-like line (fibroblastic) instead of trying to isolate chondrocytes that differentiate directly from a stem cell line. After clonal expansion of the AT805 cell line, they selected colonies that stained with the cationic dye Alcian blue, indicating the presence of cartilage. The cell line they isolated (ATDC5) grew beyond confluency when insulin was added to the media, and formed aggregates that looked like cartilage nodules and were stained with Alcian blue. The ATDC5 cell line has been well characterized and used in many studies as an *in vitro* model of chondrogenesis as it undergoes the many stages of chondrocyte differentiation, from condensation to hypertrophy and calcification (Atsumi, Miwa, et al, 1990; Chen, Fink, et al, 2005; Chen, Fink, et al, 2006; Shukunami, Ishizeki, et al, 1997). For this reason the ATDC5 line was chosen to be used in our studies because it

could be used to determine if the mutant IHH constructs interfere with the chondrogenic differentiation process.

Primary cultures are also a good *in vitro* model to use as they are isolated directly from the tissue of interest. Mouse embryonic limb bud mesenchymal cells (LBMCs) can be harvested at day E11.5 to act as chondrogenic precursors *in vitro* (Ahrens, Solursh, and Reiter, 1977). In order to preserve the chondrocyte gene expression profile and phenotype, the cells must be cultured at high density such as in a micromass culture (Mello, and Tuan, 1999; Stokes, Liu, et al, 2002). A micromass culture enables the precursor cells to differentiate into chondrocytes as it mimics the density of chondrocytes at the condensation stage of bone development. The cells are plated at a high concentration (2×10^7 cells/mL) as a drop on a dry tissue culture plate and allowed to adhere before media is added, resulting in a ball-like culture with the cells sitting upon each other (Ahrens, Solursh, and Reiter, 1977). This creates a 3D culture environment for the cells (compared to a 2D monolayer) increasing intercellular interactions and inducing chondrocyte differentiation. This method is another way to test if mutant IHH signaling interferes with the differentiation process.

3.2. Materials and Methods

3.2.1. ATDC5

3.2.1.1. ATDC5 culture and transfection

The ATDC5 cell line was obtained from the RIKEN cell bank (Ibaraki, Japan) and cultured in a 1:1 ratio of Dulbecco's Modified Eagle medium (DMEM) and F12-HAM Nutrient Mixture (Sigma-Aldrich, Oakville, ON) containing 1% GlutaMAX (Gibco,

Invitrogen, Carlsbad, CA), 1% penicillin/streptomycin (Gibco, Invitrogen, Carlsbad, CA) and 5% fetal bovine serum (FBS, Sigma-Aldrich, Oakville, ON). Cells were grown at 37°C with 5% CO_2 in plasticware from Corning Life Science (Corning, NY).

ATDC5 cells were transfected with the *IHH* plasmid DNA using the SuperFect transfection reagent (Qiagen, Mississauga, ON) at a ratio of 1 μg DNA to 2 μL SuperFect. Twenty-four hours prior to transfection, 4×10^4 cells were plated in each well of a 24-well plate. A dilution of 400 ng of plasmid DNA in 150 μL Opti-MEM (Invitrogen, Carlsbad, CA) was made and 0.8 μL of SuperFect was added. This mixture was incubated for 10 min at room temperature (RT) to allow the DNA-SuperFect complexes to form. Media was aspirated from the cells, and the cells were washed once with phosphate-buffered saline (PBS). Five hundred microlitres of media was added to the SuperFect/DNA mixture and this was added to the cells. The transfection mixture was incubated on the cells at 37°C with 5% CO_2 for 4 h, and then aspirated and the cells were washed three times with PBS. Fresh media was added to each well and the cells were grown for 48 h before being treated with trypsin to detach the cells. One quarter of the cells were plated in a 10 cm dish to allow for isolated colonies under selection of 400 μg/mL G418 (Sigma-Aldrich, Oakville, ON). The media was changed every 2-3 days and colonies were transferred to individual wells of a 24-well plate after 10-14 days. Once they reached ~80% confluency they were transferred to a well in a 6-well plate, and then to a 10 cm plate. After the 10 cm plate reached ~80% confluency, the cells were frozen in growth media without G418 and supplemented with 20% FBS and 10% dimethyl sulfoxide (DMSO). Cells were transferred to liquid nitrogen for long term storage.

3.2.1.2. Preparation of ATDC5 cell lysates

Cells were removed from the tissue culture plate using a cell scraper and were pelleted for 2 min at 10 000 ×g. They were then resuspended in a sonication buffer composed of 100 mM Tris-HCl, 0.1% NP-40, and a protease inhibitor cocktail tablet (Roche, Basel, Switzerland). Cells were sonicated in an ice water bath for three cycles of 9.9 s on/off using a Vibra cell sonicator (Sonics & Materials, Danbury, CT). Unlysed cells were then pelleted for 20 min at 10 000 ×g and discarded, while the supernatant was retained for analysis. Total protein concentration of the cell lysates was determined by Bradford assay, using the Bio-Rad Protein Assay Dye Reagent Concentrate (Bio-Rad Laboratories, Hercules, CA). Cell lysates were used immediately or stored at -20°C until required.

3.2.1.3. Western blot analysis of cell lysates

Protein samples to be analyzed (30-50 μg total cell protein) were combined with 5X Laemmli Running Buffer to a final (1X) concentration of 60 mM Tris-HCl (pH 6.8), 2% SDS, 0.01% bromophenol blue, 4% β-mercaptoethanol, and 10% glycerol and boiled at 95°C for 5 min. Samples were subsequently loaded into each well of a 12% SDS-polyacrylamide gel, along with 10 μL of the Precision Plus Protein™ Standards Dual Color ladder (Bio-Rad Laboratories, Hercules, CA) and subjected to electrophoresis at 100 V for 2 h in a Mini Protean 3 cell (Bio-Rad Laboratories, Hercules, CA) with a running buffer containing 25 mM Tris, 192 mM glycine, and 0.1% SDS.

The protein was transferred to Immobilon-P polyvinylidene difluoride (PVDF) membrane (Millipore, Billerica, MA) using a Mini Trans-Blot Cell (Bio-Rad Laboratories, Hercules,

CA) in a buffer consisting of 25 mM Tris, 192 mM glycine, and 0.025% SDS, set at a constant voltage of 50 V for 50 min.

PVDF membranes containing transferred protein were blocked in 5% milk supplemented with 1% FBS (Sigma-Aldrich, Oakville, ON) in 1X Tris-Borate saline Tween-20 (TBST) containing 25 mM Tris-HCl pH 7.4, 2.7 mM KCl, 150 mM NaCl, 0.05% Tween-20. Membranes were blocked at RT for 1 h. The membranes were probed with a rabbit polyclonal anti-Shh-N (H-160) antibody (Santa Cruz, Santa Cruz, CA) at a dilution of 1:2 000 in blocking solution (5% milk, 1% FBS in 1X TBST). The membranes were left to incubate with the primary antibody overnight at 4°C. The membranes were then washed five times for 10 min each at RT with TBST to remove unbound primary antibody. The membranes were probed with a horse-radish peroxidase-conjugated goat anti-rabbit IgG (Bethyl Laboratories, Montgomery, TX) in 5% milk in TBST at a dilution of 1:20 000 for 45 min at RT. The 10 min TBST washes were repeated five times followed by a 10 min wash with TBS (no Tween-20) prior to detection. The secondary antibody was detected using the Amersham ECL Plus Western Blotting Detection System (GE Healthcare, Buckinghamshire, UK). The treated membranes were covered in saran wrap and exposed Kodak X-OMAT Blue XB-1 film (Kodak, Rochester, NY). The film was developed using the SRX-101A tabletop processor (Konica Minolta, Mississauga, ON).

3.2.2. Primary chondrocyte cultures

3.2.2.1. Mouse embryonic limb bud mesenchymal extraction

All animal work followed procedures approved by the University of Ottawa Animal Care Committee. C57BL/6 mice were mated and the resulting embryos were obtained at E11.5.

The limb buds were clipped off using forceps and washed twice with sterile PBS followed by digestion in 0.5% trypsin, 0.1% collagenase IV in PBS at 37°C for 20 min. The cells were gently mixed to create a single cell suspension, and growth media (DMEM with 10% FBS, 1% GlutaMAX, and 1% pen/strep) was added to inactivate the enzymes. The cells were pelleted at 90×g for 5 min in an Allegra X15-R swinging bucket centrifuge (Beckman Coulter, Fullerton, CA) and resuspended in growth media before filtering through a 70 μm nylon cell strainer (Falcon, BD Biosciences, Bedford, MA).

3.2.2.2. Micromass culture and transfection

The cells were counted and adjusted to a concentration of 1×10^7 cells/mL. Next, 20 μL drops (containing 2×10^5 cells) were spotted onto dry wells of a 6-well plate and allowed to attach for 2 h at 37°C with 5% CO_2. After the cells adhered, they were transfected with the *IHH* plasmids using the cationic lipid transfection reagent Lipofectamine (Invitrogen, Carlsbad, CA). A 4:1 ratio of Lipofectamine to DNA was used. 20 μL of Lipofectamine was diluted in 250 μL Opti-MEM (Invitrogen, Carlsbad, CA) and incubated at RT for 5 min. Five micrograms of plasmid DNA was diluted in 250 μL Opti-MEM and added to the Lipofectamine dilution. The DNA/lipid complexes were allowed to form at RT for 20 min before adding to the cells with 2 mL of growth media. The mixture was incubated on the micromass cultures for 3 h at 37°C with 5% CO_2. The pEGFP-N1 expression plasmid (Clonetech) was transfected as a control, and EGFP expression was visualized after 35-40 h using an Axiovert S100 inverted microscope (Zeiss). Forty-eight hours post-transfection, the media was supplemented with 25 μg/mL L-ascorbic acid, 1 mM $CaCl_2$, and 4 mM KH_2PO_4. The media was changed every two days.

3.2.2.3. Alcian blue staining

After seven days in culture, the micromass cultures (transfected with the mutant *IHH* constructs) were stained with Alcian blue. The media was aspirated and the cells were washed three times in PBS. The cells were then fixed in 4% paraformaldehyde (PFA) in PBS for 5 min at RT followed by two washes with PBS. The cells were stained in 0.1% Alcian Blue 8GX (Sigma-Aldrich, Oakville, ON) for 2 h at RT and then rinsed three times in ddH_2O. The cells were photographed in ddH_2O using the Axiovert S100 inverted microscope (Zeiss).

3.3. Results

3.3.1. Attempts to create ATDC5 cell lines stably expressing IHH

ATDC5 were transfected with the mutant *IHH* constructs and G418 was used to select for clones with stable expression. Cell lysates were prepared after approximately five weeks, which was the length of time it took for the single clones to expand to have enough cells for the cell lysates and also to freeze stocks for long term storage in liquid nitrogen. The cell lysates were analyzed by western blot to screen clones for IHH expression, however none of the G418 resistant clones expressed IHH at a level detectable by western blot.

The control vector pEGFP-N1 (containing EGFP under the control of the CMV promoter) was transfected into ATDC5, and the transfected cells were selected with G418. However after two weeks in culture, the cells that had originally been positive for EGFP no longer had visibly detectable EGFP expression under 488 nm light using the Zeiss Axiovert S100 inverted microscope (Figure 3.1).

Figure 3.1. Decrease in EGFP expression in ATDC5 transfectants over time. ATDC5 cells transfected with pEGFP-N1 are shown 24 h and two weeks post transfection. G418 selection was maintained, however expression of EGFP was no longer detected after two weeks in culture.

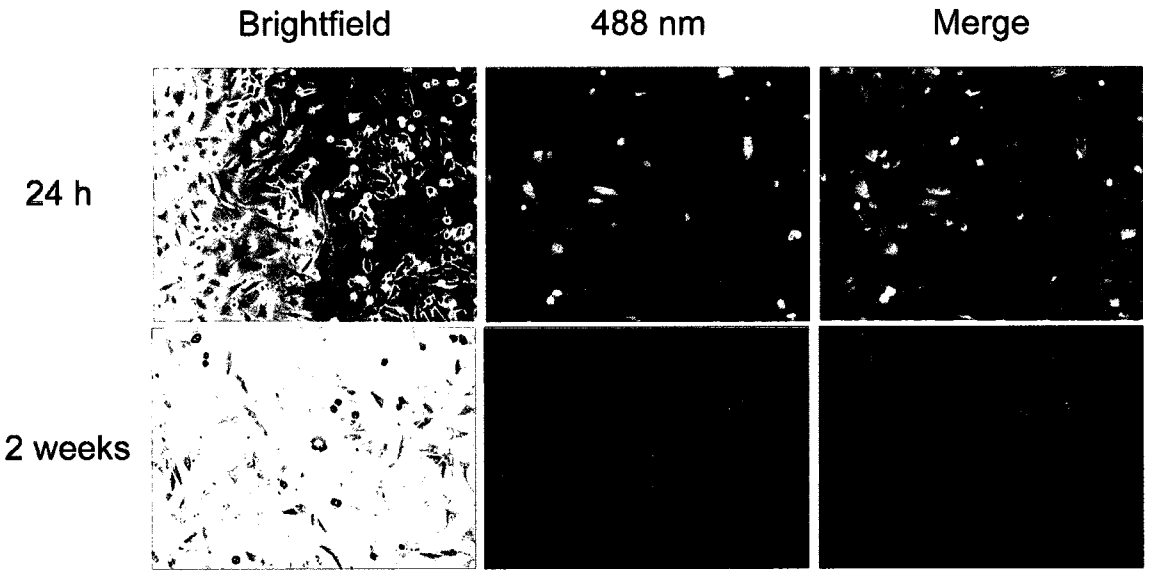
Brightfield
488 nm
Merge
24 h
2 weeks

3.3.2. Attempts to transfect mouse embryonic limb bud mesenchymal cells

The limb bud mesenchymal cells were successfully extracted and micromass cultures were established. The pEGFP-N1 vector was transfected into the primary cells as a control and EGFP expression was visualized under 488 nm light with the Axiovert S100 inverted microscope (Zeiss). Transfection efficiency was estimated to be 1% for the first transfection, but this was improved to 13% in future transfections (Figure 3.2). The micromass cultures were transfected with each of the mutant IHH constructs and grown for 7 days before staining with Alcian blue (Figure 3.3) to detect the presence of cartilage nodules. However, Lipofectamine transfection appeared to be toxic to the cells, as most of the cultures were not healthy post-transfection. The intensity of Alcian blue staining appeared to be correlated with the health and density of each culture.

3.4. Discussion

3.4.1. Long term expression of IHH in ATDC5 cells was never attained

No clones expressing IHH were recovered when they were screened five weeks post transfection. Even though G418 selection was maintained, none of the G418-resistant clones expressed IHH at a level detectable by western blot. This suggests that we were selecting for clones that had little to no expression of IHH. A G418-resistant clone that does not express IHH could be the result of a disruption of the *IHH* gene or the CMV promoter upon integration of the plasmid into the ATDC5 genome (Figure 3.4). Since integration of the plasmid into the chromosome is a random event (Murnane, Yezzi, and Young, 1990) it is

Figure 3.2. Micromass cultures of primary mouse embryonic limb bud mesenchymal cells transfected with pEGFP-N1. The micromass culture is shown at 25X to show the entire culture and the even distribution of transfected cells across the surface. The 200X magnification illustrates the low transfection efficiency, estimated to be 13%.

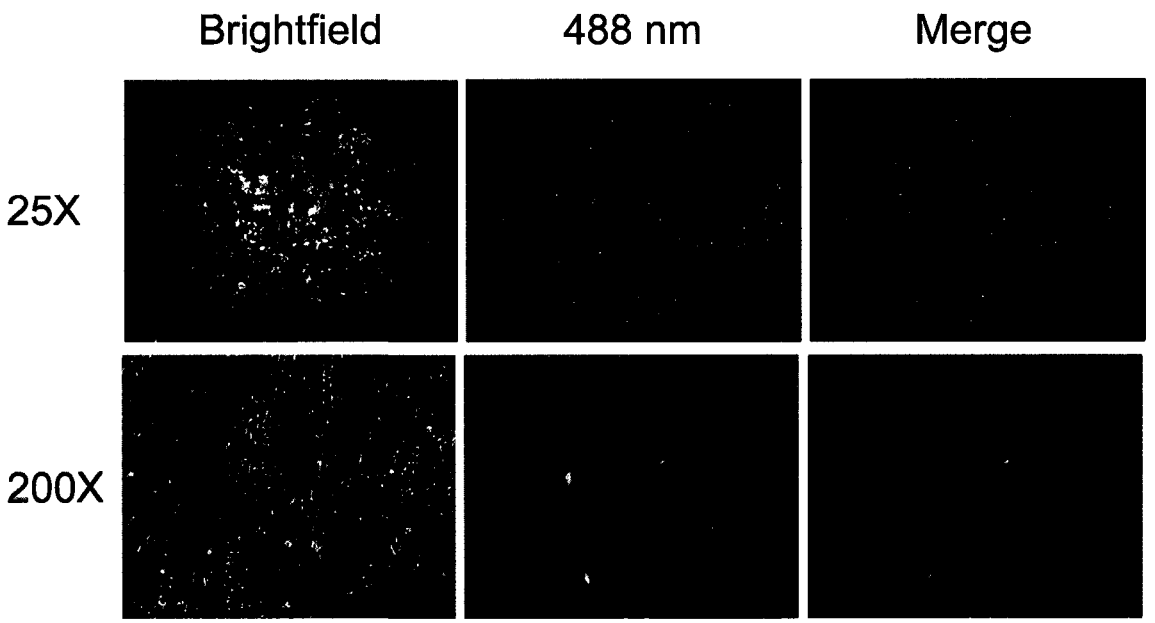
Brightfield
488 nm
Merge
25X
200X

Figure 3.3. Alcian blue staining of primary mouse embryonic limb bud mesenchymal cell micromass cultures. Micromass cultures transfected with each of the mutant *IHH* constructs were stained with Alcian blue after 7 days in culture. Cells are shown under 100X magnification with brightfield illumination. Alcian blue is a cationic dye that binds to the negatively charged glycosaminoglycans in the cartilage ECM which is produced by chondrocytes. The number of cartilage nodules (and the intensity of Alcian blue staining) appears to be correlated with the health (and density) of the micromass cultures, and not necessarily a result of mutant *IHH* expression.

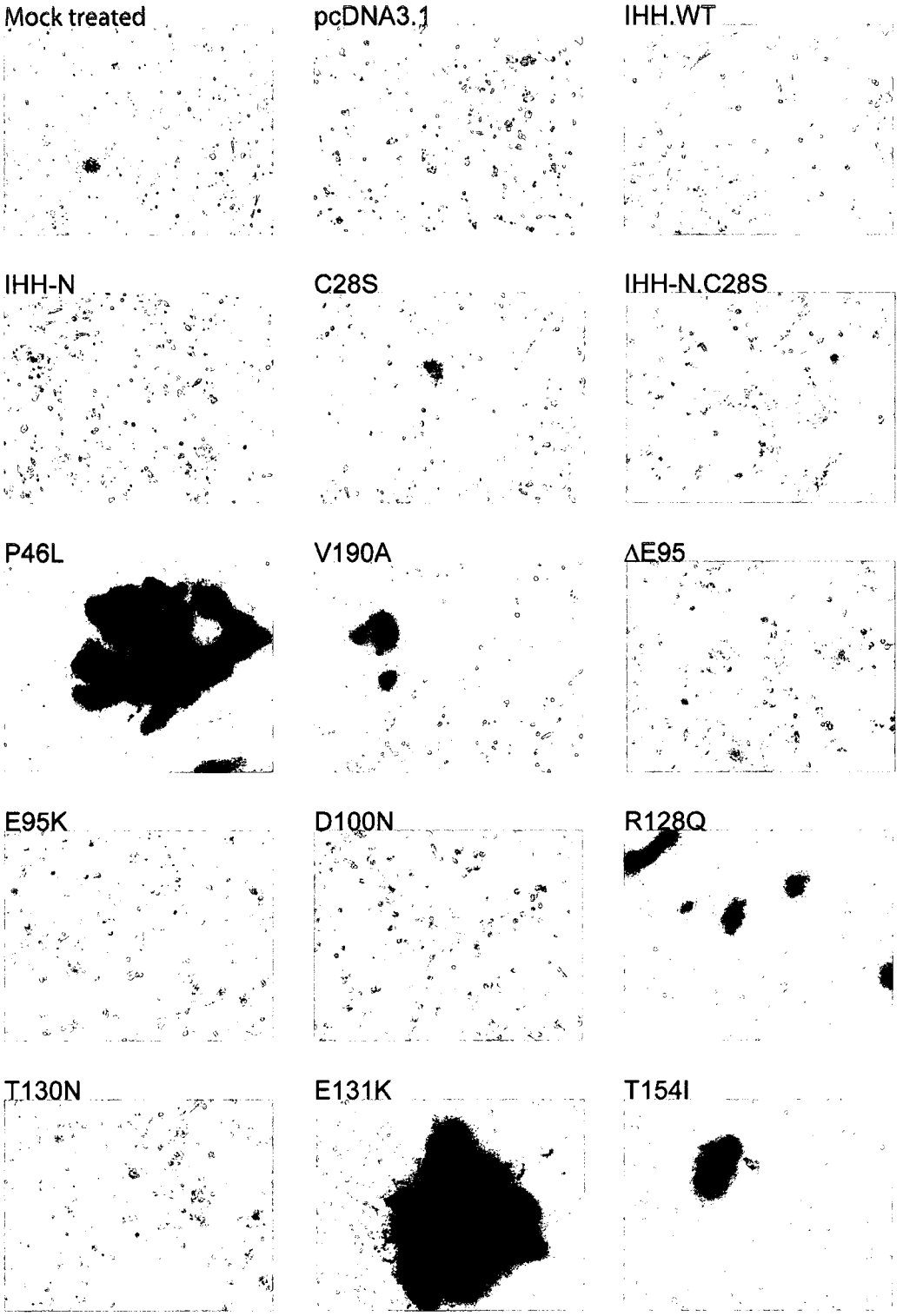
Mock treated
pcDNA3.1
IHH.WT
IHH-N
C28S
IHH-N.C28S
P46L
V190A
ΔE95
E95K
D100N
R128Q
T130N
E131K
T154I

Figure 3.4. Illustration of possible gene and promoter disruptions when the *IHH* plasmid constructs integrate into the ATDC5 genome. Disruption of either the CMV promoter (purple) or *IHH* (blue) can occur during the generation of a stable clone due to random integration of the plasmid into the transfected cells genome. The red dash indicates the break point in the plasmid, and the resulting linearized integrated plasmid is shown to the right, flanked by the transfected cells genome (in red). *IHH* is disrupted in panel A and the CMV promoter is disrupted in panel C. Panel B represents an integration event where both CMV and *IHH* remain intact and would likely result in *IHH* expression.

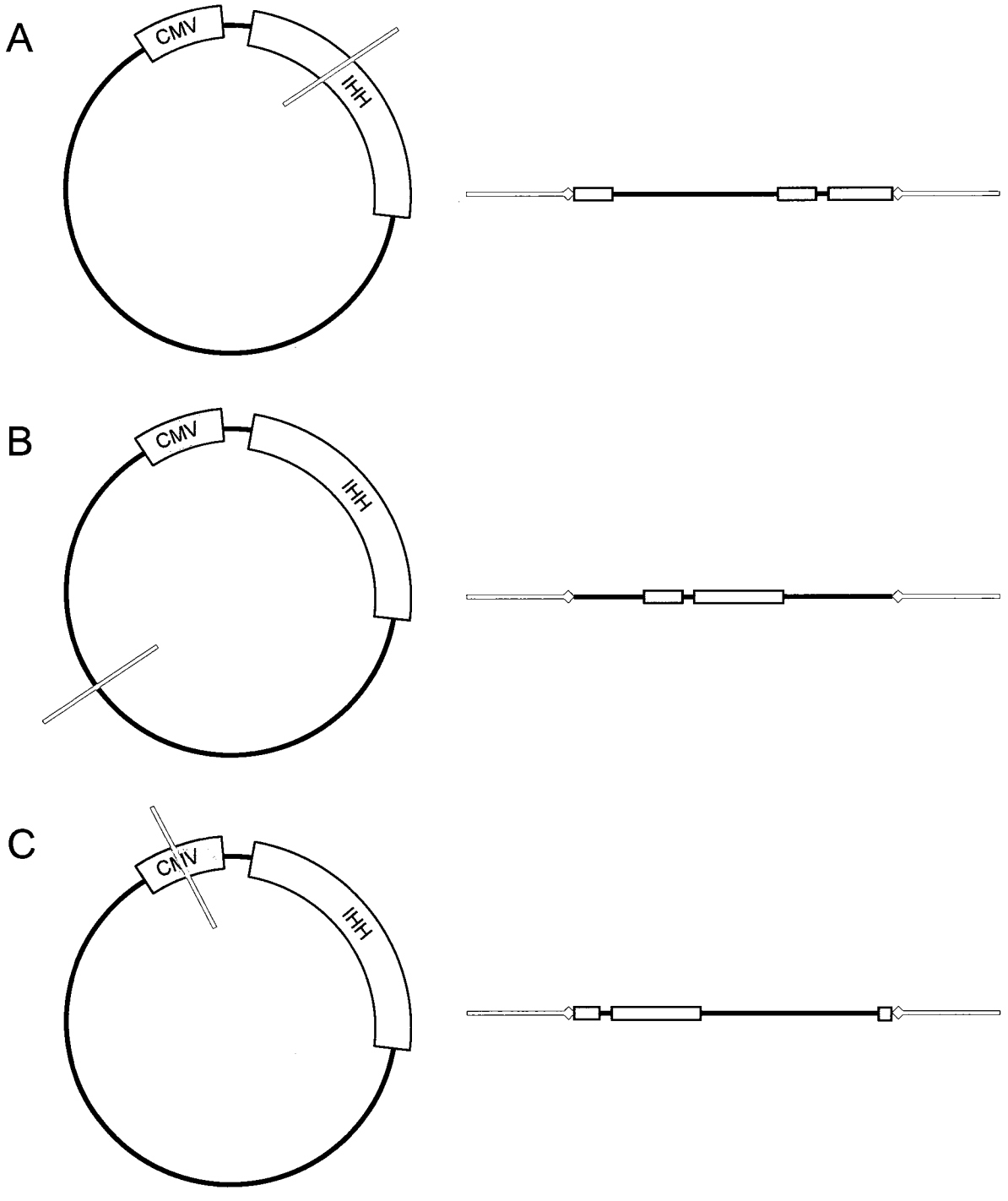
A
CMV
IHH
B
CMV
IHH
C
CMV
IHH

possible that the *IHH* gene or CMV promoter are disrupted during integration, resulting in clones with little or no expression. Also, if expression of *IHH* is toxic to the ATDC5 chondroprogenitor line, then selecting with G418 would likely select for clones that have silenced the *IHH* gene. Despite multiple attempts to stably express IHH in ATDC5 cells, long term expression was never attained. In the interest of time, the establishment of the ATDC5 stable lines was no longer pursued.

3.4.2. Low transfection efficiency of micromass cultures

Transfection of the micromass cultures was challenging because the cationic lipid transfection reagent Lipofectamine (Invitrogen, Carlsbad, CA) has been optimized for use on a monolayer culture, but the limb bud mesenchymal cells would not differentiate into chondrocytes if they were plated as a monolayer culture (Mello, and Tuan, 1999; Stokes, Liu, et al, 2002). The cell line ATDC5 was used to optimize micromass culture transfection before attempting to transfect the primary cells. Plating the micromass culture and transfecting 24 h later resulted in low transfection efficiency with only the cells on the periphery of the culture expressing EGFP. Transfection efficiency was improved (with a more even distribution of transfected cells on the surface of the culture) when the cells were transfected 2 h after plating (Figure 3.5).

Transfection of the primary micromass culture had similar results but with decreased transfection efficiency, as expected since primary chondrocytes are notorious for being difficult to transfect (Goomer, Deftos, et al, 2001; Qureshi, Ahmad, and Zafarullah, 2008). Other options included electroporation and nucleofection, however they required a large

Figure 3.5. Optimization of the transfection of micromass cultures. ATDC5 was used to optimize the transfection of micromass cultures. The cultures were plated and transfected either 24 h or 2 h after plating. Cells are under 25X magnification to show the distribution of transfected cells on the surface of the micromass culture. Transfecting the cells 24 h after plating resulted in a ring of transfected cells at the periphery of the micromass culture and low transfection efficiency at the centre. Transfecting the cells 2 h after plating yielded the best results with an even distribution of transfected cells across the entire surface of the micromass culture.

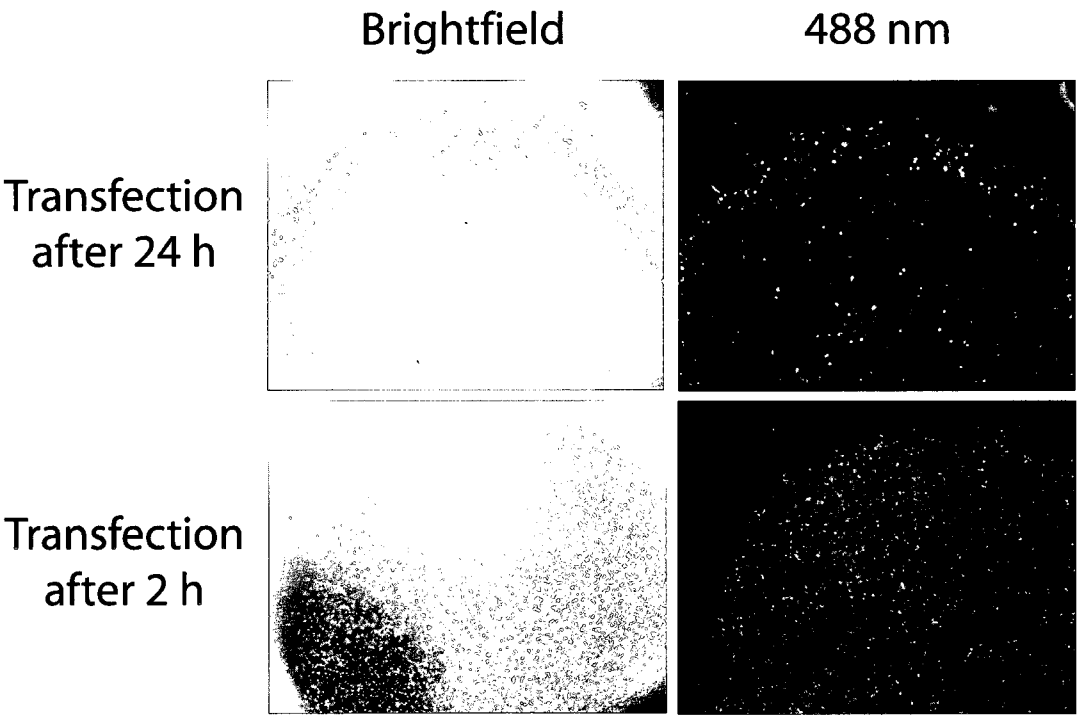
Brightfield
488 nm
Transfection after 24 h
Transfection after 2 h

number of cells. Electroporation required 80X as many cells as Lipofectamine because of the cell density and the volume required for the cuvette, in addition, half of the cells die during the procedure (DeLise, and Tuan, 2000). Nucleofection (Lonza, Cologne, Germany) was also considered as an alternative; however the enormous amount of cells needed for the optimization of the protocol was a limitation. As a future direction, the best approach may be to subclone the mutant *IHH* constructs into a retroviral vector to infect the micromass cultures (Carlberg, Pucci, et al, 2001).

Despite the low transfection efficiency, the transfected micromass cultures were stained with Alcian blue after seven days in culture to assess the degree of chondrocyte differentiation. However, the health of each culture was variable and the intensity of Alcian blue staining was correlated to the density of the cultures. This is evident as the mock treated culture has multiple Alcian blue positive cartilage nodules while the IHH^{WT} transfected culture has none (Figure 3.3). It was expected that the culture transfected with IHH^{WT} would have intense Alcian blue staining as a result of increased proliferation induced by IHH signaling. The inconsistency of health between cultures suggests that Lipofectamine is not the ideal method of transfection for these primary cells. Perhaps switching to a retroviral system is needed to first improve the transfection before continuing the characterization of mutant *IHH* expression in the *in vitro* chondrogenesis models.

Chapter 4: Characterization of mutations in *IHH*

4.1. Introduction

4.1.1. HEK293 cell line

The HEK293 cell line was chosen for stable IHH expression to avoid the difficulties encountered when attempting to overexpress IHH in a chondrogenic line as discussed in the previous chapter. The HEK293 cell line was established by Frank Graham in 1977 by transforming human embryonic kidney (HEK) cells with sheared human adenovirus type 5 (Ad5) DNA (Graham, Smiley, et al, 1977; Thomas, and Smart, 2005). This cell line is a popular choice when deciding on a mammalian expression system because the cells are easy to transfect and drive robust expression of the gene of interest when it is under the control of the CMV promoter (such as the IHH constructs in pcDNA3.1+). Other groups have successfully transfected HEK293 cells with SHH constructs which resulted in successful overexpression and secretion of the protein (Chen, Ren, et al, 2004; Couvé-Privat, Le Bret, et al, 2004; Singh, Tokhunts, et al, 2009; Traiffort, Dubourg, et al, 2004). For these reasons, the HEK293 cell line was chosen as an expression system for the IHH mutant constructs to generate high levels of protein for use in the *in vitro* assays.

4.1.2. Defects in IHH biogenesis

We wanted to determine the specific defect caused by each individual mutation to elucidate the role of certain residues in the function of the IHH protein. The mutations can be interfering in any one of the many steps of IHH biogenesis such as translation, autocleavage, post-translational modification (PTM), secretion, multimerization/trafficking,

and receptor binding. If a mutation interferes with the autocleavage reaction, we would expect to see an accumulation of full-length IHH (45 kDa on a western blot) relative to the cleaved IHH-N (19 kDa) when compared to the normal rate of cleavage of IHH^{WT}. Secretion may also be affected by mutations in IHH, which could be assessed by comparing the relative levels of IHH in the conditioned media (normalized to the level of IHH in the cell lysate) to IHH^{WT} as well.

The relative activity of the mutant IHH proteins compared to IHH^{WT} can be determined using an *in vitro* activity assay, such as the SHH-Light II system (Chen, Taipale, et al, 2002; Taipale, Chen, et al, 2000) . The SHH-Light II cell line was established by transfecting NIH/3T3 cells with a Gli-responsive firefly luciferase and a constitutively active *Renilla* luciferase (Chen, Taipale, et al, 2002; Taipale, Chen, et al, 2000). In the presence of active IHH-N, firefly luciferase is expressed and quantified using a luminometer. The constitutively active *Renilla* luciferase is used as an internal control to normalize for cell density and the resulting relative activity was compared to IHH^{WT}. The above *in vitro* assays aim to elucidate the specific defect each mutation confers during IHH biogenesis.

4.2. Materials and Methods

4.2.1. HEK293 culture and transfection

The human embryonic kidney (HEK) 293 cell line was generously donated by Dr. Robin Parks, Ottawa Hospital Research Institute (OHRI). The HEK293 cells were cultured in Minimal Essential Medium (MEM) with Earle's Balanced Salt Solution (EBSS) supplemented with 10% fetal bovine serum (FBS, Sigma-Aldrich, Oakville, ON), 1%

GlutaMAX (Gibco, Invitrogen, Carlsbad, CA), and 1% penicillin/streptomycin (Gibco, Invitrogen, Carlsbad, CA). Cells were grown at 37°C with 5% CO_2 in plasticware from Corning Life Science (Corning, NY).

HEK293 cells were transfected with the *IHH* plasmid DNA using the cationic lipid transfection reagent Lipofectamine (Invitrogen, Carlsbad, CA) at a ratio of 1 μg DNA to 2.5 μL Lipofectamine. Twenty-four hours prior to transfection, 4×10^4 cells were plated in each well of a 24-well plate. A dilution of 2 μL of Lipofectamine in 50 μL Opti-MEM (Invitrogen, Carlsbad, CA) was made and incubated at 5 min at RT while 800 ng of plasmid DNA was diluted in 50 μL Opti-MEM. The two dilutions were mixed together and this mixture was incubated for 20 min at RT to allow the DNA/lipid complexes to form. The transfection mixture was added to the cells in 500 μL growth media and incubated for 3 h at 37°C with 5% CO_2. The media was later aspirated and the cells were washed three times with PBS. Fresh media was added to each well and the cells were grown for 48 h before being treated with trypsin to detach the cells.

Half of the cells were plated in a 15 cm dish to allow for isolated colonies under selection with 400 μg/mL G418 (Sigma-Aldrich, Oakville, ON). The media was changed every 2-3 days and colonies were transferred to individual wells of a 24-well plate after 10-14 days. Once they reached ~80% confluency they were transferred to a well in a 6-well plate, and then to a 10 cm plate. After the 10 cm plate reached ~80% confluency, the cells were frozen in growth media supplemented with 10% dimethyl sulfoxide (DMSO). Cells were transferred to liquid nitrogen for long term storage.

4.2.2. Preparation of cell lysates

Protocol was followed as in section 3.2.1.2 except RIPA buffer was used to lyse the cells (50 mM Tris-Cl pH 7.5, 150 mM NaCl, 1% NP-40, 0.5% DOC, 0.1% SDS) supplemented with one protease inhibitor cocktail tablet dissolved per 10 mL of buffer (complete, Mini, EDTA-free protease inhibitor cocktail tablet, Roche, Basel, Switzerland).

4.2.3. Western blot analysis of cell lysates

See section 3.2.1.3 for methods. The mouse monoclonal anti-β-actin antibody was used at a 1:10 000 dilution with the goat anti-mouse HRP-conjugated secondary antibody at a dilution of 1:7 500. Densitometry measurements were made using the AlphaImager with the SpotDenso application in the AlphaEase®FC v6.0.0 software (Alpha Innotech Corporation, San Leandro, CA). The mean and standard error were calculated from measurements taken from three separate blots. The significance of the difference between mutant and IHH^{WT} processing was calculated using the two-sample *t*-test assuming unequal variance (Excel 2003, Microsoft Corp., Seattle, WA).

4.2.4. Concentration of conditioned media

Conditioned media (CM) from the HEK293[IHH] stable cell lines was concentrated to attempt to visualize IHH using western blot analysis. Cells and debris in the CM were pelleted at 2851×g for 5 min using the Allegra X15-R swinging bucket centrifuge (Beckman Coulter, Fullerton, CA). Media was concentrated 100X (from 50 mL to 500 μL) using the Amicon Ultra Centrifugal filter devices with a 10 MWCO pore size. This allowed the excess

liquid (and proteins smaller than 10 kDa) to flow through the filter, while both IHH species (19 kDa and 45 kDa) were retained.

4.2.5. SHH-Light II luciferase assay

The hedgehog-responsive cell line SHH-Light II was generously donated by Dr. Valerie Wallace (OHRI). The cells were cultured in DMEM (Sigma-Aldrich, Oakville, ON) supplemented with 10% FBS (Sigma-Aldrich, Oakville, ON), 2% GlutaMAX (Gibco, Invitrogen, Carlsbad, CA), 1% penicillin/streptomycin (Gibco, Invitrogen, Carlsbad, CA), 0.15 mg/mL Zeocin (Invitrogen, Carlsbad, CA), and 0.4 mg/mL G418. The SHH-Light II cells were plated in excess in a 3:1 co-culture with the HEK293[IHH] stable cell lines. A total of 4×10^4 cells were plated in each well of a 96-well plate (3×10^4 SHH-Light II and 1×10^4 HEK293[IHH] cells). The cells were grown in DMEM media with 0.5% FBS for 48 h prior to the luciferase assay.

The Dual-Luciferase® Reporter assay system (Promega Corp, Madison, WT) was used and the manufacturer's protocol was followed except for the few changes listed here. Thirty microlitres of Passive Lysis Buffer (PLB) was added to each well and the cells were lysed at RT for 2 h. The cell lysates were transferred from the 96-well plate into 5 mL polystyrene round bottom tubes (Falcon, BD Biosciences, San Jose, CA). The LumatLB 9507 luminometer (EG&G Berthold, Bad WildBad, Germany) was used for the injections of the reagents and to quantify the level of luciferase expression. One-hundred microlitres of Luciferase Assay Reagent (LARII) was injected, followed by a 2 s delay and a 10 s measurement of firefly luciferase expression. Next, 100 µL of Stop&Glo® 1X substrate was injected, followed by a 2 s delay and a 10 s measurement of *Renilla* luciferase expression.

The firefly luciferase reading was divided by the *Renilla* luciferase reading for each sample to account for differences in cell number. There were always six replicates per sample in each experiment, and each experiment was repeated at least three times. The positive and negative controls (HEK293[IHH^{WT}] and HEK293[pcDNA3], respectively) were repeated in every experiment and the activity of each mutant IHH was normalized to the IHH^{WT} for each experiment before determining the standard error across a minimum of three experiments. Significant differences between the mutants and IHH^{WT} were calculated using the two-sample *t*-test assuming unequal variance (Excel 2003, Microsoft Corp.).

4.2.6. ELISA

Cells were counted and 6×10^5 cells were plated per 6 cm plate. The cells were grown to confluency over a 48 h time period prior to collection of conditioned media and cell lysis (the lysis protocol in section 4.2.3 was followed). Cells and debris in the CM were pelleted at 2851×g for 5 min using the Allegra X15-R swinging bucket centrifuge (Beckman Coulter, Fullerton, CA). The manufacturer's protocol was followed for the mouse Shh DuoSet ELISA kit (R&D systems, Minneapolis, MN). Standard curves were measured using the recombinant mShh (included in the kit), the IHH^{WT} cell lysate, and the IHH^{WT} conditioned media to determine the optimal amount of cell lysate and CM to maintain the absorbance readings within the accurate range. Using the standard curves, it was determined that 15 µg of cell lysate and 15 µl of conditioned media were the best amounts to analyze for each cell line. The absorbance at 450 nm and 540 nm (for correction) was read using the SPECTRAmax 190 ROM version 3.12 plate reader (Molecular Devices Corp, Sunnyvale, CA).

4.3. Results

4.3.1. Establishment of HEK293 cell lines stably expressing the IHH mutants

The stable cell lines were successfully established, and IHH expression of each clone was determined by western blot analysis of the cell lysates. Clones with detectable IHH expression were chosen for future experiments, and an attempt was made to choose clones with fairly similar levels of IHH expression. However, the clones of the HEK293[IHH^{WT}] line consistently had high IHH expression, and every clone of the IHH^{P46L}, IHH^{V190A}, and IHH^{E95K} lines had very low IHH expression (Figure 4.1).

4.3.2. Processing defects of the IHH mutants

Originally, equal amounts of each cell lysate (in μg of total protein) were analyzed by western blot to determine defects in autocleavage. However, due to differences in expression of the stable cell lines, the 19 kDa band of IHH^{WT} quickly saturated the blot while the 19 kDa band of IHH^{E95K}, for example, was not visible. For this reason, various amounts of each cell line were analyzed (from 2 μg of IHH^{WT} to 60 μg of IHH^{E95K}) in an attempt to make the 19 kDa band of each line similar in intensity (Figure 4.1). The differences in the β-actin loading control show the relative amounts of cell lysate loaded for each cell line. Densitometry was used to quantify the intensity of each band (45 kDa and 19 kDa) for each clone. Then the two IHH species (full-length and IHH-N) were expressed as a percent of the total amount of IHH present in that lane to avoid the inaccuracy of comparing across cell lines. After analyzing three separate blots, the significance of the difference between each

Figure 4.1. Reduction of autocleavage in several IHH mutants. The processing of full-length IHH into IHH-N was assessed by immunoblotting whole cell lysates of HEK293[IHH] stable cell lines with the anti-Shh antibody. Panel A shows a representative blot with various amounts of sample loaded (panel B, β-actin) to normalize the intensity of IHH-N (19 kDa, arrowhead) for each sample. Presence of accumulated IHH precursor (45 kDa, chevron) is visible in several mutants, indicating a defect in processing into the active IHH-N form. The relative amounts of IHH-N and full-length IHH were quantified by densitometry expressed as the percent of total IHH detected in that lane (panel C). The relative amounts presented in panel C are the mean of four independent experiments and the error bars represent ±SE. Asterisks denote a $p < 0.05$ when comparing each mutant sample to IHH^{WT} using the two-sample *t*-test assuming unequal variances (Excel 2003, Microsoft Corp., Seattle, WA).

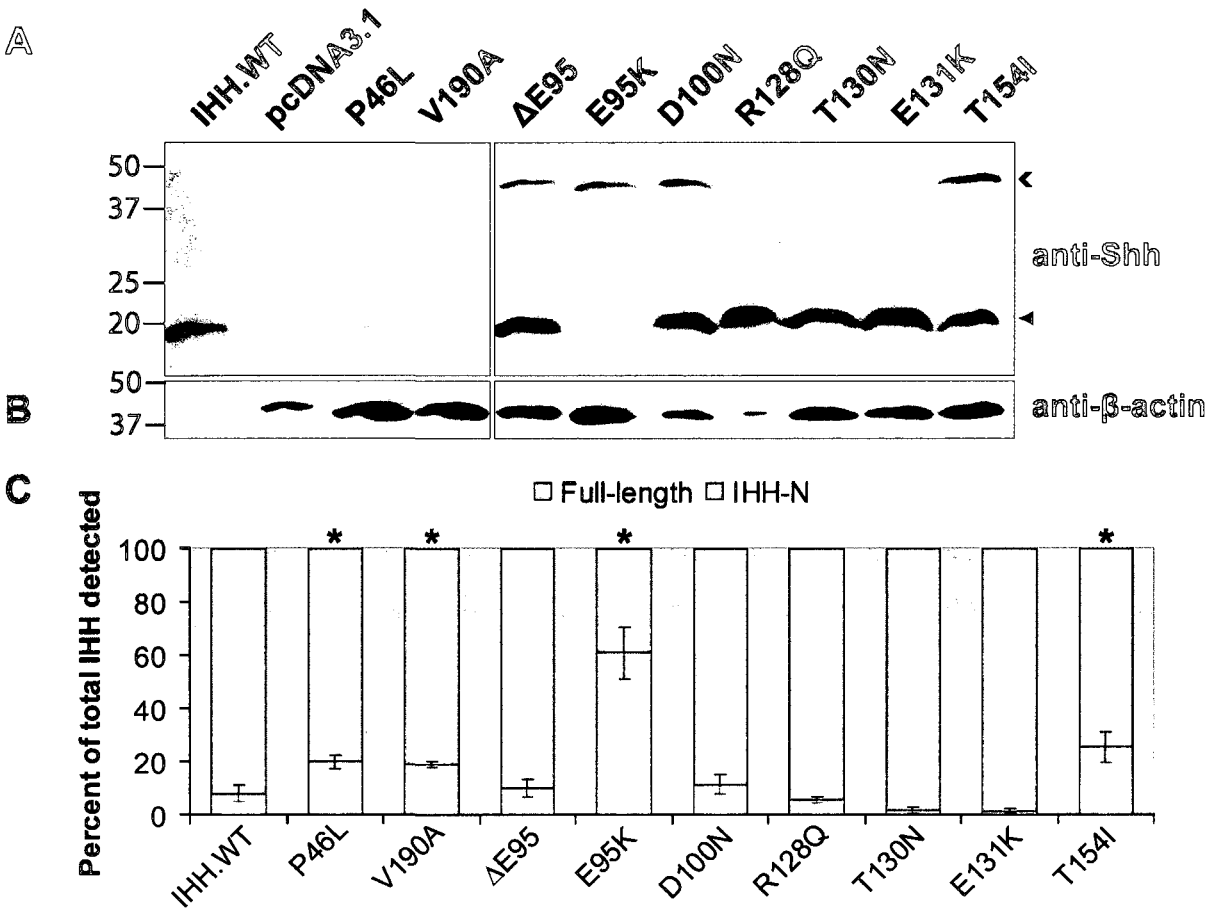
A
IHH.WT
pcDNA3.1
P46L
V190A
ΔE95
E95K
D100N
R128Q
T130N
E131K
T154I
50
37
25
20
anti-Shh
B
50
37
anti-β-actin
C
□ Full-length □ IHH-N
Percent of total IHH detected
100
80
60
40
20
0
*
IHH.WT
P46L
V190A
ΔE95
E95K
D100N
R128Q
T130N
E131K
T154I

mutant and IHH^{WT} was calculated using the two-sample *t*-test assuming unequal variance (Excel 2003, Microsoft Corp.).

Both of the ACFD mutants (IHH^{P46L} and IHH^{V190A}) and two of the BDA1 mutants (IHH^{E95K} and IHH^{T154I}) had significantly more IHH full-length than IHH^{WT} when compared to the same amount of IHH-N. A significant accumulation of full-length IHH could be due to a defect in processing. The IHH^{WT} full-length made up about 10% of the total IHH detected, indicative of efficient processing of the full-length into the cleaved form. The ACFD mutants had and accumulation of full-length: IHH^{P46L} was 20% full-length and 80% IHH-N (p value = 0.002) and IHH^{V190A} was 19% full-length and 81% IHH-N (p value = 4×10^{-4}). The BDA1 mutant IHH^{E95K} had a large accumulation of full-length IHH, roughly 60% of the total IHH detected was in the full-length form and only 40% was cleaved (p value = 0.006). This suggests that there is a significant defect in processing of the IHH^{E95K} mutant into its active form. Another BDA1 mutant, IHH^{T154I}, also had an accumulation of full-length IHH with 25% as full-length and 75% cleaved IHH-N (p value = 0.043).

4.3.3. Concentration of conditioned media to detect secreted IHH

Conditioned media was collected from confluent 15 cm plates of the HEK293[IHH^{WT}], empty vector, IHH^{P46L}, and IHH^{V190A} cell lines. The media was concentrated because IHH was not detected in the CM when analyzed by western blot, likely due to the lipid modifications anchoring the IHH protein to the cell membrane.

As a first attempt, only the CM from the ACFD mutants were concentrated, along with IHH^{WT} as a positive control and an HEK293 clone transfected with empty vector (HEK293[pcDNA3.1]) as a negative control. After concentrating 100X, the 19 kDa IHH-N

band was visible for IHH^{WT}, however it was still quite faint for the IHH^{P46L} and IHH^{V190A} lines (Figure 4.2). The amount of IHH^{WT} present in the CM was determined by using densitometry to compare the intensity of the 19 kDa band to a known amount of purified recombinant Shh (generously donated by Dr. Valerie Wallace). Next, a standard curve was generated measuring the induction of firefly luciferase in the SHH-Light II line by treating the cells with increasing amounts of IHH^{WT} concentrated media (Figure 4.3, panel A). HEK293[pcDNA3.1] CM was also concentrated and the SHH-Light II cells were "treated" with this media as a negative control. The untreated sample was another negative control in which the SHH-Light II cells were simply grown in the assay media (DMEM with 0.5% FBS).

The first observation was that the induction of firefly luciferase expression was very low and similar to the pcDNA3.1 negative control when the volumes were equal (such as in the pcDNA3.1 control and the 0.5 μg/mL IHH^{WT} sample in figure 4.3, panel A). This suggested that perhaps the small amount of activity we saw was simply due to a non-specific induction of the Gli-firefly luciferase reporter from treatment with concentrated media. When the samples were normalized to the total amount of protein the cells were treated with, the activity at all IHH^{WT} concentrations was similar to the negative controls (Figure 4.3, panel B). This suggests that treating the SHH-Light II cells with concentrated CM is not a viable assay to use because the amount of IHH present is too low to induce a response above the background level in the SHH-Light II cell line.

Figure 4.2. Concentration of conditioned media. The schematic in panel A illustrates the experimental procedure for concentrating the conditioned media from the HEK293[IHH] stable cell lines using the centrifugal filter device. Proteins larger than the 10 kDa pore size (such as full-length IHH and IHH-N, 45 kDa and 19 kDa, respectively) are retained in the filter. In panel B, 16 µl of 100X concentrated media was immunoblotted with the anti-Shh antibody. The negative control was conditioned media collected from the HEK293 cells transfected with empty vector (HEK293[pcDNA3.1]). The purified recombinant Shh (rShh) was used as a control to determine the amount of IHH in the media, (a generous gift from Dr. Valerie Wallace, OHRI).

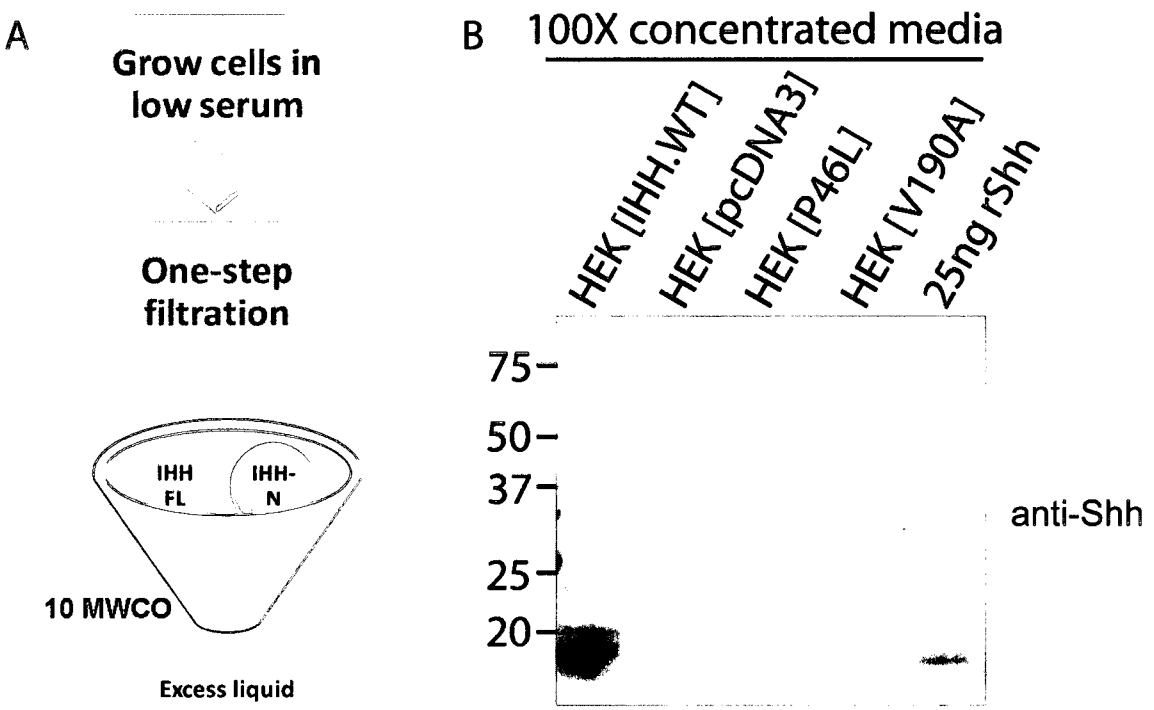
A
Grow cells in low serum
One-step filtration
IHH FL
IHH-N
10 MWCO
Excess liquid
B
100X concentrated media
HEK [IHH.WT]
HEK [pcDNA3]
HEK [P46L]
HEK [V190A]
25ng rShh
75
50
37
25
20
anti-Shh

Figure 4.3. Standard curve of concentrated HEK293[IHH^{WT}] media treatment of SHH-Light II cells. Conditioned media from the HEK293[IHH^{WT}] stable cell line was collected and concentrated. The quantity of IHH^{WT} in the concentrated media was determined using densitometry to compare the intensity of the 19 kDa IHH^{WT} band to a known amount of purified recombinant Shh (generously donated by Dr. Valerie Wallace, OHRI). Increasing amounts of IHH^{WT} were added to SHH-Light II cells to determine the optimal amount to use for future experiments (panel A). However the induction of firefly luciferase expression was quite low and when the activities were normalized to the total amount of protein present, there was no difference between the IHH^{WT} treated cells (green) and the untreated cells (red, panel B).

A

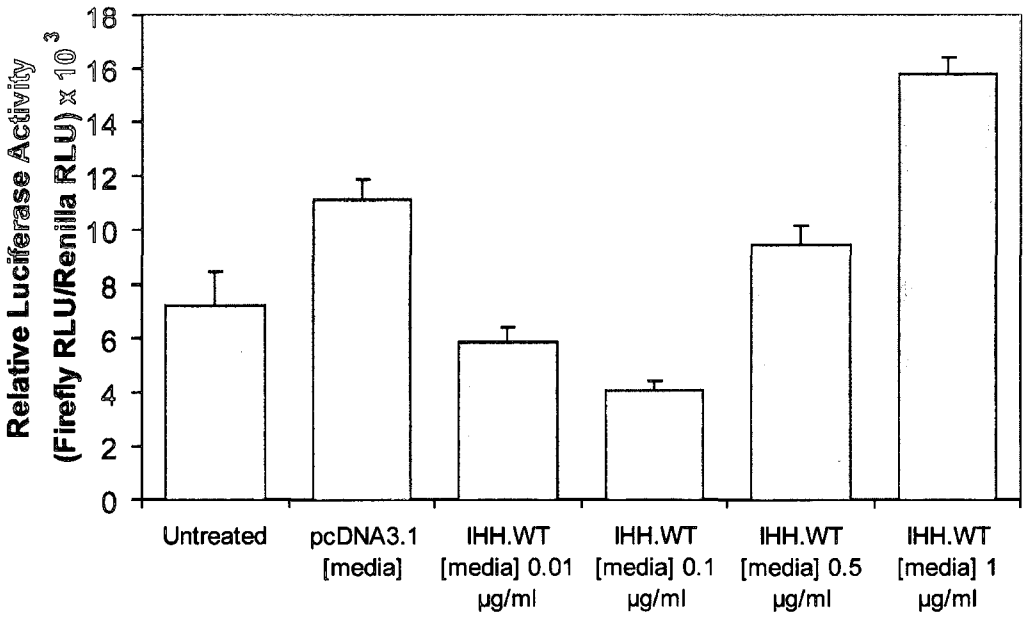
Relative Luciferase Activity
(Firefly RLU/Renilla RLU) x 10³
18
16
14
12
10
8
6
4
2
0
Untreated
pcDNA3.1 [media]
IHH.WT [media] 0.01 µg/ml
IHH.WT [media] 0.1 µg/ml
IHH.WT [media] 0.5 µg/ml
IHH.WT [media] 1 µg/ml

B

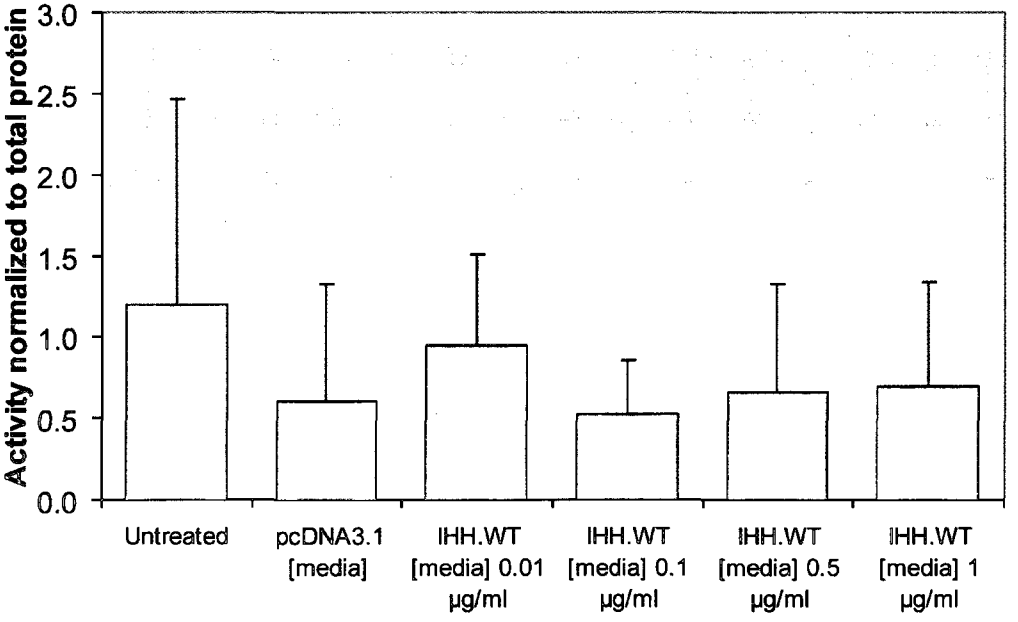
Activity normalized to total protein
3.0
2.5
2.0
1.5
1.0
0.5
0.0
Untreated
pcDNA3.1 [media]
IHH.WT [media] 0.01 µg/ml
IHH.WT [media] 0.1 µg/ml
IHH.WT [media] 0.5 µg/ml
IHH.WT [media] 1 µg/ml

4.3.4. SHH-Light II and HEK293[IHH] co-culture to quantify activity of the IHH mutants

Due to the small quantity of IHH in the conditioned media, treating the SHH-Light II cells with CM yielded unsatisfactory results because activity of IHH^{WT} CM was similar to background. As an alternative, the HEK293[IHH] stable lines were co-cultured with the SHH-Light II line to bypass the need for secretion of IHH since the membranes of the different cell lines would be in direct contact. This approach was recently used by Singh *et al* when screening a panel of SHH mutations that cause HPE (Singh, Tokhunts, et al, 2009).

The SHH-Light II cells were co-cultured 3:1 with each HEK293[IHH] stable cell line and the induction of firefly luciferase was roughly 100-fold higher than in the previous experiments when the SHH-Light II cells were treated with concentrated CM. In order to account for differences in cell numbers between samples, the firefly luciferase was normalized to the constitutively active *Renilla* luciferase. The activity of IHH^{WT} was set to one and the activities of each IHH mutant were expressed relative to that (Figure 4.4). The activity of the palmitate mutant IHH^{C28S} was roughly half of IHH^{WT} (p value = 0.011), and the activity of the mutant lacking both lipids (IHH-N^{C28S}) was only a quarter of IHH^{WT} (p value = 3×10^{-4}). The activities of both of the ACFD mutants (IHH^{P46L} and IHH^{V190A}) were roughly half of IHH^{WT} as well (52% and 60% with p values of 0.002 and 0.021 for IHH^{P46L} and IHH^{V190A}, respectively). The activities of two BDA1 mutants, IHH^{E95K} and IHH^{R128Q} were just over a third of the IHH^{WT} activity, at 37% and 34% (with p values of 0.004 and 0.017), respectively. The remaining BDA1 mutants did not seem to have defective activity as they were roughly 80-90% as active as IHH^{WT}.

Figure 4.4. Several IHH mutants have decreased activity. SHH-Light II cells were co-cultured 3:1 with each of the HEK293[IHH] stable lines for 48 h, followed by a dual-luciferase assay to quantify activity. SHH-Light II cells contain a Gli-responsive firefly luciferase as a marker for hedgehog pathway activation, and a constitutively active *Renilla* luciferase used as a control for cell number. Activity is represented as the mean of n $\geq$3 experiments, relative to IHH^{WT} activity, and the error bars represent +SE. Asterisks denote a $p < 0.05$ when comparing each mutant sample to IHH^{WT} using the two-sample *t*-test assuming unequal variances (Excel 2003, Microsoft Corp, Seattle, WA). The negative controls are shown in red, the IHH^{WT} in green, the lipid mutant controls in dark blue, the ACFD mutants in yellow, and the BDA1 mutants in light blue.

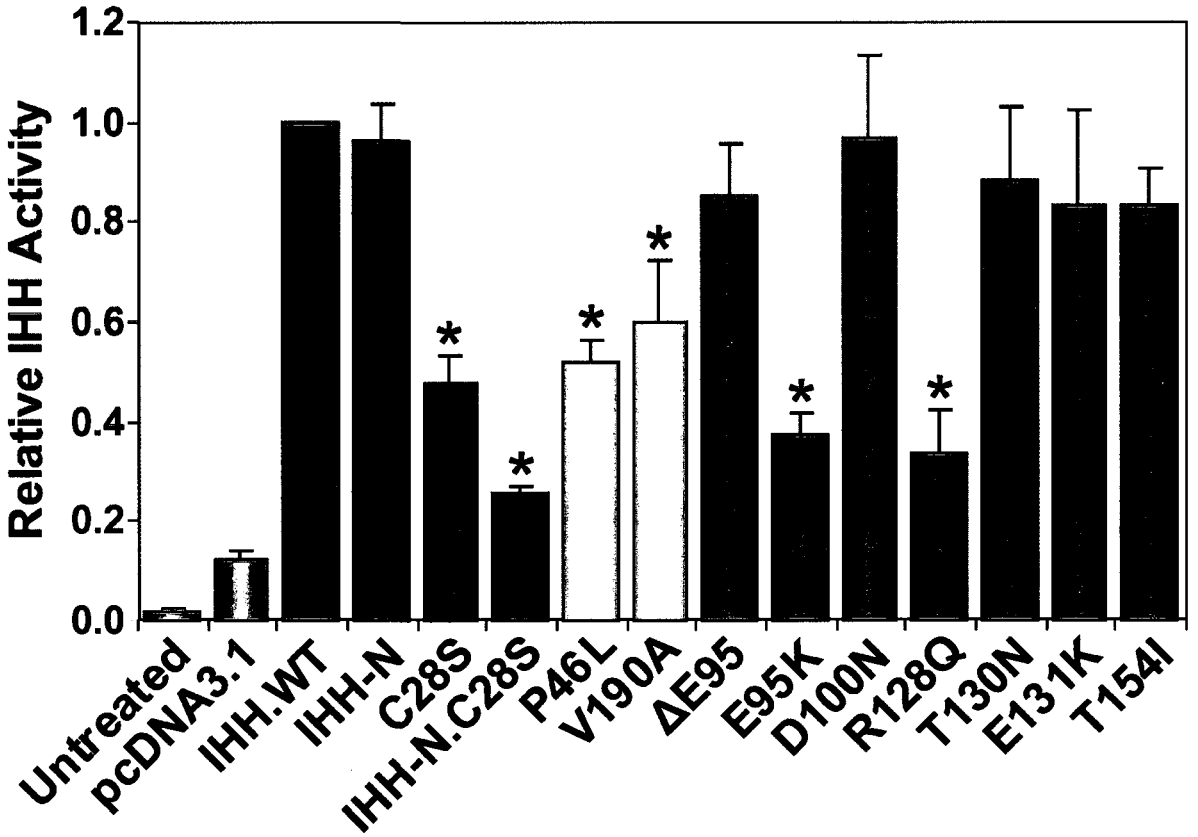
Relative IHH Activity
1.2
1.0
0.8
0.6
0.4
0.2
0.0
*
Untreated
pcDNA3.1
IHH.WT
IHH-N
C28S
IHH-N.C28S
P46L
V190A
ΔE95
E95K
D100N
R128Q
T130N
E131K
T154I

4.3.5. ELISA of conditioned media to quantify secretion

Since western blotting is not sensitive enough to detect the small quantities of IHH in the conditioned media of the HEK293[IHH] stable lines, ELISA was used to quantify the amount of IHH in the media. The sandwich ELISA was performed in a 96-well plate with 15 μg of cell lysate and 15 μl of CM analyzed for each stable cell line. The above amounts were used to maintain the absorbance readings within the accurate range of the standard curve (data not shown). The amount of IHH in the media and the cell lysate were expressed as a percent of total IHH detected for that cell line, to account for differences in expression between the cell lines (Figure 4.5). The IHH^{WT} construct appears to be evenly distributed between the cell lysate and the media, with approximately 50% of IHH in the media. The lipid mutant controls lacking either palmitate (C28S) or both lipids (IHH-N^{C28S}) were secreted more efficiently than the membrane-tethered IHH^{WT}, as expected. The distribution of IHH^{C28S} was approximately 80% in the media, and 20% in the cell lysates, while IHH-N^{C28S} had 90% in the media and only 10% retained in the cell. However, the cholesterol mutant IHH-N has the same distribution as IHH^{WT}, which is unexpected as the lack of cholesterol should increase the amount of IHH in the media. The ACFD mutant IHH^{P46L} has a large proportion of IHH in the media (80%), similar to that of the IHH^{C28S} palmitate mutant which suggests that the p.P46L substitution may interfere with palmitate addition. The BDA1 mutants IHH^{E95K} and IHH^{T154I} both have approximately 70% of IHH in the media and 30% in the cell lysate. All of the mutant constructs (except for IHH^{R128Q}) appear to be secreted more efficiently than IHH^{WT} because there is relatively more mutant IHH detected in the media than in the cell.

Figure 4.5. Quantification of the proportion of IHH in the cell lysates versus conditioned media from the HEK293[IHH] stable cell lines. ELISA was used to quantify the amount of IHH in the cell lysate (15 μg) and conditioned media (15 μl) of each HEK293[IHH] stable cell line (panel A). The relative amounts in the media and cell lysate were expressed as a percent of total IHH detected for that cell line. The error bars represent ±SE and n = 4. Asterisks denote a $p < 0.05$ when comparing each mutant sample to IHH^{WT} using the two-sample *t*-test assuming unequal variances (Excel 2003, Microsoft Corp., Seattle, WA).

Cell lysates
Conditioned media
Percent of total IHH detected
100
90
80
70
60
50
40
30
20
10
0
IHH-WT
IHH-N
C28S
IHH-N-C28S
P46L
V190A
ΔE95
E95K
D100N
R128Q
T130N
E131K
T154I
*

4.4. Discussion

4.4.1. Establishment of the HEK293[IHH] stable cell lines

Stable cell lines are useful tools to characterize a protein of interest because they are a continual source of protein, with consistent expression that can be maintained by antibiotic selection. However, the expansion of clones originating from a single cell takes a significant amount of time, and this process selects for only the healthiest cells. If expression of the protein is toxic to a particular cell, only the clones that have silenced the gene (or express very small quantities of it) will be selected for. Since every clone expressing the ACFD IHH mutants had very low IHH expression levels, this suggests that either mutant IHH expression may be harmful to the cell, or that the mRNA and/or protein are being degraded. If the mutations cause a problem with translation or folding of the mutant protein, that could result in accumulation of misfolded protein in the ER leading to ER stress and the unfolded protein response (reviewed in Schröder, and Kaufman, 2005). Among other things, the unfolded protein response (UPR) involves decreasing the translation rate in the cells to reduce the level of ER stress, and can induce apoptosis of the cell if the ER stress is not relieved (Schröder, and Kaufman, 2005). A UPR-mediated decrease in translation could explain why we were unable to isolate clones that stably express ACFD mutant IHH (or IHH^{E95K}) at a high level.

4.4.2. Decreased processing of mutant IHH into the active form

The accumulation of full-length IHH was assessed by western blot of cell lysates and was used as an indicator for a decreased rate of autocleavage. It appeared that IHH^{WT} did not exist in the full-length form for very long, as only a small fraction (10%) of the IHH present

in the cell was uncleaved. This suggests that the autocleavage was relatively efficient for IHH^{WT} and accumulation of mutant full-length above this expected 10% was considered to be indicative of a defect in processing. The autocleavage of both of the ACFD mutants (IHH^{P46L} and IHH^{V190A}) and two of the BDA1 mutants (IHH^{E95K} and IHH^{T154I}) appeared to be less efficient than that of IHH^{WT} (Figure 4.1) resulting in an accumulation of full-length up to six times more than expected based on IHH^{WT}. This would result in decreased production of active IHH-N even if expression levels of the mutants were the same as IHH^{WT}.

The analysis of the HEK293 stable lines also suggests that the expression level of both of the ACFD mutants may be low (perhaps due to defects in protein folding). If this is in fact the case *in vivo*, then not only would the ACFD IHH mutants be expressed at a low level, but what little mutant IHH is made may not be properly processed into its active IHH-N form. This theory is supported by the fact that ACFD is a recessive trait, suggesting that it results from a significantly decreased amount of functional protein at the growth plate.

The amino acid substitutions resulting from the ACFD mutations also suggest that the mutant protein may not fold properly *in vivo*. The substitution of a proline with a leucine (p.P46L) could disrupt folding as proline is unique in its capability to form tight turns within a protein, is less hydrophobic than leucine. The valine to alanine substitution (p.V190A) could result in a disruption of folding as alanine is much smaller and more hydrophobic than valine. Also, the nearby residue H187 (H182 in human Shh) is involved in zinc binding, which has been shown to be important for human SHH protein stability (Day, Wen, et al, 1999; Hall, Porter, et al, 1995). If the alanine substitution at residue 190 disrupted the local tertiary structure resulting in reduced zinc binding by residue H187, this could have a detrimental effect on the structural stability of the entire protein.

4.4.3. Several IHH mutants have decreased activity relative to IHH^{WT}

The *in vitro* activity of each of the IHH mutants was compared to IHH^{WT} using the SHH-Light II assay system. In the literature, this cell line has been used to test the activity of hedgehog constructs by treating the cells with purified Shh (Chen, Taipale, et al, 2002; Taipale, Chen, et al, 2000) or treating the cells with conditioned media containing Shh (Chen, Li, et al, 2004; Goetz, Singh, et al, 2006). We used the co-culture system, similar to a recent study (Singh, Tokhunts, et al, 2009) since the dual lipid-modified IHH constructs are not secreted into the media at a sufficient level to induce a response in the SHH-Light II line (Figure 4.3). The activity of the lipid mutant constructs were consistent with what was expected based on the literature and served as a good control for the assay. By using an *in vivo* assay, Chen *et al* found that Shh lacking palmitate has decreased activity relative to Shh^{WT}, and the Shh construct lacking both palmitate and cholesterol is even less active (Chen, Li, et al, 2004). The same results were seen with the IHH^{C28S} and IHH-N^{C28S} mutants in our SHH-Light II cell-based assay. The activity of IHH-N was similar to IHH^{WT} which was also expected based on the theory that cholesterol is not essential for potency (reviewed in Wendler, Franch-Marro, and Vincent, 2006).

The potency of the ACFD mutants (IHH^{P46L} and IHH^{V190A}) appears to be roughly half of IHH^{WT}. As ACFD is a recessive condition, a 50% reduction in mutant IHH activity follows the expected pattern for recessive disease. Only two of the BDA1 mutants had significantly decreased activities (IHH^{E95K} and IHH^{R128Q}) in the assay; the potency of both was only roughly a third of IHH^{WT}.

As BDA1 is a dominant condition, a simple reduction in activity of the mutants does not necessarily explain the basis for disease, and it is not surprising that the majority of BDA1

mutant IHH had similar activity to IHH^{WT}. It is more likely that the mutations act in a dominant negative manner. To test this hypothesis, equal amounts of IHH^{WT} expressing cells and BDA1 mutant IHH expressing cells were co-cultured with the SHH-Light II line (Figure 4.6). However, there was no significant difference between the activity of IHH^{WT} alone (with the empty vector control, pcDNA3.1) or mixed with each of the BDA1 mutants, suggesting there is not a large dominant negative effect in this particular assay. However, activity of the mixtures was lower than expected since most BDA1 mutants are almost as active as IHH^{WT} when assayed individually (Figure 4.4). The mixtures would be expected to be more active than IHH^{WT} alone and the fact that they were not suggests that there may be a slight dominant negative effect of the mutant on IHH^{WT} activity. Also, this assay does not co-express the mutant and IHH^{WT} in the same cell, nor does it require secretion of the IHH constructs. It could be that the dominant negative effect of the BDA1 mutant IHH is in the interference of the formation of IHH multimers, which would be detrimental to secretion, trafficking, and signaling (Chen, Li, et al, 2004; Zeng, Goetz, et al, 2001). Further studies characterizing the ability of mutant IHH to form multimers would have to be conducted to be certain.

4.4.4. Mutant IHH is found at higher levels in the media than in the cell lysate

Defects in secretion of the IHH mutants were determined by comparing the relative levels of IHH in the CM to the amount of IHH in the cell lysate. Because certain clones expressed IHH at a higher level than others, it would not be accurate to compare the amount of IHH in the media without first taking into account the amount of IHH produced by the cells. The amount of IHH in the conditioned media and cell lysates of the HEK293[IHH] stable lines

Figure 4.6. Co-culture of BDA1 mutant IHH with IHH^{WT} to test for dominant negative effect on activity. SHH-Light II cells were co-cultured 3:1 with an equal mixture of the HEK293[IHH] stable lines (3×10^4 SHH-Light II cells with 5×10^3 HEK[IHH^{WT}] and 5×10^3 HEK[BDA1 IHH] cells). The IHH^{WT} cells were also cultured with the empty vector cells (pcDNA3.1) as a control. The cells were grown for 48 h, followed by a dual-luciferase assay to quantify activity.

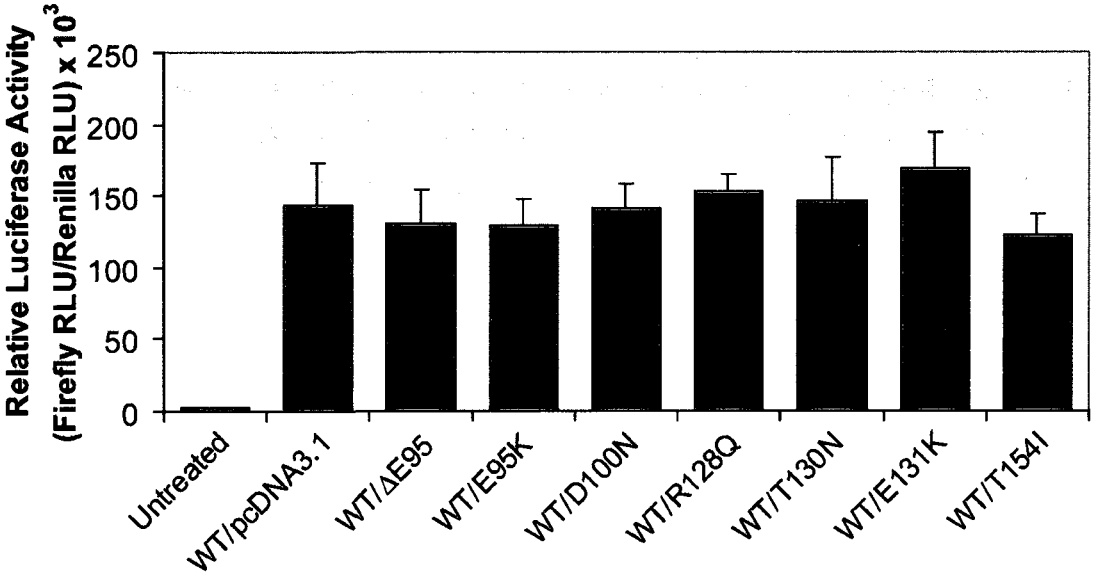
Relative Luciferase Activity
(Firefly RLU/Renilla RLU) x 10^3
250
200
150
100
50
0
Untreated
WT/pcDNA3.1
WT/ΔE95
WT/E95K
WT/D100N
WT/R128Q
WT/T130N
WT/E131K
WT/T154I

was quantified using the sandwich ELISA. The specificity of the sandwich ELISA is high compared to western blotting since the protein must bind both the capture antibody and the detection antibody in order to be detected. The sensitivity of ELISA is also greater than western blotting, partly because the epitopes on the protein are not destroyed as they can be under the denaturing conditions of SDS-PAGE. For these reasons, ELISA was chosen to analyze the relative amounts of IHH in the media and cell lysates of the stable cell lines.

The IHH-N^{C28S} mutant displayed the highest level of secretion, which was expected since it is lacking both lipid modifications and should be easily secreted from the cell. The IHH^{C28S} palmitate mutant was also secreted more efficiently than IHH^{WT}; however the secretion of the cholesterol mutant IHH-N was similar to IHH^{WT}. I would have expected the secretion of IHH-N to be higher than IHH^{WT} based on the literature (Bumcrot, Takada, and McMahon, 1995; Porter, Von Kessler, et al, 1995; Porter, Young, and Beachy, 1996). However, if the secreted proteins do in fact form multimers, they will likely exist in that state during the assay and may prevent accurate quantification of the total amount of IHH in the sample. Perhaps IHH^{WT} forms multimers in the media samples, which may allow for more efficient binding to the capture antibody. However, IHH-N would not form multimers as well, and more of the IHH-N in the media would remain unbound. This would result in an apparent decrease of IHH-N in the media fraction as compared to IHH^{WT}.

There are other limitations to the ELISA assay, for example, there is no way to differentiate between full-length and cleaved IHH-N as would be possible on a western blot. As well, the antibodies in the ELISA kit have been designed to be very specific for mouse Shh with only a small amount of cross-reactivity with human IHH. For this reason, it is possible that the concentration of IHH is underestimated. However, for the purposes of this experiment, relative secretion can still be calculated by comparing the relative amounts of

IHH in the media to the amount of IHH in the cell lysates without the need to calculate the actual concentration of IHH present.

Overall, the *in vitro* assays indicate that there are defects in mutant IHH biogenesis, and that the individual mutations interfere at different stages including the translation/folding of the protein, processing, secretion, and signaling activity. Table 4.1 summarizes the results from the assays and lists the potential defects caused by the mutations, using insights from recent studies in the literature.

Table 4.1. Summary of the defects in biogenesis of the mutant IHH proteins. The amino acid substitutions are shown along with a description of the possible defects based on the properties of the amino acids and recent results from the literature. The p.P46L and p.V190A mutations are the recessive ACFD mutations, the remaining are the dominant BDA1 mutations. Arrows indicate an increase or decrease compared to IHH^{WT}, the number of arrows indicates the degree of change from IHH^{WT}.

Mutation	Potential defects caused by amino acid substitution	IHH expression in HEK293	Processing	Activity	Relative secretion
p.P46L	Potential misfolding since leucine is less compact and less hydrophobic	⬇⬇⬇	⬇	⬇	⬆⬆⬆
p.V190A	Potential misfolding since alanine is smaller and more hydrophobic. Overall protein instability if zinc coordination is disrupted at residue H187 (Hall *et al*, 1995; Day *et al*, 1999)	⬇⬇⬇	⬇	⬇	⬆⬆
p.ΔE95	Residue E95 is the IHH equivalent of an Shh residue involved in Ca^{2+} coordination, important for receptor binding (McLellan *et al*, 2008)	⬇⬇	Normal	Normal	⬆
p.E95K	Substitution changes the negative charge to positive. Residue E95 is the IHH equivalent of an Shh residue involved in Ca^{2+} coordination, important for receptor binding (McLellan *et al*, 2008)	⬇⬇⬇	⬇⬇	⬇⬇	⬆⬆
p.D100N	Substitution changes the negative charge to neutral. Potentially disrupted Ca^{2+} coordination resulting in decreased Ptc and Hip binding (McLellan *et al*, 2008)	⬇	Normal	Normal	⬆
p.R128Q	Substitution changes the positive charge to neutral. Residue R128 is the IHH equivalent of the CDO binding site identified in Shh (McLellan *et al*, 2008)	⬇	Normal	⬇⬇	Normal
p.T130N	Potential misfolding since asparagine is not hydrophobic.	⬇⬇	Normal	Normal	⬆
p.E131K	Substitution changes negative charge to positive. Residue E131 is involved in Ca^{2+} coordination, substitution results in decreased receptor binding (McLellan *et al*, 2008)	⬇⬇	Normal	Normal	⬆
p.T154I	Residue T154 lies within a β-sheet based on Shh 3D structure (Liu *et al*, 2006). Substitution with isoleucine could disrupt the β-sheet since it is larger and more hydrophobic.	⬇⬇⬇	⬇	Normal	⬆⬆

Chapter 5: Discussion and conclusions

5.1. Summary of defects in the BDA1 and ACFD IHH mutants

The autosomal dominant disorder brachydactyly type A1 was identified over a century ago (Farabee, 1903), however the nine missense mutations and one deletion mutation in *IHH* which cause the disease were only identified within the past decade (Byrnes, Racacho, et al, 2009; Gao, Guo, et al, 2001; Giordano, Gennari, et al, 2003; Kirkpatrick, Au, et al, 2003; Liu, Wang, et al, 2006; Lodder, Hoogeboom, et al, 2008; McCready, Sweeney, et al, 2002; McCready, Grimsey, et al, 2005; Stattin, Lindén, et al, 2009; Zhu, Ke, et al, 2007). The recessive condition acrocapitofemoral dysplasia and the causative mutations in *IHH* were both identified six years ago (Hellemans, Coucke, et al, 2003; Mortier, Kramer, et al, 2003). Due to the fairly recent discovery of the BDA1 and ACFD mutations, the mechanism by which the mutant IHH causes a disease phenotype is still unknown. We are the first group to attempt to characterize the ACFD mutations and the entire panel of BDA1 mutations. The different mutations can act as useful tools in analyzing the importance of certain residues and domains on IHH protein function. The biogenesis of IHH is a highly conserved and regulated process, and the mutations may interfere with any number of steps including translation/folding, processing, secretion, multimerization/trafficking, or receptor binding.

Most BDA1 mutations caused no significant defects in processing or activity. However, all BDA1 mutant constructs displayed reduced protein expression relative to the IHH^{WT} line, suggesting that the mutants may be misfolding and accumulating in the ER, or perhaps they are unstable and targeted for degradation. This is supported by the results from the ELISA where the proportion of mutant IHH in the cell lysates was consistently lower than the

amount of mutant IHH in the media. This may also suggest that the mutant IHH constructs have low intracellular stability or may be targeted for degradation.

Unfortunately, the attempts to characterize mutant IHH function in the *in vitro* chondrogenesis models were unsuccessful. Stable long term expression of *IHH* in the ATDC5 chondroprogenitor cell line was never established, possibly due to toxicity of overexpression of *IHH* in this system. Transfection of the primary mouse limb bud mesenchymal cells was unsuccessful using a cationic lipid transfection reagent, and the number of cells needed for electroporation and nucleofection were prohibitive. Future work should include subcloning each mutant *IHH* cDNA construct from the pcDNA3.1+ vector into a viral vector, as other groups have had success with using infection to transfer DNA into primary limb bud mesenchymal cells (Carlberg, Pucci, et al, 2001; Stott, and Chuong, 2000).

5.1.1. BDA1 mutations

5.1.1.1. The p.E95K mutation

The BDA1 p.E95K mutation had the most detrimental effect on IHH biogenesis resulting in significantly decreased expression, processing, and activity compared to IHH^{WT}. It should be noted that the protein expression level of each cell line was compared by assessing western blots of cell lysates, so it could in fact represent instability of the protein or mRNA as opposed to low expression levels. It was recently discovered that the equivalent residue of E95 in mouse Shh (E91) is involved in coordinating two calcium ions, which was found to be essential for receptor binding (McLellan, Zheng, et al, 2008). The equivalent mutation (E91K) resulted in decreased binding to the receptors Hip and Ptc, with only 10% and 40%

binding compared to wild-type, respectively (McLellan, Zheng, et al, 2008). Since Hip is a negative regulator of Hh signaling (Chuang, and McMahon, 1999), decreased Hip binding would result in an increased range of IHH^{E95K} signaling at the growth plate. However, the decreased Ptc binding would result in a decreased potency of the IHH^{E95K} mutant. This increase in signaling range but decrease in potency was confirmed in a recent study in which the $IHH^{E95K/E95K}$ mouse model was generated (Gao, Hu, et al, 2009). The group performed a cell-based binding assay and found that the affinity of IHH^{E95K} for Ptc was roughly 70% that of IHH^{WT}, which may explain the decreased potency in IHH short range signaling. However, they found that long range signaling of IHH^{E95K} was increased, possibly owing to the decreased affinity for Ptc and Hip resulting in increased diffusion of IHH^{E95K} away from the IHH producing cells (Gao, Hu, et al, 2009). These two studies help to explain the mechanism of the dominant negative effect of the BDA1 mutations, and in the case of p.E95K, it is likely a result of decreased receptor binding leading to a disruption of the normal concentration gradient of IHH at the growth plate. McLellan *et al* found that the mShh residues equivalent to D100 and E131 in IHH are also involved in calcium coordination, suggesting that the p.D100N and p.E131K mutants may behave in the same manner as p.E95K (McLellan, Zheng, et al, 2008).

5.1.1.2. The p.R128Q mutation

The p.R128Q IHH BDA1 mutant was similar to IHH^{WT} in processing and secretion, and expression was only slightly less than IHH^{WT} in the HEK293 cell line. However, the activity of IHH^{R128Q} was only a third of IHH^{WT} in the SHH-Light II reporter assay. McLellan *et al* showed that the R128 equivalent residue in Shh (R124) is involved in binding to CDO

(McLellan, Zheng, et al, 2008). CDO is a positive regulator of Hh signaling (Allen, Tenzen, and McMahon, 2007) and decreased CDO binding (due to the positive to neutral charge substitution in the p.R128Q mutation) could explain the decreased activity of the IHH^{R128Q} mutant in the SHH-Light II reporter assay. Overall, the p.R128Q mutation results in a protein that is produced and secreted at a level similar to wild-type, however it is significantly less efficient at binding to its receptors, resulting in decreased potency.

5.1.1.3. The p.T154I mutation

The p.T154I IHH BDA1 mutant had very low expression (or intracellular stability) and its processing was also less efficient than IHH^{WT}. However, the activity of IHH^{T154I} was similar to IHH^{WT}, and relative secretion of the mutant was more efficient than IHH^{WT}. Based on the Shh 3D structure, residue T154 in IHH is within a β-sheet (Liu, Wang, et al, 2006) which could potentially be disrupted by the p.T154I mutation. Misfolding as a result of this substitution could be the cause for the observed decrease in IHH protein production, and could perhaps interfere with the autocleavage reaction. It appears that the p.T154I mutation interferes with the early steps in IHH biogenesis, resulting in low intracellular levels of the mutant protein. Even though it is not physiologically relevant, it is interesting to note that what little IHH^{T154I} is produced is secreted efficiently and is as potent as IHH^{WT}.

5.1.2. ACFD mutations

Both ACFD mutations appeared to interfere with many steps during IHH biogenesis. Both were expressed at very low levels, suggesting that either mRNA levels are low, or that

intracellular protein stability may be low due to misfolding or degradation. The processing and activity of both the IHH^{P46L} and IHH^{V190A} mutants were significantly less than IHH^{WT}. The relative secretion of the p.P46L IHH mutant appeared to be increased compared to IHH^{WT} and resembled the secretion level of the palmitate mutant, IHH^{C28S}. It would have to be confirmed in future experiments whether or not this is a result of decreased palmitate addition due to the p.P46L substitution (see future directions). Residue P46 is also near the Cardin-Weintraub sequence which is important for heparin binding (Cardin, and Weintraub, 1989; Rubin, Choi, and Segal, 2002). If the p.P46L mutation disrupted HSPG binding, the long-range signaling of IHH at the growth plate could be reduced as illustrated in a recent paper showing the importance of HSPG and CSPG interactions with IHH at the growth plate (Cortes, Baria, and Schwartz, 2009). As stated previously, the p.V190A mutation lies near a histidine residue important for zinc coordination, and disruption could result in protein instability (Day, Wen, et al, 1999; Hall, Porter, et al, 1995).

Overall, the *in vitro* assays to test the biogenesis of mutant IHH shed some light on the mechanism of the dominant mutations in BDA1 and the recessive mutations in ACFD. As the two conditions follow different inheritance patterns, it is expected that the defect caused by the mutations will also be different. The basis of dominant inheritance is that the mutant protein interferes in some way with the function of the wild-type protein, resulting in a disease phenotype when only one copy of the mutant gene is present. However in a recessive condition, the heterozygous carriers of the mutation are phenotypically normal, and there is only a disease phenotype when both copies of the gene are mutated. This means that the recessive mutations do not confer a dominant negative effect on wild-type function, instead they result in a decrease (or total loss) of function of the mutant protein.

As expected, the recessive ACFD mutations lead to a protein that is severely compromised both in protein levels and activity, consistent with a partial loss-of-function mutation. It is evident that the ACFD mutant IHH retains some of its signaling ability, since an IHH null mutation would not be expected to be viable based on studies with $IHH^{-/-}$ mice (St-Jacques, Hammerschmidt, and McMahon, 1999). A few of the dominant BDA1 mutations lead to decreased processing or signaling, however many of the BDA1 mutants performed similar to IHH^{WT} in the *in vitro* assays. It is likely that the BDA1 mutants confer a dominant-negative effect, however further studies will have to be pursued to determine the exact mechanism.

5.2. BDA1 disease model

The mutations in IHH which result in the autosomal dominant condition BDA1 are likely gain-of-function mutations. It is not likely that the disease is caused by haploinsufficiency because mice heterozygous for an IHH null mutation are phenotypically normal (Gao, Hu, et al, 2009). One question about the BDA1 phenotype is why the middle phalanges of the digits are so severely shortened, while other long bones seem relatively unaffected. *IHH* is expressed in the condensation stage of digit formation (Gao, Hu, et al, 2009) and aberrant IHH signaling at this stage could lead to the formation of a small cartilage template. Since the middle phalanges are the last to ossify (O'Rahilly, and Gardner, 1975) they would be the worst affected by the shortened cartilage template (Fitch, 1979).

Using data from our assays as well as recently published results from other groups, a model for BDA1 can be postulated in which the expression level of mutant IHH in the

prehypertrophic chondrocytes is decreased (Figure 5.1). Both the mutant and wild-type forms of IHH would be secreted and the mutant form would diffuse further than IHH^{WT} due to decreased Hip and Ptc binding (Gao, Hu, et al, 2009; McLellan, Zheng, et al, 2008). Since the mutant IHH diffuses further and is less potent, overall there is less IHH signaling at the growth plate due to a dilution of the normal concentration gradient. This would result in decreased chondrocyte proliferation and cause the decreased bone growth seen in the BDA1 phenotype. The relatively small size of the growth plates in the digits amplifies the dominant negative effect of the BDA1 mutants since the mutant IHH protein can travel beyond the boundary of the developing bone (Gao, Hu, et al, 2009). This could result in aberrant induction of PTHrP at the periarticular perichondrium and in the interzone between the developing phalanges (Gao, Hu, et al, 2009) disrupting the regulation of chondrocyte proliferation and differentiation.

5.3. ACFD disease model

Based on the results of our assays, the ACFD mutations result in mutant proteins whose intracellular levels are low either due to decreased expression or stability. This observation is consistent with the fact that ACFD is an autosomal recessive condition, likely caused by a mutation that causes a partial loss-of-function. The heterozygous carriers of the ACFD mutations appear phenotypically normal, and it was only discovered upon X-ray analysis that a few carriers have mild shortening of various phalanges. Significantly decreased levels of IHH at the growth plate could be the mechanism for the pathology of ACFD, resulting in decreased induction of PTHrP (Figure 5.2). This would lead to an increased rate of

Figure 5.1. Increased signaling range of BDA1 mutant IHH. A schematic of the growth plate is shown with the ranges of the mutant and wildtype IHH proteins. The BDA1 mutant has defective trafficking due to decreased receptor binding resulting in the ablation a the concentration gradient, while the IHH^{WT} concentration gradient is maintained. The BDA1 mutants also have decreased signaling ability, leading to an overall decrease in the induction of PTHrP. This combination of decreased IHH and PTHrP signaling would result in chondrocytes exiting the proliferation stage prematurely.

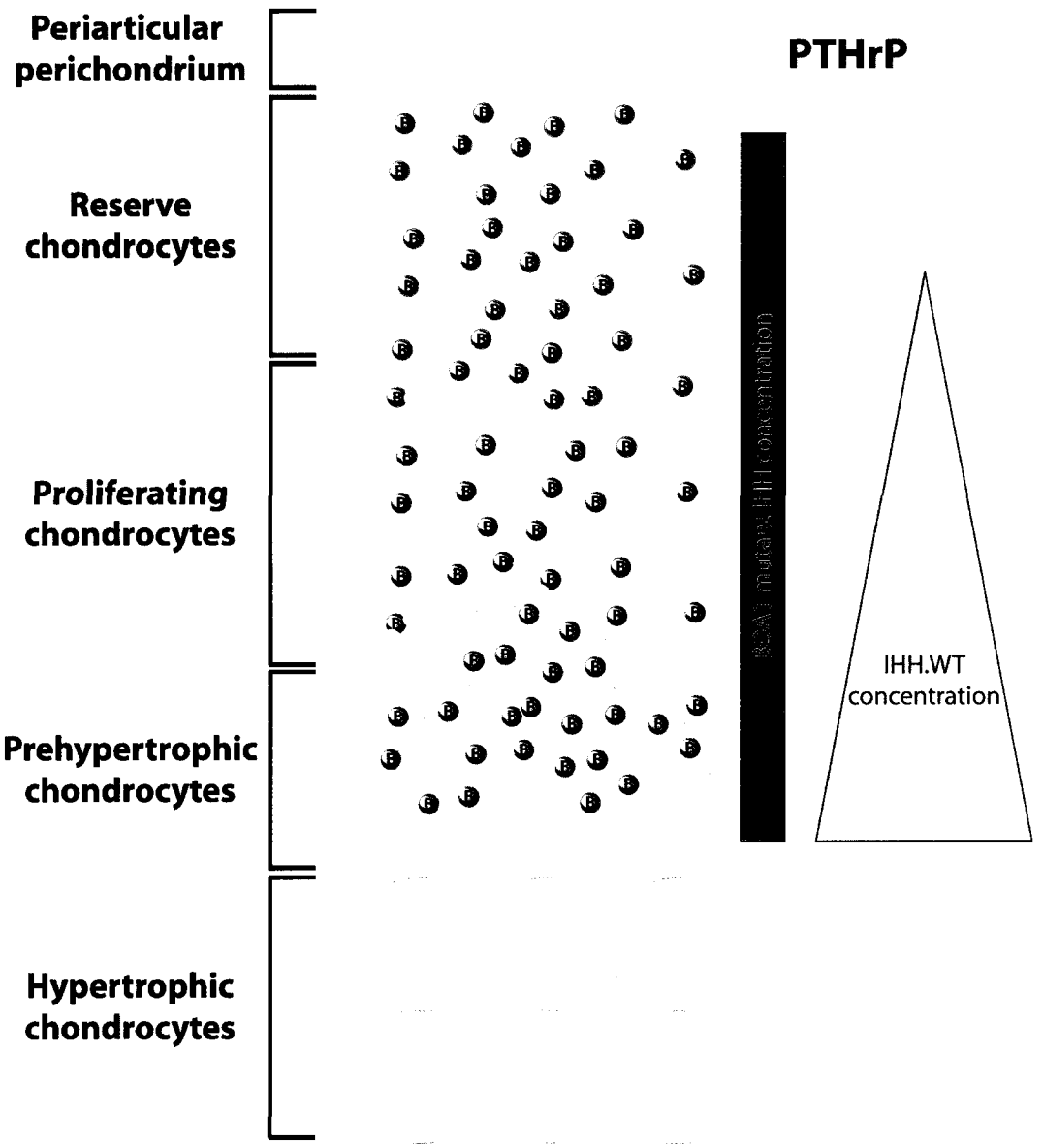
Periarticular perichondrium
Reserve chondrocytes
Proliferating chondrocytes
Prehypertrophic chondrocytes
Hypertrophic chondrocytes
PTHrP
IHH.WT concentration

differentiation of the proliferating chondrocytes into prehypertrophic chondrocytes, which could result in premature epiphyseal closure (Hellemans, Coucke, et al, 2003). The cone-shaped epiphyses seen in the ACFD patients are also indicative of a disruption in the normal rate of chondrocyte differentiation/proliferation (Hellemans, Coucke, et al, 2003) as it appears that differentiation occurs earlier in the centre of the growth plate. This could be due to a reduced concentration gradient of ACFD mutant IHH at the growth plate as a result of decreased IHH production by the prehypertrophic chondrocytes.

5.4. Conclusions and future directions

The *in vitro* characterization of a panel of BDA1 and ACFD mutations gave some insight into the molecular basis of the pathogenesis of both skeletal dysplasias. The recessive condition ACFD may be caused by partial loss-of-function mutations which result in low levels of IHH at the growth plate. What little ACFD mutant IHH is produced is also less active than IHH^{WT}, resulting in significant decrease of IHH signaling at the growth plate. The result is a skeletal dysplasia with a variety of defects in many of the long bones of the upper and lower limbs.

The autosomal dominant condition BDA1 is likely caused by a gain-of-function of the mutant IHH protein, resulting in aberrant IHH signaling at the growth plate. The majority of BDA1 mutants showed no defects in processing, secretion, or activity in our *in vitro* assays. However, all BDA1 mutants had decreased expression compared to IHH^{WT}, possibly due to decreased intracellular stability or misfolding because of the disruptive amino acid substitutions.

Figure 5.2. Decreased production and stability of ACFD mutant IHH. A schematic of the growth plate is shown illustrating the severe defect in ACFD mutant IHH production. Decreased expression and processing of the mutant *IHH* would result in very little functional protein in the growth plate. This would lead to reduced induction of PTHrP and proliferation. A decreased rate of proliferation coupled with an increased rate of differentiation could lead to premature epiphyseal closure and result in a shortening of the bones.

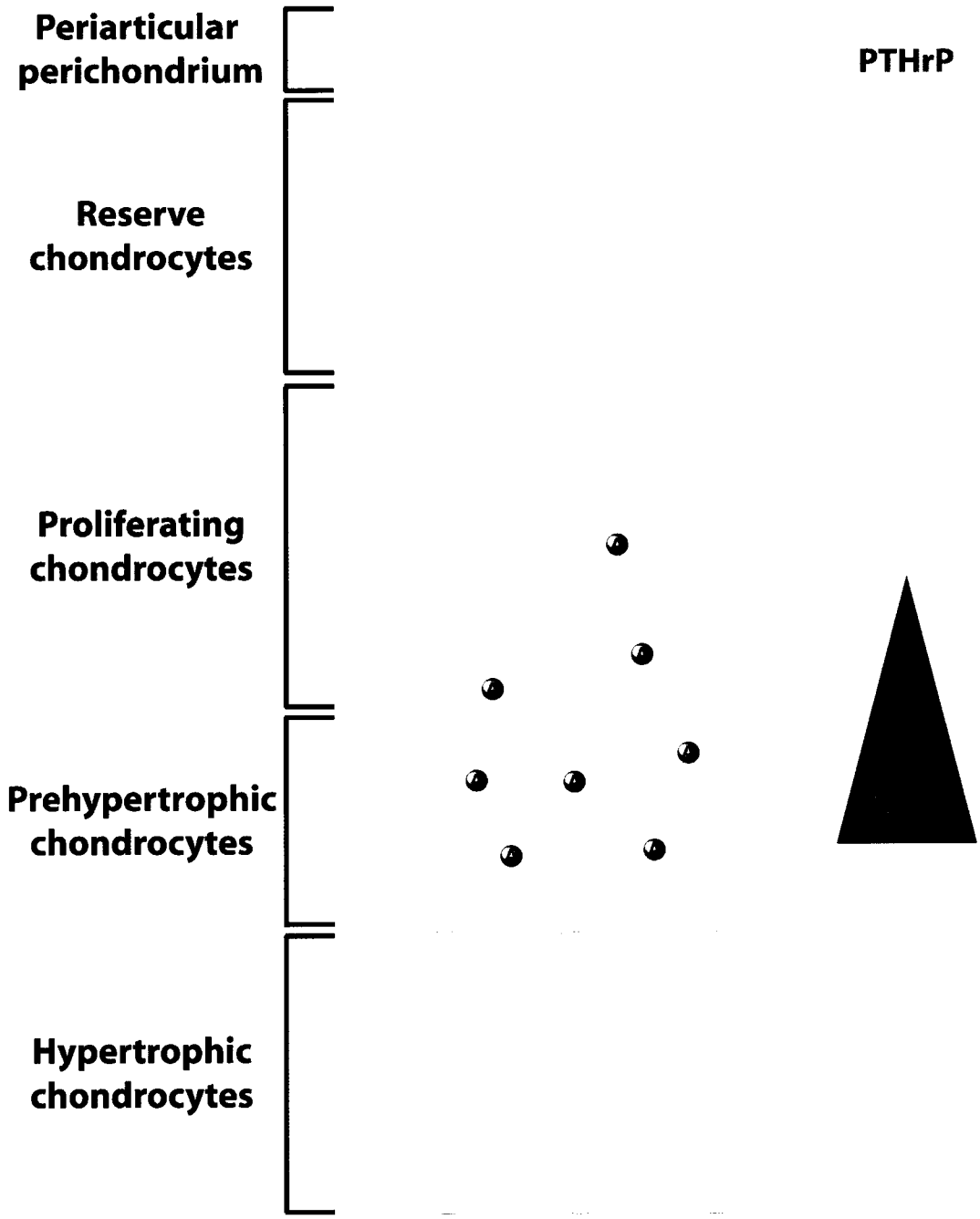
Periarticular perichondrium
Reserve chondrocytes
Proliferating chondrocytes
Prehypertrophic chondrocytes
Hypertrophic chondrocytes
PTHrP

No specific dominant negative effect was determined in the cell-based activity assay. However, the co-culture system eliminates the requirement for secretion or multimerization of the IHH constructs, so future experiments could address this issue. Gel filtration of conditioned media could be used to separate the secreted IHH monomers and multimers. This method can be used to compare the ability of the individual IHH mutants to multimerize, and could also be used to test the activity of the purified monomer and multimer fractions (Chen, Li, et al, 2004). Analysis of conditioned media from cells co-expressing IHH^{WT} and one of each of the BDA1 mutants could determine if the mutant interferes with the ability of IHH^{WT} to multimerize, and could also test the activity of the heterogeneous mutant/WT multimers.

Defective multimerization could be caused by a lack of addition of cholesterol or palmitate during IHH processing. The efficiency of lipid modification of the ACFD and BDA1 mutants could be tested by incubating the HEK293 cells stably expressing the IHH constructs with tritiated palmitate or cholesterol. The incorporation of the tritiated lipid would be determined by western blot analysis of immunoprecipitated IHH from the cell lysates, followed by exposure of an autoradiograph (Chen, Li, et al, 2004; Singh, Tokhunts, et al, 2009). The HEK293 cells stably expressing the lipid mutant constructs would be useful as negative controls for these experiments.

As stated previously, recent evidence suggests that the range of certain BDA1 IHH mutants is increased due to decreased Hip and Ptc binding, and the potency of the mutants is decreased due to decreased Ptc, CDO, and Gas1 binding (Gao, Hu, et al, 2009; McLellan, Zheng, et al, 2008). Our *in vitro* assays confirm that two of the BDA1 mutants have decreased potency in a short-range signaling assay, likely due to the disrupted receptor binding described in those studies. The dominant negative effects of the BDA1 mutants

were not seen in our assays but may be elucidated if future experiments are designed to analyze long-range signaling. To date, no other group has attempted to characterize the ACFD mutations, and our *in vitro* assays suggest that the recessive condition is in fact due to a partial loss-of-function of mutant IHH, resulting in decreased IHH signaling at the growth plate.

Overall, the *in vitro* assays have provided some insight into the molecular mechanism behind the skeletal dysplasias BDA1 and ACFD. The ACFD mutations appear to interfere early on in IHH biogenesis, resulting in very little production of functional IHH-N. The BDA1 mutations introduce defects later on in IHH biogenesis by interfering with the ability of mutant IHH to activate the signaling cascade. Further studies are needed to determine the lipid modification of the mutants, which would have implications on the multimerization and long-range signaling capacity of the mutants at the growth plate.

References

Abad, V., Meyers, J.L., Weise, M., Gafni, R.I., Barnes, K.M., Nilsson, O., Bacher, J.D., and Baron, J. (2002). The role of the resting zone in growth plate chondrogenesis. Endocrinology *143,* 1851-1857.

Ahrens, P.B., Solursh, M., and Reiter, R.S. (1977). Stage-related capacity for limb chondrogenesis in cell culture. Developmental Biology *60,* 69-82.

Allen, B.L., Tenzen, T., and McMahon, A.P. (2007). The Hedgehog-binding proteins Gas1 and Cdo cooperate to positively regulate Shh signaling during mouse development. Genes and Development *21,* 1244-1257.

Arnold, M.A., Kim, Y., Czubryt, M.P., Phan, D., McAnally, J., Qi, X., Shelton, J.M., Richardson, J.A., Bassel-Duby, R., and Olson, E.N. (2007). MEF2C Transcription Factor Controls Chondrocyte Hypertrophy and Bone Development. Developmental Cell *12,* 377-389.

Atsumi, T., Miwa, Y., Kimata, K., and Ikawa, Y. (1990). A chondrogenic cell line derived from a differentiating culture of AT805 teratocarcinoma cells. Cell Differentiation and Development *30,* 109-116.

Ballock, R.T., and O'Keefe, R.J. (2003). Current concepts review: The biology of the growth plate. Journal of Bone and Joint Surgery - Series A *85,* 715-726.

Bell, J. (1951). On brachydactyly and symphalangism. In Treasury of Human Inheritance. Volume 5. Penrose, Lionel ed., (London: Cambridge University Press) pp. 1-31.

Bijlsma, M.F., Spek, C.A., Zivkovic, D., Van De Water, S., Rezaee, F., and Peppelenbosch, M.P. (2006). Repression of smoothened by patched-dependent (pro-)vitamin D3 secretion. PLoS Biology *4,* 1397-1410.

Bitgood, M.J., and McMahon, A.P. (1995). Hedgehog and Bmp genes are coexpressed at many diverse sites of cell-cell interaction in the mouse embryo. Dev. Biol. *172,* 126-138.

Bitgood, M.J., Shen, L., and McMahon, A.P. (1996). Sertoli cell signaling by Desert hedgehog regulates the male germline. Current Biology *6,* 298-304.

Buglino, J.A., and Resh, M.D. (2008). Hhat is a palmitoylacyltransferase with specificity for N-palmitoylation of Sonic Hedgehog. The Journal of Biological Chemistry *283,* 22076-22088.

Bumcrot, D.A., Takada, R., and McMahon, A.P. (1995). Proteolytic processing yields two secreted forms of sonic hedgehog. Mol. Cell. Biol. *15,* 2294-2303.

Burdan, F., Szumiło, J., Korobowicz, A., Farooquee, R., Patel, S., Patel, A., Dave, A., Szumiło, M., Solecki, M., Klepacz, R., and Dudka, J. (2009). Morphology and physiology of the epiphyseal growth plate. Folia Histochemica Et Cytobiologica *47,* 5-16.

Burke, R., Nellen, D., Bellotto, M., Hafen, E., Senti, K., Dickson, B.J., and Basler, K. (1999). Dispatched, a Novel Sterol-Sensing Domain Protein Dedicated to the Release of Cholesterol-Modified Hedgehog from Signaling Cells. Cell *99,* 803-815.

Byrnes, A.M., Racacho, L., Grimsey, A., Hudgins, L., Kwan, A.C., Sangalli, M., Kidd, A., Yaron, Y., Lau, Y.-., Nikkel, S.M., and Bulman, D.E. (2009). Brachydactyly A-1 mutations restricted to the central region of the N-terminal active fragment of Indian Hedgehog. European Journal of Human Genetics *17,* 1112-1120.

Cardin, A.D., and Weintraub, H.J.R. (1989). Molecular modeling of protein-glycosaminoglycan interactions. Arteriosclerosis *9,* 21-32.

Carlberg, A.L., Pucci, B., Rallapalli, R., Tuan, R.S., and Hall, D.J. (2001). Efficient chondrogenic differentiation of mesenchymal cells in micromass culture by retroviral gene transfer of BMP-2. Differentiation *67,* 128-138.

Chen, J.K., Taipale, J., Young, K.E., Maiti, T., and Beachy, P.A. (2002). Small molecule modulation of smoothened activity. Proceedings of the National Academy of Sciences of the United States of America *99,* 14071-14076.

Chen, L., Fink, T., Ebbesen, P., and Zachar, V. (2006). Temporal transcriptome of mouse ATDC5 chondroprogenitors differentiating under hypoxic conditions. Experimental Cell Research *312,* 1727-1744.

Chen, L., Fink, T., Zhang, X.-., Ebbesen, P., and Zachar, V. (2005). Quantitative transcriptional profiling of ATDC5 mouse progenitor cells during chondrogenesis. Differentiation *73,* 350-363.

Chen, M.-., Li, Y.-., Kawakami, T., Xu, S.-., and Chuang, P.-. (2004). Palmitoylation is required for the production of a soluble multimeric Hedgehog protein complex and long-range signaling in vertebrates. Genes and Development *18,* 641-659.

Chen, W., Ren, X.-., Nelson, C.D., Barak, L.S., Chen, J.K., Beachy, P.A., De Sauvage, F., and Lefkowitz, R.J. (2004). Activity-dependent internalization of smoothened mediated by β-Arrestin 2 and GRK2. Science *306,* 2257-2260.

Chiang, C., Litingtung, Y., Lee, E., Young, K.E., Corden, J.L., Westphal, H., and Beachy, P.A. (1996). Cyclopia and defective axial patterning in mice lacking Sonic hedgehog gene function. Nature *383,* 407-413.

Chuang, P.-., and McMahon, A.P. (1999). Vertebrate hedgehog signalling modulated by induction of a hedgehog- binding protein. Nature *397,* 617-621.

Corcoran, R.B., and Scott, M.P. (2006). Oxysterols stimulate Sonic hedgehog signal transduction and proliferation of medulloblastoma cells. Proc. Natl. Acad. Sci. U. S. A. *103,* 8408-8413.

Cortes, M., Baria, A.T., and Schwartz, N.B. (2009). Sulfation of chondroitin sulfate proteoglycans is necessary for proper Indian hedgehog signaling in the developing growth plate. Development *136,* 1697-1706.

Couvé-Privat, S., Le Bret, M., Traiffort, E., Queille, S., Coulombe, J., Bouadjar, B., Avril, M.F., Ruat, M., Sarasin, A., and Daya-Grosjean, L. (2004). Functional analysis of novel sonic hedgehog gene mutations identified in basal cell carcinomas from xeroderma pigmentosum patients. Cancer Res. *64,* 3559-3565.

Cunningham, G.R.M. (2008). *In Vitro* and *In Vivo* Characterization of Mutations In the Human Indian Hedgehog Gene Associated with Brachydactyly Type A1 and Acrocapitofemoral Dysplasia.

Day, E.S., Wen, D., Garber, E.A., Hong, J., Avedissian, L.S., Rayhorn, P., Shen, W., Zeng, C., Bailey, V.R., Reilly, J.O. *et al.* (1999). Zinc-dependent structural stability of human sonic hedgehog. Biochemistry *38,* 14868-14880.

DeLise, A.M., and Tuan, R.S. (2000). Electroporation-mediated DNA transfection of embryonic chick limb mesenchymal cells. Methods Mol. Biol. *137,* 377-382.

Drinkwater, H. (1915). A second brachydactylous family. J Genet *4,* 323-339.

Drinkwater, H. (1912). Account of a family showing minor brachydactyly. J Genet *2,* 21-40.

Drinkwater, H. (1908). An account of a brachydactylous family. Proc R Soc Edin *28,* 35-57.

Echelard, Y., Epstein, D.J., St-Jacques, B., Shen, L., Mohler, J., McMahon, J.A., and McMahon, A.P. (1993). Sonic hedgehog, a member of a family of putative signaling molecules, is implicated in the regulation of CNS polarity. Cell *75,* 1417-1430.

Ehlen, H.W.A., Buelens, L.A., and Vortkamp, A. (2006). Hedgehog signaling in skeletal develoment. Birth Defects Research Part C - Embryo Today: Reviews *78,* 267-279.

Eugster, C., Panáková, D., Mahmoud, A., and Eaton, S. (2007). Lipoprotein-Heparan Sulfate Interactions in the Hh Pathway. Developmental Cell *13,* 57-71.

Farabee, W.C. (1903). Hereditary and sexual influence in meristic variation: A study of malformations in man.

Fitch, N. (1979). Classification and identification of inherited brachydactylies. J. Med. Genet. *16,* 36-44.

Gao, B., Guo, J., She, C., Shu, A., Yang, M., Tan, Z., Yang, X., Guo, S., Feng, G., and He, L. (2001). Mutations in IHH, encoding Indian hedgehog, cause brachydactyly type A-1. Nature Genetics *28,* 386-388.

Gao, B., Hu, J., Stricker, S., Cheung, M., Ma, G., Law, K.F., Witte, F., Briscoe, J., Mundlos, S., He, L., Cheah, K.S.E., and Chan, D. (2009). A mutation in Ihh that causes digit abnormalities alters its signalling capacity and range. Nature *458,* 1196-1200.

Giordano, N., Gennari, L., Bruttini, M., Mari, F., Meloni, I., Baldi, C., Capoccia, S., Geraci, S., Merlotti, D., Amendola, A. *et al.* (2003). Mild brachydactyly type A 1 maps to chromosome 2q35-q36 and is caused by a novel IHH mutation in a three generation family [3]. J. Med. Genet. *40,* 132-135.

Girirajan, S., and Elsea, S.H. (2005). Brachydactyly A1: New relatives for old families? Journal of Genetics *84,* 95-98.

Goetz, J.A., Singh, S., Suber, L.M., Kull, F.J., and Robbins, D.J. (2006). A highly conserved amino-terminal region of Sonic Hedgehog is required for the formation of its freely diffusible multimeric form. J. Biol. Chem. *281,* 4087-4093.

Goomer, R.S., Deftos, L.J., Terkeltaub, R., Maris, T., Lee, M.C., Harwood, F.L., and Amiel, D. (2001). High-efficiency non-viral transfection of primary chondrocytes and perichondrial cells for ex-vivo gene therapy to repair articular cartilage defects. Osteoarthritis and Cartilage *9,* 248-256.

Graham, F.L., Smiley, J., Russell, W.C., and Nairn, R. (1977). Characteristics of a human cell line transformed by DNA from human adenovirus type 5. J. Gen. Virol. *36,* 59-72.

Guo, J., Chung, U.-., Yang, D., Karsenty, G., Bringhurst, F.R., and Kronenberg, H.M. (2006). PTH/PTHrP receptor delays chondrocyte hypertrophy via both Runx2-dependent and -independent pathways. Dev. Biol. *292,* 116-128.

Hall, T.H.T., Porter, J.A., Beachy, P.A., and Leahy, D.J. (1995). A potential catalytic site revealed by the 1.7 A° crystal structure of the amino terminal signalling domain of Sonic hedgehog. Nature *378,* 212-216.

Haycraft, C.J., Banizs, B., Aydin-Son, Y., Zhang, Q., Michaud, E.J., and Yoder, B.K. (2005). Gli2 and Gli3 localize to cilia and require the intraflagellar transport protein polaris for processing and function. PLoS Genetics *1,* 0480-0488.

Hellemans, J., Coucke, P.J., Giedion, A., De Paepe, A., Kramer, P., Beemer, F., and Mortier, G.R. (2003). Homozygous mutations in IHH cause acrocapitofemoral dysplasia, an autosomal recessive disorder with cone-shaped epiphyses in hands and hips. American Journal of Human Genetics *72,* 1040-1046.

Hirao, M., Tamai, N., Tsumaki, N., Yoshikawa, H., and Myoui, A. (2006). Oxygen tension regulates chondrocyte differentiation and function during endochondral ossification. J. Biol. Chem. *281,* 31079-31092.

Huangfu, D., and Anderson, K.V. (2005). Cilia and Hedgehog responsiveness in the mouse. Proc. Natl. Acad. Sci. U. S. A. *102,* 11325-11330.

Jeong, J., and McMahon, A.P. (2005). Growth and pattern of the mammalian neural tube are governed by partially overlapping feedback activities of the hedgehog antagonists patched 1 and Hhip1. Development *132,* 143-154.

Karp, S.J., Schipani, E., St-Jacques, B., Hunzelman, J., Kronenberg, H., and McMahon, A.P. (2000). Indian Hedgehog coordinates endochondral bone growth and morphogenesis via Parathyroid Hormone related-Protein-dependent and -independent pathways. Development *127,* 543-548.

Karsenty, G. (2003). The complexities of skeletal biology. Nature *423,* 316-318.

Kirkpatrick, T.J., Au, K.-., Mastrobattista, J.M., McCready, M.E., Bulman, D.E., and Northrup, H. (2003). Identification of a mutation in the Indian Hedgehog (IHH) gene causing brachydactyly type A1 and evidence for a third locus [1]. Journal of Medical Genetics *40,* 42-44.

Kobayashi, T., Soegiarto, D.W., Yang, Y., Lanske, B., Schipani, E., McMahon, A.P., and Kronenberg, H.M. (2005). Indian hedgehog stimulates periarticular chondrocyte differentiation to regulate growth plate length independently of PTHrP. J. Clin. Invest. *115,* 1734-1742.

Krauss, S., Concordet, J.-., and Ingham, P.W. (1993). A functionally conserved homolog of the Drosophila segment polarity gene hh is expressed in tissues with polarizing activity in zebrafish embryos. Cell *75,* 1431-1444.

Kronenberg, H.M. (2003). Developmental regulation of the growth plate. Nature *423,* 332-336.

Lanske, B., Karaplis, A.C., Lee, K., Luz, A., Vortkamp, A., Pirro, A., Karperien, M., Defize, L.H.K., Ho, C., Mulligan, R.C. *et al.* (1996). PTH/PTHrP receptor in early development and Indian hedgehog-regulated bone growth. Science *273,* 663-666.

Lee, C.S., Buttitta, L., and Fan, C.-. (2001). Evidence that the WNT-inducible growth arrest-specific gene 1 encodes an antagonist of sonic hedgehog signaling in the somite. Proc. Natl. Acad. Sci. U. S. A. *98,* 11347-11352.

Lee, K., Lanske, B., Karaplis, A.C., Deeds, J.D., Kohno, H., Nissenson, R.A., Kronenberg, H.M., and Segre, G.V. (1996). Parathyroid hormone-related peptide delays terminal differentiation of chondrocytes during endochondral bone development. Endocrinology *137,* 5109-5118.

Lefebvre, V., and Smits, P. (2005). Transcriptional control of chondrocyte fate and differentiation. Birth Defects Research Part C - Embryo Today: Reviews *75,* 200-212.

Liu, A., Wang, B., and Niswander, L.A. (2005). Mouse intraflagellar transport proteins regulate both the activator and repressor functions of Gli transcription factors. Development *132,* 3103-3111.

Liu, M., Wang, X., Cai, Z., Tang, Z., Cao, K., Liang, B., Ren, X., Liu, J.Y., and Wang, Q.K. (2006). A novel heterozygous mutation in the Indian hedgehog gene (IHH) is associated with brachydactyly type A1 in a Chinese family. Journal of Human Genetics *51,* 727-731.

Lodder, E.M., Hoogeboom, A.J.M., Coert, J.H., and De Graaff, E. (2008). Deletion of 1 amino acid in indian hedgehog leads to Brachydactylya. American Journal of Medical Genetics, Part A *146,* 2152-2154.

Long, F., Zhang, X.M., Karp, S., Yang, Y., and McMahon, A.P. (2001). Genetic manipulation of hedgehog signaling in the endochondral skeleton reveals a direct role in the regulation of chondrocyte proliferation. Development *128,* 5099-5108.

Lu, X., Liu, S., and Kornberg, T.B. (2006). The C-terminal tail of the Hedgehog receptor Patched regulates both localization and turnover. Genes and Development *20,* 2539-2551.

Ma, G., Xiao, Y., and He, L. (2008). Recent progress in the study of Hedgehog signaling. Journal of Genetics and Genomics *35,* 129-137.

Mackie, E.J., Ahmed, Y.A., Tatarczuch, L., Chen, K.-., and Mirams, M. (2008). Endochondral ossification: How cartilage is converted into bone in the developing skeleton. International Journal of Biochemistry and Cell Biology *40,* 46-62.

Mann, R.K., and Beachy, P.A. (2004). Novel lipid modifications of secreted protein signals. Annual Review of Biochemistry *73,* 891-923.

Martinelli, D.C., and Fan, C.-. (2007). Gas1 extends the range of Hedgehog action by facilitating its signaling. Genes and Development *21,* 1231-1243.

May, S.R., Ashique, A.M., Karlen, M., Wang, B., Shen, Y., Zarbalis, K., Reiter, J., Ericson, J., and Peterson, A.S. (2005). Loss of the retrograde motor for IFT disrupts localization of Smo to cilia and prevents the expression of both activator and repressor functions of Gli. Dev. Biol. *287,* 378-389.

McCready, M.E., Grimsey, A., Styer, T., Nikkel, S.M., and Bulman, D.E. (2005). A century later Farabee has his mutation. Human Genetics *117,* 285-287.

McCready, M.E., Sweeney, E., Fryer, A.E., Donnai, D., Baig, A., Racacho, L., Warman, M.L., Hunter, A.G.W., and Bulman, D.E. (2002). A novel mutation in the IHH gene causes brachydactyly type A1: A 95-year-old mystery resolved. Hum. Genet. *111,* 368-375.

McLellan, J.S., Zheng, X., Hauk, G., Ghirlando, R., Beachy, P.A., and Leahy, D.J. (2008). The mode of Hedgehog binding to Ihog homologues is not conserved across different phyla. Nature *455,* 979-983.

McMahon, A.P., Ingham, P.W., and Tabin, C.J. (2003). 1 Developmental roles and clinical significance of Hedgehog signaling. Current Topics in Developmental Biology *53,* 1-114.

Mello, M.A., and Tuan, R.S. (1999). High density micromass cultures of embryonic limb bud mesenchymal cells: An in vitro model of endochondral skeletal development. In Vitro Cellular and Developmental Biology - Animal *35,* 262-269.

Melrose, J., Smith, S.M., Smith, M.M., and Little, C.B. (2008). The use of Histochoice™® for histological examination of articular and growth plate cartilages, intervertebral disc and meniscus. Biotechnic and Histochemistry *83,* 47-53.

Mirsky, R., Parmantier, E., McMahon, A.P., and Jessen, K.R. (1999). Schwann cell-derived desert hedgehog signals nerve sheath formation. Annals of the New York Academy of Sciences *883,* 196-202.

Mortier, G.R., Kramer, P.P.G., Giedion, A., and Beemer, F.A. (2003). Acrocapitofemoral dysplasia: An autosomal recessive skeletal dysplasia with cone shaped epiphyses in the hands and hips [2]. Journal of Medical Genetics *40,* 201-207.

Murnane, J.P., Yezzi, M.J., and Young, B.R. (1990). Recombination events during integration of transfected DNA into normal human cells. Nucleic Acids Res. *18,* 2733-2738.

Nusslein-Volhard, C., and Wieschaus, E. (1980). Mutations affecting segment number and polarity in Drosophila. Nature *287,* 795-801.

Okada, A., Charron, F., Morin, S., Shin, D.S., Wong, K., Fabre, P.J., Tessier-Lavigne, M., and McConnell, S.K. (2006). Boc is a receptor for sonic hedgehog in the guidance of commissural axons. Nature *444,* 369-373.

O'Rahilly, R., and Gardner, E. (1975). The timing and sequence of events in the development of the limbs in the human embryo. Anat. Embryol. *148,* 1-23.

Panáková, D., Sprong, H., Marois, E., Thiele, C., and Eaton, S. (2005). Lipoprotein particles are required for Hedgehog and Wingless signalling. Nature *435,* 58-65.

Pepinsky, R.B., Zeng, C., Went, D., Rayhorn, P., Baker, D.P., Williams, K.P., Bixler, S.A., Ambrose, C.M., Garber, E.A., Miatkowski, K. *et al.* (1998). Identification of a palmitic acid-modified form of human Sonic hedgehog. Journal of Biological Chemistry *273,* 14037-14045.

Porter, J.A., Von Kessler, D.P., Ekker, S.C., Young, K.E., Lee, J.J., Moses, K., and Beachy, P.A. (1995). The product of hedgehog autoproteolytic cleavage active in local and long-range signalling. Nature *374,* 363-366.

Porter, J.A., Young, K.E., and Beachy, P.A. (1996). Cholesterol modification of hedgehog signaling proteins in animal development. Science *274,* 255-259.

Provot, S., Kempf, H., Murtaugh, L.C., Chung, U.-., Kim, D.-., Chyung, J., Kronenberg, H.M., and Lassar, A.B. (2006). Nkx3.2/Bapx1 acts as a negative regulator of chondrocyte maturation. Development *133,* 651-662.

Qureshi, H.Y., Ahmad, R., and Zafarullah, M. (2008). High-efficiency transfection of nucleic acids by the modified calcium phosphate precipitation method in chondrocytes. Anal. Biochem. *382,* 138-140.

Rohatgi, R., Milenkovic, L., and Scott, M.P. (2007). Patched1 regulates hedgehog signaling at the primary cilium. Science *317,* 372-376.

Rubin, J.B., Choi, Y., and Segal, R.A. (2002). Cerebellar proteoglycans regulate sonic hedgehog responses during development. Development *129,* 2223-2232.

Schipani, E., Ryan, H.E., Didrickson, S., Kobayashi, T., Knight, M., and Johnson, R.S. (2001). Hypoxia in cartilage: HIF-1α is essential for chondrocyte growth arrest and survival. Genes and Development *15,* 2865-2876.

Schröder, M., and Kaufman, R.J. (2005). The mammalian unfolded protein response. Annual Review of Biochemistry *74,* 739-789.

Shukunami, C., Ishizeki, K., Atsumi, T., Ohta, Y., Suzuki, F., and Hiraki, Y. (1997). Cellular hypertrophy and calcification of embryonal carcinoma-derived chondrogenic cell line ATDC5 in vitro. Journal of Bone and Mineral Research *12,* 1174-1188.

Simpson, F., Kerr, M.C., and Wicking, C. (2009). Trafficking, development and hedgehog. Mech. Dev. *126,* 279-288.

Singh, S., Tokhunts, R., Baubet, V., Goetz, J.A., Huang, Z.J., Schilling, N.S., Black, K.E., MacKenzie, T.A., Dahmane, N., and Robbins, D.J. (2009). Sonic hedgehog mutations identified in holoprosencephaly patients can act in a dominant negative manner. Hum. Genet. *125,* 95-103.

Singla, V., and Reiter, J.F. (2006). The primary cilium as the cell's antenna: Signaling at a sensory organelle. Science *313,* 629-633.

Stattin, E.-., Lindén, B., Lönnerholm, T., Schuster, J., and Dahl, N. (2009). Brachydactyly type A1 associated with unusual radiological findings and a novel Arg158Cys mutation in the Indian hedgehog (IHH) gene. European Journal of Medical Genetics *52,* 297-302.

St-Jacques, B., Hammerschmidt, M., and McMahon, A.P. (1999). Indian hedgehog signaling regulates proliferation and differentiation of chondrocytes and is essential for bone formation. Genes and Development *13,* 2072-2086.

Stokes, D.G., Liu, G., Coimbra, I.B., Piera-Velazquez, S., Crowl, R.M., and Jiménez, S.A. (2002). Assessment of the gene expression profile of differentiated and dedifferentiated human fetal chondrocytes by microarray analysis. Arthritis and Rheumatism *46,* 404-419.

Stott, N.S., and Chuong, C.M. (2000). Retroviral gene transduction in limb bud micromass cultures. Methods Mol. Biol. *135,* 509-513.

Taipale, J., Chen, J.K., Cooper, M.K., Wang, B., Mann, R.K., Milenkovic, L., Scott, M.P., and Beachy, P.A. (2000). Effects of oncogenic mutations in Smoothened and Patched can be reversed by cyclopamine. Nature *406,* 1005-1009.

Taipale, J., Cooper, M.K., Maiti, T., and Beachy, P.A. (2002). Patched acts catalytically to suppress the activity of smoothened. Nature *418,* 892-897.

Tenzen, T., Allen, B.L., Cole, F., Kang, J.-., Krauss, R.S., and McMahon, A.P. (2006). The Cell Surface Membrane Proteins Cdo and Boc Are Components and Targets of the Hedgehog Signaling Pathway and Feedback Network in Mice. Developmental Cell *10,* 647-656.

Thomas, P., and Smart, T.G. (2005). HEK293 cell line: A vehicle for the expression of recombinant proteins. Journal of Pharmacological and Toxicological Methods *51,* 187-200.

Traiffort, E., Dubourg, C., Faure, H., Rognan, D., Odent, S., Durou, M.-., David, V., and Ruat, M. (2004). Functional characterization of Sonic hedgehog mutations associated with holoprosencephaly. Journal of Biological Chemistry *279,* 42889-42897.

Vega, R.B., Matsuda, K., Oh, J., Barbosa, A.C., Yang, X., Meadows, E., McAnally, J., Pomajzl, C., Shelton, J.M., Richardson, J.A., Karsenty, G., and Olson, E.N. (2004). Histone deacetylase 4 controls chondrocyte hypertrophy during skeletogenesis. Cell *119,* 555-566.

Vortkamp, A., Lee, K., Lanske, B., Segre, G.V., Kronenberg, H.M., and Tabin, C.J. (1996). Regulation of rate of cartilage differentiation by Indian Hedgehog and PTH-related protein. Science *273,* 613-622.

Weise, M., De-Levi, S., Barnes, K.M., Gafni, R.I., Abad, V., and Baron, J. (2001). Effects of estrogen on growth plate senescence and epiphyseal fusion. Proc. Natl. Acad. Sci. U. S. A. *98,* 6871-6876.

Wendler, F., Franch-Marro, X., and Vincent, J.-. (2006). How does cholesterol affect the way Hedgehog works? Development *133,* 3055-3061.

Yang, X., She, C., Guo, J., Yu, A.C.H., Lu, Y., Shi, X., Feng, G., and He, L. (2000). A locus for brachydactyly type A-1 maps to chromosome 2q35-q36. Am. J. Hum. Genet. *66,* 892-903.

Yoshida, C.A., Yamamoto, H., Fujita, T., Furuichi, T., Ito, K., Inoue, K.-., Yamana, K., Zanma, A., Takada, K., Ito, Y., and Komori, T. (2004). Runx2 and Runx3 are essential for chondrocyte maturation, and Runx2 regulates limb growth through induction of Indian hedgehog. Genes and Development *18,* 952-963.

Zelzer, E., and Olsen, B.R. (2003). The genetic basis for skeletal diseases. Nature *423,* 343-348.

Zeng, X., Goetz, J.A., Suber, L.M., Scott Jr., W.J., Schreiner, C.M., and Robbins, D.J. (2001). A freely diffusible form of Sonic hedgehog mediates long-range signalling. Nature *411,* 716-720.

Zhang, W., Kang, J.-., Cole, F., Yi, M.-., and Krauss, R.S. (2006). Cdo Functions at Multiple Points in the Sonic Hedgehog Pathway, and Cdo-Deficient Mice Accurately Model Human Holoprosencephaly. Developmental Cell *10,* 657-665.

Zhou, G., Zheng, Q., Engin, F., Munivez, E., Chen, Y., Sebald, E., Krakow, D., and Lee, B. (2006). Dominance of SOX9 function over RUNX2 during skeletogenesis. Proc. Natl. Acad. Sci. U. S. A. *103,* 19004-19009.

Zhu, G., Ke, X., Liu, Q., Li, J., Chen, B., Shao, C., and Gong, Y. (2007). Recurrence of the D100N mutation in a Chinese family with brachydactyly type A1: Evidence for a mutational hot spot in the Indian hedgehog gene [2]. American Journal of Medical Genetics, Part A *143,* 1246-1248.

SPRINGER LICENSE
TERMS AND CONDITIONS

Sep 15, 2009

This is a License Agreement between Kelly Patterson ("You") and Springer ("Springer") provided by Copyright Clearance Center ("CCC"). The license consists of your order details, the terms and conditions provided by Springer, and the payment terms and conditions.

All payments must be made in full to CCC. For payment instructions, please see information listed at the bottom of this form.

License Number	2247880847168
License date	Aug 14, 2009
Licensed content publisher	Springer
Licensed content publication	Human Genetics
Licensed content title	A century later Farabee has his mutation
Licensed content author	M. Elizabeth McCready
Licensed content date	Jul 1, 2005
Volume number	117
Issue number	2
Type of Use	Thesis/Dissertation
Portion	Figures
Author of this Springer article	No
Order reference number	
Title of your thesis / dissertation	Biochemical characterization of Indian Hedgehog mutations associated with Brachydactyly Type A1 and Acrocapitofemoral Dysplasia
Expected completion date	Sep 2009
Estimated size(pages)	100
Total	0.00 CAD

Terms and Conditions

Introduction

The publisher for this copyrighted material is Springer Science + Business Media. By clicking "accept" in connection with completing this licensing transaction, you agree that the following terms and conditions apply to this transaction (along with the Billing and Payment terms and conditions established by Copyright Clearance Center, Inc. ("CCC"), at

the time that you opened your Rightslink account and that are available at any time at http://myaccount.copyright.com).

Limited License
With reference to your request to reprint in your thesis material on which Springer Science and Business Media control the copyright, permission is granted, free of charge, for the use indicated in your enquiry. Licenses are for one-time use only with a maximum distribution equal to the number that you identified in the licensing process.

This License includes use in an electronic form, provided it is password protected or on the university's intranet, destined to microfilming by UMI and University repository. For any other electronic use, please contact Springer at (permissions.dordrecht@springer.com or permissions.heidelberg@springer.com)

The material can only be used for the purpose of defending your thesis, and with a maximum of 100 extra copies in paper.

Although Springer holds copyright to the material and is entitled to negotiate on rights, this license is only valid, provided permission is also obtained from the (co) author (address is given with the article/chapter) and provided it concerns original material which does not carry references to other sources (if material in question appears with credit to another source, authorization from that source is required as well). Permission free of charge on this occasion does not prejudice any rights we might have to charge for reproduction of our copyrighted material in the future.

Altering/Modifying Material: Not Permitted
However figures and illustrations may be altered minimally to serve your work. Any other abbreviations, additions, deletions and/or any other alterations shall be made only with prior written authorization of the author(s) and/or Springer Science + Business Media. (Please contact Springer at permissions.dordrecht@springer.com or permissions.heidelberg@springer.com)

Reservation of Rights
Springer Science + Business Media reserves all rights not specifically granted in the combination of (i) the license details provided by you and accepted in the course of this licensing transaction, (ii) these terms and conditions and (iii) CCC's Billing and Payment terms and conditions.

Copyright Notice:
Please include the following copyright citation referencing the publication in which the material was originally published. Where wording is within brackets, please include verbatim.
"With kind permission from Springer Science+Business Media: <book/journal title, chapter/article title, volume, year of publication, page, name(s) of author(s), figure number(s), and any original (first) copyright notice displayed with material>."

Warranties: Springer Science + Business Media makes no representations or warranties with respect to the licensed material.

Indemnity
You hereby indemnify and agree to hold harmless Springer Science + Business Media and CCC, and their respective officers, directors, employees and agents, from and against any and all claims arising out of your use of the licensed material other than as specifically authorized pursuant to this license.

No Transfer of License
This license is personal to you and may not be sublicensed, assigned, or transferred by you to any other person without Springer Science + Business Media's written permission.

No Amendment Except in Writing
This license may not be amended except in a writing signed by both parties (or, in the case of Springer Science + Business Media, by CCC on Springer Science + Business Media's behalf).

Objection to Contrary Terms
Springer Science + Business Media hereby objects to any terms contained in any purchase order, acknowledgment, check endorsement or other writing prepared by you, which terms are inconsistent with these terms and conditions or CCC's Billing and Payment terms and conditions. These terms and conditions, together with CCC's Billing and Payment terms and conditions (which are incorporated herein), comprise the entire agreement between you and Springer Science + Business Media (and CCC) concerning this licensing transaction. In the event of any conflict between your obligations established by these terms and conditions and those established by CCC's Billing and Payment terms and conditions, these terms and conditions shall control.

Jurisdiction
All disputes that may arise in connection with this present License, or the breach thereof, shall be settled exclusively by the country's law in which the work was originally published.

v1.2

Gratis licenses (referencing $0 in the Total field) are free. Please retain this printable license for your reference. No payment is required.

If you would like to pay for this license now, please remit this license along with your payment made payable to "COPYRIGHT CLEARANCE CENTER" otherwise you will be invoiced within 30 days of the license date. Payment should be in the form of a check or money order referencing your account number and this license number 2247880847168.
If you would prefer to pay for this license by credit card, please go to http://www.copyright.com/creditcard to download our credit card payment authorization form.

Make Payment To:

ELSEVIER LICENSE
TERMS AND CONDITIONS

Sep 15, 2009

This is a License Agreement between Kelly Patterson ("You") and Elsevier ("Elsevier") provided by Copyright Clearance Center ("CCC"). The license consists of your order details, the terms and conditions provided by Elsevier, and the payment terms and conditions.

All payments must be made in full to CCC. For payment instructions, please see information listed at the bottom of this form.

Supplier	Elsevier Limited The Boulevard,Langford Lane Kidlington,Oxford,OX5 1GB,UK
Registered Company Number	1982084
Customer name	Kelly Patterson
Customer address	
License Number	2250280565583
License date	Aug 15, 2009
Licensed content publisher	Elsevier
Licensed content publication	The American Journal of Human Genetics
Licensed content title	Homozygous Mutations in *IHH* Cause Acrocapitofemoral Dysplasia, an Autosomal Recessive Disorder with Cone-Shaped Epiphyses in Hands and Hips
Licensed content author	Jan Hellemans, Paul J. Coucke, Andres Giedion, Anne De Paepe, Peter Kramer, Frits Beemer and Geert R. Mortier
Licensed content date	April 2003
Volume number	
Issue number	
Pages	0
Type of Use	Thesis / Dissertation
Portion	Figures/table/illustration/abstracts
Portion Quantity	2

Format	Print
You are an author of the Elsevier article	No
Are you translating?	No
Order Reference Number	
Expected publication date	Sep 2009
Elsevier VAT number	GB 494 6272 12
Permissions price	0.00 USD
Value added tax 0.0%	0.00 USD
Total	0.00 USD

Terms and Conditions

INTRODUCTION

1. The publisher for this copyrighted material is Elsevier. By clicking "accept" in connection with completing this licensing transaction, you agree that the following terms and conditions apply to this transaction (along with the Billing and Payment terms and conditions established by Copyright Clearance Center, Inc. ("CCC"), at the time that you opened your Rightslink account and that are available at any time at http://myaccount.copyright.com).

GENERAL TERMS

2. Elsevier hereby grants you permission to reproduce the aforementioned material subject to the terms and conditions indicated.

3. Acknowledgement: If any part of the material to be used (for example, figures) has appeared in our publication with credit or acknowledgement to another source, permission must also be sought from that source. If such permission is not obtained then that material may not be included in your publication/copies. Suitable acknowledgement to the source must be made, either as a footnote or in a reference list at the end of your publication, as follows:

"Reprinted from Publication title, Vol /edition number, Author(s), Title of article / title of chapter, Pages No., Copyright (Year), with permission from Elsevier [OR APPLICABLE SOCIETY COPYRIGHT OWNER]." Also Lancet special credit - "Reprinted from The Lancet, Vol. number, Author(s), Title of article, Pages No., Copyright (Year), with permission from Elsevier."

4. Reproduction of this material is confined to the purpose and/or media for which permission is hereby given.

5. Altering/Modifying Material: Not Permitted. However figures and illustrations may be

altered/adapted minimally to serve your work. Any other abbreviations, additions, deletions and/or any other alterations shall be made only with prior written authorization of Elsevier Ltd. (Please contact Elsevier at permissions@elsevier.com)

6. If the permission fee for the requested use of our material is waived in this instance, please be advised that your future requests for Elsevier materials may attract a fee.

7. Reservation of Rights: Publisher reserves all rights not specifically granted in the combination of (i) the license details provided by you and accepted in the course of this licensing transaction, (ii) these terms and conditions and (iii) CCC's Billing and Payment terms and conditions.

8. License Contingent Upon Payment: While you may exercise the rights licensed immediately upon issuance of the license at the end of the licensing process for the transaction, provided that you have disclosed complete and accurate details of your proposed use, no license is finally effective unless and until full payment is received from you (either by publisher or by CCC) as provided in CCC's Billing and Payment terms and conditions. If full payment is not received on a timely basis, then any license preliminarily granted shall be deemed automatically revoked and shall be void as if never granted. Further, in the event that you breach any of these terms and conditions or any of CCC's Billing and Payment terms and conditions, the license is automatically revoked and shall be void as if never granted. Use of materials as described in a revoked license, as well as any use of the materials beyond the scope of an unrevoked license, may constitute copyright infringement and publisher reserves the right to take any and all action to protect its copyright in the materials.

9. Warranties: Publisher makes no representations or warranties with respect to the licensed material.

10. Indemnity: You hereby indemnify and agree to hold harmless publisher and CCC, and their respective officers, directors, employees and agents, from and against any and all claims arising out of your use of the licensed material other than as specifically authorized pursuant to this license.

11. No Transfer of License: This license is personal to you and may not be sublicensed, assigned, or transferred by you to any other person without publisher's written permission.

12. No Amendment Except in Writing: This license may not be amended except in a writing signed by both parties (or, in the case of publisher, by CCC on publisher's behalf).

13. Objection to Contrary Terms: Publisher hereby objects to any terms contained in any purchase order, acknowledgment, check endorsement or other writing prepared by you, which terms are inconsistent with these terms and conditions or CCC's Billing and Payment terms and conditions. These terms and conditions, together with CCC's Billing and Payment terms and conditions (which are incorporated herein), comprise the entire agreement between you and publisher (and CCC) concerning this licensing transaction. In

the event of any conflict between your obligations established by these terms and conditions and those established by CCC's Billing and Payment terms and conditions, these terms and conditions shall control.

14. Revocation: Elsevier or Copyright Clearance Center may deny the permissions described in this License at their sole discretion, for any reason or no reason, with a full refund payable to you. Notice of such denial will be made using the contact information provided by you. Failure to receive such notice will not alter or invalidate the denial. In no event will Elsevier or Copyright Clearance Center be responsible or liable for any costs, expenses or damage incurred by you as a result of a denial of your permission request, other than a refund of the amount(s) paid by you to Elsevier and/or Copyright Clearance Center for denied permissions.

LIMITED LICENSE

The following terms and conditions apply only to specific license types:

15. **Translation**: This permission is granted for non-exclusive world **English** rights only unless your license was granted for translation rights. If you licensed translation rights you may only translate this content into the languages you requested. A professional translator must perform all translations and reproduce the content word for word preserving the integrity of the article. If this license is to re-use 1 or 2 figures then permission is granted for non-exclusive world rights in all languages.

16. **Website**: The following terms and conditions apply to electronic reserve and author websites:
Electronic reserve: If licensed material is to be posted to website, the web site is to be password-protected and made available only to bona fide students registered on a relevant course if:
This license was made in connection with a course,
This permission is granted for 1 year only. You may obtain a license for future website posting,
All content posted to the web site must maintain the copyright information line on the bottom of each image,
A hyper-text must be included to the Homepage of the journal from which you are licensing at http://www.sciencedirect.com/science/journal/xxxxx or the Elsevier homepage for books at http://www.elsevier.com , and
Central Storage: This license does not include permission for a scanned version of the material to be stored in a central repository such as that provided by Heron/XanEdu.

17. **Author website** for journals with the following additional clauses:

All content posted to the web site must maintain the copyright information line on the bottom of each image, and
he permission granted is limited to the personal version of your paper. You are not allowed to download and post the published electronic version of your article (whether PDF or

HTML, proof or final version), nor may you scan the printed edition to create an electronic version,
A hyper-text must be included to the Homepage of the journal from which you are licensing at http://www.sciencedirect.com/science/journal/xxxxx , As part of our normal production process, you will receive an e-mail notice when your article appears on Elsevier's online service ScienceDirect (www.sciencedirect.com). That e-mail will include the article's Digital Object Identifier (DOI). This number provides the electronic link to the published article and should be included in the posting of your personal version. We ask that you wait until you receive this e-mail and have the DOI to do any posting.
Central Storage: This license does not include permission for a scanned version of the material to be stored in a central repository such as that provided by Heron/XanEdu.

18. **Author website** for books with the following additional clauses:
Authors are permitted to place a brief summary of their work online only.
A hyper-text must be included to the Elsevier homepage at http://www.elsevier.com

All content posted to the web site must maintain the copyright information line on the bottom of each image
You are not allowed to download and post the published electronic version of your chapter, nor may you scan the printed edition to create an electronic version.
Central Storage: This license does not include permission for a scanned version of the material to be stored in a central repository such as that provided by Heron/XanEdu.

19. **Website** (regular and for author): A hyper-text must be included to the Homepage of the journal from which you are licensing at http://www.sciencedirect.com/science/journal/xxxxx. or for books to the Elsevier homepage at http://www.elsevier.com

20. **Thesis/Dissertation**: If your license is for use in a thesis/dissertation your thesis may be submitted to your institution in either print or electronic form. Should your thesis be published commercially, please reapply for permission. These requirements include permission for the Library and Archives of Canada to supply single copies, on demand, of the complete thesis and include permission for UMI to supply single copies, on demand, of the complete thesis. Should your thesis be published commercially, please reapply for permission.

21. **Other Conditions**None

v1.6

Gratis licenses (referencing $0 in the Total field) are free. Please retain this printable license for your reference. No payment is required.

If you would like to pay for this license now, please remit this license along with your payment made payable to "COPYRIGHT CLEARANCE CENTER" otherwise you will be invoiced within 30 days of the license date. Payment should be in the form of a check or money order referencing your account number and this license number 2250280565583.
If you would prefer to pay for this license by credit card, please go to http://www.copyright.com/creditcard to download our credit card payment authorization form.

Make Payment To:
Copyright Clearance Center
Dept 001
P.O. Box 843006
Boston, MA 02284-3006

If you find copyrighted material related to this license will not be used and wish to cancel, please contact us referencing this license number 2250280565583 and noting the reason for cancellation.

Questions? customercare@copyright.com or +1-877-622-5543 (toll free in the US) or +1-978-646-2777.
